



**Titre:** Relations rhéologie-morphologie dans les mélanges de polymères  
Title: immiscibles

**Auteur:** Christophe Lacroix  
Author:

**Date:** 1998

**Type:** Mémoire ou thèse / Dissertation or Thesis

**Référence:** Lacroix, C. (1998). Relations rhéologie-morphologie dans les mélanges de polymères immiscibles [Ph.D. thesis, École Polytechnique de Montréal].  
Citation: PolyPublie. <https://publications.polymtl.ca/6785/>

 **Document en libre accès dans PolyPublie**  
Open Access document in PolyPublie

**URL de PolyPublie:** <https://publications.polymtl.ca/6785/>  
PolyPublie URL:

**Directeurs de recherche:**  
Advisors:

**Programme:** Unspecified  
Program:

## INFORMATION TO USERS

This manuscript has been reproduced from the microfilm master. UMI films the text directly from the original or copy submitted. Thus, some thesis and dissertation copies are in typewriter face, while others may be from any type of computer printer.

**The quality of this reproduction is dependent upon the quality of the copy submitted.** Broken or indistinct print, colored or poor quality illustrations and photographs, print bleedthrough, substandard margins, and improper alignment can adversely affect reproduction.

In the unlikely event that the author did not send UMI a complete manuscript and there are missing pages, these will be noted. Also, if unauthorized copyright material had to be removed, a note will indicate the deletion.

Oversize materials (e.g., maps, drawings, charts) are reproduced by sectioning the original, beginning at the upper left-hand corner and continuing from left to right in equal sections with small overlaps. Each original is also photographed in one exposure and is included in reduced form at the back of the book.

Photographs included in the original manuscript have been reproduced xerographically in this copy. Higher quality 6" x 9" black and white photographic prints are available for any photographs or illustrations appearing in this copy for an additional charge. Contact UMI directly to order.

**UMI<sup>®</sup>**

Bell & Howell Information and Learning  
300 North Zeeb Road, Ann Arbor, MI 48106-1346 USA  
800-521-0600



UNIVERSITÉ DE MONTRÉAL

RELATIONS RHÉOLOGIE-MORPHOLOGIE DANS  
LES MÉLANGES DE POLYMÈRES IMMISCIBLES

CHRISTOPHE LACROIX  
DÉPARTEMENT DE GÉNIE CHIMIQUE  
ÉCOLE POLYTECHNIQUE DE MONTRÉAL

THÈSE PRÉSENTÉE EN VUE DE L'OBTENTION  
DU DIPLÔME DE PHILOSOPHIAE DOCTOR (Ph.D.)  
(GÉNIE CHIMIQUE)

AVRIL 1998





**National Library  
of Canada**

**Acquisitions and  
Bibliographic Services**

**395 Wellington Street  
Ottawa ON K1A 0N4  
Canada**

**Bibliothèque nationale  
du Canada**

**Acquisitions et  
services bibliographiques**

**395, rue Wellington  
Ottawa ON K1A 0N4  
Canada**

*Your file Votre référence*

*Our file Notre référence*

The author has granted a non-exclusive licence allowing the National Library of Canada to reproduce, loan, distribute or sell copies of this thesis in microform, paper or electronic formats.

The author retains ownership of the copyright in this thesis. Neither the thesis nor substantial extracts from it may be printed or otherwise reproduced without the author's permission.

L'auteur a accordé une licence non exclusive permettant à la Bibliothèque nationale du Canada de reproduire, prêter, distribuer ou vendre des copies de cette thèse sous la forme de microfiche/film, de reproduction sur papier ou sur format électronique.

L'auteur conserve la propriété du droit d'auteur qui protège cette thèse. Ni la thèse ni des extraits substantiels de celle-ci ne doivent être imprimés ou autrement reproduits sans son autorisation.

0-612-38722-4



UNIVERSITÉ DE MONTRÉAL

ÉCOLE POLYTECHNIQUE DE MONTRÉAL

Cette thèse intitulée :

RELATIONS RHÉOLOGIE-MORPHOLOGIE DANS  
LES MÉLANGES DE POLYMÈRES IMMISCIBLES

présentée par: LACROIX Christophe

en vue de l'obtention du diplôme de: Philosophiae Doctor

a été dûment acceptée par le jury d'examen constitué de:

M. LEGROS Robert, Ph.D., président

M. CARREAU Pierre J., Ph.D., membre et directeur de recherche

M. GRMELA Miroslav, Ph.D., membre et codirecteur de recherche

M. AIT-KADI Abdellatif, Ph.D., membre

M. LAFLEUR Pierre G., Ph.D., membre

***“ Espérer sans essayer est une faute mais  
essayer sans espérer est le pire mensonge à soi”***

Libre Propos d’Alain, 1932, Minerve ou de la sagesse (p.155, Hartmann)

***A ma femme, Carol***

## REMERCIEMENTS

Ces remerciements s'adressent à :

Monsieur Pierre Carreau, pour ses conseils scientifiques et pour la liberté qu'il m'a accordée tout au long de cette thèse;

Monsieur Miroslav Grmela, pour sa disponibilité et son implication pertinente dans la partie théorique de ce projet;

Monsieur Alain Michel qui a participé à l'élaboration initiale de l'étude avec Messieurs Alain Bouilloux et Benoît Ernst d'Elf-Atochem;

Messieurs Jean-François Pierson et Jacques Bodelle d'Elf-Atochem pour l'intérêt dont ils ont témoigné vis-à-vis de ces recherches et la société Elf-Atochem pour son support financier.

Que le personnel du CRASP, ainsi que les étudiants au doctorat et à la maîtrise que j'ai côtoyés durant ces nombreuses années trouvent l'expression de ma profonde reconnaissance.

Enfin, merci à Carol pour son soutien inconditionnel et ses encouragements.

## RÉSUMÉ

Ce travail est consacré à l'étude des relations entre la rhéologie et la morphologie dans les mélanges de polymères immiscibles. Ces systèmes sont caractérisés par des morphologies biphasiques dans les cas les plus simples. Cette morphologie est sensible aux conditions d'écoulement rencontrées durant les diverses étapes de mise en forme. Etant donné que les propriétés finales des matériaux hétérogènes sont intimement reliées à leur microstructure, il est essentiel, dans un souci d'optimisation du développement de nouveaux mélanges, d'établir des modèles rhéologiques qui peuvent prendre en compte les changements de morphologie se produisant dans les écoulements.

La première partie de ce travail a consisté en une caractérisation des propriétés viscoélastiques linéaires de différents mélanges. Une étude comparative des modèles de Palierne (1990) et de Lee et Park (1994) a été effectuée sur ces systèmes à l'état fondu. Le modèle de Palierne, qui est limité au domaine des faibles déformations, prédit parfaitement le comportement rhéologique des mélanges. Le modèle de Lee et Park, initialement développé pour prendre en considération les phénomènes de coalescence et de rupture se produisant dans le domaine des fortes déformations, s'avère lui aussi apte à décrire de façon satisfaisante les propriétés rhéologiques des mélanges dans le domaine de la viscoélasticité linéaire. A la différence du modèle de Palierne, le modèle de Lee et Park requiert l'ajustement d'un paramètre. Comme les temps caractéristiques associés à l'interface sont du même ordre de grandeur pour les deux modèles et se comparent aux temps issus du spectre de relaxation pondéré, il a été possible de proposer une méthode approximative d'estimation du paramètre ajustable. Néanmoins, des déficiences entre les prédictions du modèle de Lee et Park et les données rhéologiques à hautes fréquences ont été observées dans le cas où le comportement rhéologique de chacune des phases est fort différent. La loi de mélange incluse dans le modèle de Lee et Park a donc été modifiée empiriquement de façon à retrouver le comportement prédit par le modèle de Palierne à hautes fréquences et à satisfaire l'équation limite d'Einstein dans le cas d'une suspension de sphères dures diluée.

Analyser les prédictions du modèle de Lee et Park dans le domaine de la viscoélasticité linéaire constituait la première étape du travail avant d'aborder l'étude de cette équation d'état dans le domaine des fortes déformations. Dans une seconde partie, les expériences menées en régime transitoire sur les mélanges immiscibles ont permis de mettre l'accent sur l'étude des propriétés viscoélastiques non linéaires. Ces tests, caractérisés par l'apparition d'un "overshoot" lors du démarrage en cisaillement, pour des mélanges présentant une phase dispersée déformable, reflètent l'évolution de morphologie se produisant dans l'écoulement. Le modèle de Lee et Park, sa version modifiée (proposée dans la première partie de ce travail) et une version modifiée du modèle de Grmela et Ait-Kadi (1994) ont été utilisés pour décrire les données rhéologiques en régime transitoire. Ces relations permettent ainsi de prédire soit qualitativement, soit quantitativement les changements de morphologie induits par l'écoulement. Pour un mélange polypropylène (PP)/ éthylène vinylacétate (EVA)-éthylène méthylacrylate (EMA) des phénomènes de rupture et de coalescence ont été observés sur un domaine relativement faible de taux de cisaillement. Ces changements de morphologie ont aussi été caractérisés à partir de mesures effectuées dans le domaine de la viscoélasticité linéaire à l'aide du modèle d'émulsion de Palierne. Sur des systèmes inverses pour lesquels la phase dispersée n'était pas déformable, les prédictions des différents modèles n'ont pas été satisfaisantes.

La troisième partie de cette thèse est dédiée à l'étude de la morphologie induite par des écoulements en cisaillement simple ou par des écoulements préférentiellement élongationnels. Les prédictions des différents modèles, utilisés pour décrire le comportement rhéologique du mélange PP/EVA-EMA, apparaissent moins satisfaisantes avec un mélange polystyrène (PS)/polyéthylène (PE). Les résultats dépendent de manière très significative de la règle de mélange utilisée pour décrire les propriétés des deux composantes. Dans des écoulements majoritairement élongationnels, l'influence du rapport de viscosité sur la morphologie finale du mélange est étudiée en utilisant des mélanges PP/EVA-EMA de compositions inverses. Les données de viscosité élongationnelle nécessaires à la résolution du modèle de Lee et Park ont été obtenues à partir de mesures de pertes de pression dans une

filière hyperbolique. Les prédictions du modèles sont cependant uniquement qualitatives. Ces résultats permettent malgré tout de mettre en évidence l'importance du type d'écoulement, car quelque soit le rapport de viscosité, une transition d'une morphologie nodulaire vers une morphologie fibrillaire est observée.



## ABSTRACT

This work is devoted to the study of the relationships between rheology and morphology in immiscible polymer blends. These systems show a two phase morphology which can be affected by the flow during the processing. As the design of specific materials of required properties is controlled by the final microstructure, it is essential for optimizing the manufacture of new polymer blends to develop rheological models that can describe the morphological changes occurring during processing.

In the first part of this work, the linear viscoelastic properties of several molten blends with immiscible components have been investigated. A comparative study of the Palierne (1990) and Lee and Park (1994) models has been carried out. The Palierne model, which is restricted to small amplitude oscillatory shear flows, is shown to predict well the linear behavior of all the blends. The Lee and Park model, developed to take into account the relationships between the rheological behavior and the morphological changes under large strain flows, is also shown to describe relatively well the behavior of the blends. In this latter case, one adjusting parameter has to be fitted. The characteristic times associated with the interface and derived from the Palierne and Lee and Park models are of the same order of magnitude and compare well with those obtained from the weighted relaxation spectra. An approximate method is then proposed to estimate this adjustable parameter. Nevertheless, discrepancies have been observed for the Lee and Park predictions with blends for which the rheological properties of the components are considerably different. The description of the bulk properties has been therefore empirically modified in order to retrieve the mixing rule embedded in the Palierne model at high frequencies and recover the Einstein limiting case when dealing with dilute suspensions of rigid spheres.

This was the first step before assessing the Lee and Park model for large deformation flows. In the second part, non linear viscoelastic properties of immiscible polymer blends have been investigated via transient shear flow tests. These experiments reflect the structural

changes of the blends during flow. Characteristic overshoots have been observed at the onset of steady shear rate when the dispersed phase was deformable. The transient rheological data have been fitted by the Lee and Park model, its modified version (established in the first part of this work), and by a modified version of the Grmela and Ait-Kadi model (1994). These models have been used to predict the morphological evolution of the blends under moderately large deformation flows. The very large morphological changes induced by the flow have been predicted either qualitatively or quantitatively by the modified versions of the Lee and Park and the Grmela and Ait-Kadi models. For a polypropylene (PP)/ ethylene vinylacetate (EVA)-ethylene methacrylate (EMA) blend, coalescence as well as breakup have been observed in a relative small range of shear rates. Linear viscoelastic measurements and the Palierne emulsion model have also been used to characterize the morphological changes of the blend during simple shear flow. Finally, for transient shear flow experiments with undeformable dispersed phase, the predictions of the different models have been found unsatisfactory.

In the third part of this thesis, the morphological evolution of immiscible polymer blends induced by both shear and extensional flows is studied. The predictions of the different models appear to be less satisfactory with a polystyrene (PS)/polyethylene (PE) blend than with the PP/EVA-EMA blend investigated previously. It is shown that the model predictions are very sensitive to the choice of the mixing rule used to describe the bulk properties of the blend. Limitations of the different relations are underlined. For dominant elongational flows, the study is conducted with two blends of PP/EVA-EMA in order to evaluate the influence of the viscosity ratio. The extensional viscosity data that are needed to solve the interface governing equations included in the Lee and Park model have been obtained from pressure drop measurements through an hyperbolic die. The results are, however, only qualitative. The transition from a spherical to a fibrillar morphology, irrespectively of the zero shear viscosity ratio, shows that large morphological changes can be obtained in elongational flow.

## TABLE DES MATIERES

RESUME .....	vi
ABSTRACT .....	ix
LISTE DES TABLEAUX .....	xiv
LISTE DES FIGURES .....	xv
LISTE DES SYMBOLES .....	xviii
CHAPITRE 1 - INTRODUCTION ET OBJECTIFS .....	1
1.1) Objectifs .....	2
CHAPITRE 2 - REVUE BIBLIOGRAPHIQUE .....	4
2.1) Introduction .....	4
2.2) Rhéologie des systèmes multiphasés .....	5
2.2.1) Introduction .....	5
2.2.2) Modèles théoriques .....	6
2.2.3) Rhéologie et développement de morphologie .....	12
2.2.4) Conclusion .....	14
CHAPITRE 3 - PRESENTATION DES ARTICLES .....	15
CHAPITRE 4 - Linear viscoelastic behavior of molten polymer blends: A comparative study of the Palierne and Lee and Park models .....	17
4.1) Abstract .....	18
4.2) Introduction .....	19

4.3) Theoretical Background .....	20
4.4) Experimental .....	27
4.5) Results and discussions .....	30
4.6) Conclusions .....	52
4.7) References .....	53

## **CHAPITRE 5 - Relationships between rheology and morphology for immiscible molten blends of polypropylene and ethylene copolymers under shear flow .....**

5.1) Synopsis .....	57
5.2) Introduction .....	58
5.3) Rheological models .....	61
5.3.1) Lee and Park model (1994) .....	61
5.3.2) Grmela and Ait-Kadi model (1994) .....	64
5.4) Experimental .....	67
5.4.1) Blending procedure .....	68
5.4.2) Rheological measurements .....	68
5.4.3) Scanning electron microscope .....	69
5.5) Results and discussion .....	70
5.5.1) Linear viscoelasticity .....	70
5.5.2) Non linear viscoelasticity .....	72
5.5.3) Stress growth results .....	75
5.5.4) Predictions of the morphological changes .....	80
5.6) Conclusions .....	90
5.7) References .....	92

## **CHAPITRE 6 - Morphological evolution of immiscible polymer blends in simple shear and elongational flows .....**

6.1) Abstract .....	96
6.2) Introduction .....	97

6.3) Relationships between rheology and morphology .....	97
6.4) Experimental .....	102
6.4.1) Materials .....	102
6.4.2) Technique .....	103
6.4.3) Cogswell analysis. ....	106
6.4.4) Binding's analysis .....	108
6.4.5) Mackay and Astarita's analysis .....	111
6.5) Results and discussion .....	112
6.5.1) Morphology and simple shear flow properties .....	112
6.5.2) Morphology and elongational flow .....	123
6.6) Concluding remarks .....	135
6.7) References .....	137
 CHAPITRE 7 - CONCLUSIONS ET PERSPECTIVES .....	 141
 CHAPITRE 8- Références .....	 144

## LISTE DES TABLEAUX

Table 4.1 : Morphological data, interfacial tension and parameters used for predicting the rheological behavior. ....	32
Table 4.2 : Comparison of different interface relaxation times .....	49
Table 5.1 : Parameters used for predicting the transient rheological behavior of the blend with the LPL and LGC models; comparison between predicted radii values and experimentally 70/30 PP/(EVA-EMA) determined values .....	79
Table 6.1: Parameters used for predicting the transient rheological behavior of the 80/20 PS/PE blend with the different models; comparison between predicted radii values and SEM determined values. ....	114
Table 6.2 : Parameters used for predicting the transient rheological behavior of the 80/20 PS/PE blend and the 70/30 PP/EVA-EMA blend with the LGC non affine model. ....	118
Table 6.3 : Power-law parameters in shear of the different systems. ....	123
Table 6.4 : Power-law parameters in elongation from the Binding and Mackay/Astarita analysis. ....	126
Table 6.5 : Morphology obtained after extrusion through both hyperbolic shaped dies. ....	133

## LISTE DES FIGURES

Figure 4.1 : Comparison between experimental data and model predictions for the 80/20 PS/PE blend; $T=200^{\circ}\text{C}$ . . . . .	31
Figure 4.2 : Influence of the parameter $d_i$ on the predictions of the Lee and Park model for the 80/20 PS/PE blend; $T=200^{\circ}\text{C}$ . . . . .	35
Figure 4.3 : Comparison between experimental data and model predictions for the 80/20 PETG/EVA blend; $T=210^{\circ}\text{C}$ . . . . .	36
Figure 4.4 : Comparison between experimental data and model predictions for two PP/EVA blends: a) 70/30 PP/EVA, b) 65/35 PP/EVA; $T=200^{\circ}\text{C}$ . . . . .	38
Figure 4.5 : Comparison between experimental data and the Palierne emulsion model predictions for the 65/35 PP/EVA blend; influence of the interfacial tension value on the model predictions; $T=200^{\circ}\text{C}$ . . . . .	39
Figure 4.6 : Comparison between the Lee-Park and modified Lee-Park model predictions for two PP/EVA blends : a) 70/30 PP/EVA, b) 65/35 PP/EVA; $T=200^{\circ}\text{C}$ . . . . .	43
Figure 4.7 : Weighted relaxation spectra for the PS, PE and the 80/20 PS/PE blend; $T=200^{\circ}\text{C}$ . . . . .	46
Figure 4.8 : Weighted relaxation spectra for the PP and the PP/EVA blends for various compositions of EVA; $T=200^{\circ}\text{C}$ . . . . .	47
Figure 4.9 : Comparison between experimental data and the Lee and Park model predictions for two PS/PE blends : a) PS/PE 90/10, b) PS/PE 80/20; — best fits; ..... using $d_i$ calculated from Eq (4.24). . . . .	51
Figure 5.1 : Linear viscoelastic properties of the PP, EVA-EMA and 70/30 PP/(EVA-EMA) blend at $T=200^{\circ}\text{C}$ : (a) Complex viscosities and dynamic moduli of the PP and EVA-EMA components. (b) Comparison between linear data and model predictions for the 70/30 PP/(EVA-EMA) blend. . . . .	71
Figure 5.2 : Transient viscosity in creep as a function of time for a 70/30 PP/(EVA-EMA) blend; $T=200^{\circ}\text{C}$ . . . . .	74

- Figure 5.3 : Comparison between stress growth viscosity data and models predictions for the 70/30 PP/(EVA- EMA) blend at  $T=200^{\circ}\text{C}$  : (a)  $\dot{\gamma} = 0.0126 \text{ s}^{-1}$ , (b)  $\dot{\gamma} = 0.0317 \text{ s}^{-1}$ , (c)  $\dot{\gamma} = 0.126 \text{ s}^{-1}$ , (d)  $\dot{\gamma} = 0.318 \text{ s}^{-1}$  ..... 76
- Figure 5.4 : Evolution with time of the normalized interfacial area predicted for the LGC model for the 70/30 PP/(EVA-EMA) blend in stress growth and relaxation experiment at  $T=200^{\circ}\text{C}$ : (a) imposed shear rate of  $\dot{\gamma} = 0.0126 \text{ s}^{-1}$ ; (b) imposed shear rate of  $\dot{\gamma} = 0.318 \text{ s}^{-1}$  ..... 81
- Figure 5.5 : Comparison between linear data after relaxation and Palierne model predictions for the 70/30 PP/(EVA-EMA)blend at  $T=200^{\circ}\text{C}$  using the radius values determined following relaxation after stress growth experiment at : (a)  $\dot{\gamma} = 0.0126 \text{ s}^{-1}$ , (b)  $\dot{\gamma} = 0.0317 \text{ s}^{-1}$ , (c)  $\dot{\gamma} = 0.126 \text{ s}^{-1}$ , (d)  $\dot{\gamma} = 0.318 \text{ s}^{-1}$  . ..... 83
- Figure 5.6 : (a) Predicted evolution with time of the anisotropy tensor component  $q_{12}$  for an imposed shear rate of  $\dot{\gamma} = 0.0126 \text{ s}^{-1}$ ; (b) scanning electron micrograph of the 70/30 PP/(EVA-EMA) blend sample after relaxation. .... 85
- Figure 5.7 : (a) Predicted evolution with time of the anisotropy tensor component  $q_{12}$  for an imposed shear rate of  $\dot{\gamma} = 0.126 \text{ s}^{-1}$ ; (b) scanning electron micrograph of the 70/30 PP/(EVA-EMA) blend sample after relaxation. .... 86
- Figure 5.8 : Transient viscosity in creep as a function of time for the 30/70 PP/(EVA-EMA) blend;  $T=200^{\circ}\text{C}$ . .... 88
- Figure 5.9 : Stress growth viscosity at two different shear rates for the 30/70 PP/(EVA-EMA) blend;  $T=200^{\circ}\text{C}$ . .... 89
- Figure 6.1 : extrusion setup ..... 105
- Figure 6.2 : Comparison between stress growth viscosity data and models predictions for a 80/20 PS/PE blend at  $T = 200^{\circ}\text{C}$  : (a)  $\dot{\gamma} = 0.0507 \text{ s}^{-1}$ , (b)  $\dot{\gamma} = 0.101 \text{ s}^{-1}$ , (c)  $\dot{\gamma} = 0.32 \text{ s}^{-1}$  ..... 115
- Figure 6.3 : Comparison between stress growth viscosity data and models predictions for a 70/30 PP/EVA-EMA blend at  $T = 200^{\circ}\text{C}$  : (a)  $\dot{\gamma} = 0.0126 \text{ s}^{-1}$ , (b)  $\dot{\gamma} = 0.126 \text{ s}^{-1}$  120
- Figure 6.4 : (a) Evolution with time of the normalized interfacial area predicted for the LGC



model for the 70/30 PP/EVA-EMA blend in stress growth and relaxation experiment at $T = 200^{\circ}\text{C}$ with an imposed shear rate of $\dot{\gamma} = 0.126 \text{ s}^{-1}$ ; (b) Evolution of the conformation tensor $\mathbf{C}'$ during stress growth and relaxation. ....	122
Figure 6.5 : Complex and steady shear viscosities of the PP and the EVA-EMA at $T = 200^{\circ}\text{C}$ . ....	124
Figure 6.6 : Elongational viscosity of : (a) PP, (b) EVA-EMA, (c) 70/30 PP/EVA-EMA, (d) 30/70 PP/EVA-EMA. ....	127
Figure 6.7 : Trouton ratio for the PP, EVA-EMA and the 70/30 PP/EVA-EMA, 30/70 PP/EVA-EMA.blends ....	130
Figure 6.8 : Micrographs of the blends before the converging section : (a) 70/30 PP/EVA-EMA, (b) 30/70 PP/EVA-EMA. ....	131
Figure 6.9 : Micrographs of the blends after the converging section with the die D2 at the lowest flow rate : (a) 70/30 PP/EVA-EMA, (b) 30/70 PP/EVA-EMA. ....	132

## LISTE DES SYMBOLES

- $\alpha$  : tension interfaciale  
 $\beta$  : inverse du rapport de contraction dans le convergent  
 $\delta$  : delta Kronecker  
 $\Delta P_s$  : perte de pression due au cisaillement  
 $\Delta P_e$  : perte de pression due à l'élongation  
 $\dot{\epsilon}$  : taux de déformation élongationnelle uniaxiale  
 $\eta_M$  : viscosité de la matrice en cisaillement simple  
 $\eta_I$  : viscosité de l'inclusion en cisaillement simple  
 $\eta_e$  : viscosité élongationnelle apparente  
 $\dot{\gamma}_{ij}$  : composante du tenseur taux de déformation  
 $\dot{\gamma}_a$  : taux de cisaillement apparent  
 $\kappa_{ij}$  : composante du tenseur gradient de vitesse  
 $\Phi$  : potentiel thermodynamique  
 $\phi$  : fraction volumique d'inclusion  
 $\Psi$  : potentiel dissipatif  
 $\sigma_{ij}$  : composante du tenseur des contraintes  
 $\xi$  : paramètre de glissement
- C** : tenseur de conformation  
 $d_1, d_2, d_3$  : paramètre du modèle de Lee et Park  
 $G_B^*$  : module complexe du mélange  
 $G_I^*$  : module complexe de l'inclusion  
 $G_M^*$  : module complexe de la matrice  
**k** : rapport de viscosité  
**K** : indice de loi de puissance de la viscosité en cisaillement  
 $l_d$  : longueur de la filière  
**L** : indice de loi de puissance de la viscosité en élongation

$n$  : paramètre de loi de puissance de la viscosité en cisaillement

$\mathbf{q}$  : tenseur d'orientation d'interface

$Q$  : aire interfaciale par unité de volume

$Q_f$  : débit volumique

$R_1$  : rayon d'entrée du convergent

$R_0$  : rayon de sortie du convergent

$R_{(z)}$  : profil du convergent suivant  $z$

$R_v$  : rayon en volume des inclusions

$t$  : indice de loi de puissance de la viscosité en élongation

$\dot{W}_s$  : puissance dissipée en cisaillement par unité de volume

$\dot{W}_e$  : puissance dissipée en élongation par unité de volume

$W$  : puissance dissipée

## CHAPITRE 1 - INTRODUCTION ET OBJECTIFS

Les mélanges de polymères représentent une alternative moins coûteuse à la synthèse de nouveaux matériaux. Ils offrent de plus une grande flexibilité pour répondre aux exigences du marché. Ces mélanges sont constitués de différents homopolymères et/ou copolymères qui, dans la grande majorité des cas, sont thermodynamiquement immiscibles. Leur développement industriel reste conditionné par les propriétés finales obtenues. L'action de mélange peut se traduire par une diminution ou par une synergie des propriétés de chacun des polymères. Ces caractéristiques physiques obtenues à l'issue du mélange sont étroitement reliées à l'état de dispersion de chacune des phases. Un renforcement des propriétés chocs ou une amélioration des propriétés barrières résultent de la combinaison de différents polymères mais aussi de la formation de morphologie bien spécifiques. Du fait de la complexité et de la multiplicité des paramètres qui interviennent dans les mécanismes de développement des morphologies en cours de mélange à l'état fondu, le sujet de recherche demeure extrêmement vaste et ouvert.

Les nombreuses études relatives à l'établissement des morphologies dans les systèmes multiphasés montrent que les propriétés rhéologiques des composantes constituent des paramètres de toute première importance. Un certain nombre de ces travaux visent à contrôler et à stabiliser la morphologie parfois évolutive de ces mélanges (phénomènes de coalescence) par l'addition de copolymère ou par voie chimique. En effet, les diverses étapes de transformation sont susceptibles d'affecter la microstructure des matériaux. Afin d'optimiser les procédés de fabrication (extrusion, injection), il est essentiel dans un cadre de modélisation, de pouvoir développer des équations constitutives spécifiques aux mélanges. Cependant, le comportement rhéologique des mélanges s'avère très rapidement complexe, dépendant de multiples facteurs comme la composition, les propriétés des composantes, la morphologie, les interactions entre les phases...

Les morphologies des mélanges de polymères immiscibles peuvent se subdiviser en deux grandes catégories. Soit des morphologies nodulaires, où une des phases (inclusions) est parfaitement dispersée dans l'autre (matrice), soit des morphologies co-continues. Ces dernières sont généralement obtenues pour des mélanges de composition intermédiaire (de l'ordre de 30% à 70% des composants) et dans ces gammes de concentrations des phénomènes d'inversion de phase peuvent se produire.

### **1.1) Objectifs**

L'établissement d'une morphologie lors d'une étape de transformation est un processus dynamique. Divers phénomènes compétitifs interviennent et un très grand nombre d'interrogations subsistent quant aux relations existantes entre les mécanismes de dispersion et le comportement intrinsèque des phases dans l'outillage utilisé. Une grande partie des recherches se concentrent sur l'étude de systèmes modèles newtoniens, généralement dilués et dans des écoulements parfaitement contrôlés. Même si ces travaux sont indispensables pour une meilleure compréhension des phénomènes, ils paraissent relativement éloignés des conditions industrielles.

La production de mélanges de polymères s'effectue principalement à l'aide d'extrudeuse bi-vis. Dans ce type d'appareil les écoulements sont très complexes. L'objectif du travail consiste donc à cerner les facteurs qui vont influencer et participer à l'établissement de la morphologie de mélanges de fluides viscoélastiques. Pour ce faire, une démarche systématique sera adoptée et les principaux écoulements rencontrés dans les machines de transformation seront découplés. L'approche retenue repose principalement sur l'analyse du comportement rhéologique des mélanges en regard de leur morphologie. Cette étape indispensable dans l'optimisation d'une stratégie de fabrication implique l'utilisation ou le développement de modèles rhéologiques spécifiques aux mélanges. En effet, ces relations associent des grandeurs macroscopiques, mesurées expérimentalement, et des paramètres microscopiques reliés à la structure du matériau. La modélisation du

comportement rhéologique des mélanges peut ainsi contribuer à établir des corrélations entre la rhéologie et la morphologie qui gouverne les propriétés du produit fini.

## CHAPITRE 2 - REVUE BIBLIOGRAPHIQUE

### 2.1) Introduction

Les propriétés rhéologiques des mélanges de polymères immiscibles sont très complexes et se trouvent affectées par la composition, le type de morphologie, le degré d'interaction entre les phases, le processus de mélange... Depuis des années, les systèmes multiphasés ou plus simplement biphasiques font l'objet d'intenses recherches dans le domaine de la rhéologie. La littérature est très abondante sur ce sujet et cette revue ne se veut pas une énumération exhaustive des multiples études et modèles qui existent. En revanche, afin de situer le cadre dans lequel s'inscrivent les modèles rhéologiques utilisés pour l'analyse des résultats expérimentaux, un bref historique du développement des relations caractérisant les systèmes biphasiques sera présenté. Les conditions de validité et les limites de ces différents modèles seront alors soulignées. Enfin, les modèles utilisés dans le cadre du présent travail seront analysés dans les différents articles constituant le coeur de ce mémoire.

Le but ultime du développement d'équations constitutives spécifiques aux suspensions ou aux émulsions est d'être capable de prédire les propriétés rhéologiques du système hétérogène connaissant les propriétés des inclusions et du médium suspendant. Mesurer et prédire le comportement rhéologique de systèmes multiphasés se révèle d'intérêt pratique pour contrôler et optimiser les conditions de mise en oeuvre. Comme l'état de dispersion est influencé par les propriétés rhéologiques et réciproquement, il est essentiel de pouvoir caractériser et corréler ces propriétés. Ces modèles associent donc des grandeurs macroscopiques et microscopiques, constituant ainsi un lien entre la rhéologie et la morphologie. Qu'elles soient prédictives ou descriptives, ces relations sont utilisées dans le but de mieux cerner les facteurs agissant sur l'interface et susceptibles de gouverner le développement de la morphologie.

## **2.2) Rhéologie des systèmes multiphasés**

### **2.2.1) Introduction**

Pour de fortes déformations, comme celles rencontrées dans des écoulement élongationnels, en rhéométrie capillaire, etc..., la morphologie du mélange évolue durant la mesure et les propriétés rhéologiques ne sont plus caractéristiques d'une morphologie initiale. Cette évolution de morphologie affecte aussi la rhéologie du mélange. Cependant, ces propriétés décrivent le système à un instant donné dans un écoulement particulier. Ces expériences peuvent donc s'avérer très utiles pour détecter et analyser des changements de structures induits par l'écoulement. De plus, ces types d'écoulement correspondent beaucoup plus aux écoulements rencontrés dans les machines de transformation industrielles. En revanche, dans le domaine de la viscoélasticité linéaire, pour de très faibles déformations, la structure du système polyphasé n'évolue pas avec le cisaillement. Ces mesures peuvent alors fournir des informations intéressantes pour corréler la morphologie aux propriétés viscoélastiques des mélanges. Selon la composition et la rhéologie de chacune des phases, les morphologies des systèmes biphasiques immiscibles se subdivisent en trois catégories :

- des morphologies nodulaires ou fibrillaires,
- des morphologies lamellaires,
- des morphologies co-continues, lorsque les deux phases sont à la fois continues et interpénétrées.

La procédure expérimentale permettant de quantifier une morphologie nodulaire est plus aisée et beaucoup plus répandue que la caractérisation quantitative d'une interface dans un système co-continu. Les modèles rhéologiques associés aux morphologies de type émulsion sont fréquemment rencontrés dans la littérature. En revanche, l'essentiel des études se restreignent souvent au domaine des faibles déformations. Pour des morphologies et des interfaces plus compliquées à caractériser, ce qui se trouve être notamment le cas avec des mélanges présentant des morphologies co-continues ou dans des écoulements complexes, les quelques théories sont très récentes et le sujet est en exploration. Les travaux concernant la



rhéologie des mélanges de polymères dans des domaines de fortes déformations sont peu nombreux et seront abordés dans les chapitres suivants. Les diverses approches menant à l'obtention des modèles utiles à cette étude seront donc mises en évidence.

### 2.2.2) Modèles théoriques

Les modèles développés pour l'étude des systèmes multiphasés peuvent se subdiviser en deux grandes catégories : soit des modèles de type émulsion, soit de type suspension. Dans les paragraphes qui suivent les deux types de modèles seront abordés afin d'introduire les fondements des équations constitutives découvertes ces dernières années. Cet historique permettra de souligner les limitations majeures de ces relations et de mettre en relief le travail qu'il reste à accomplir en matière de modélisation.

L'étude de la rhéologie des systèmes biphasiques débute avec les travaux d'Einstein (1906,1911). Einstein a montré que l'addition de sphères indéformables dans un liquide newtonien de viscosité  $\eta_0$  augmentait sa viscosité et, que pour une suspension infiniment diluée, celle-ci était définie par :

$$\eta = \eta_0 \left( 1 + \frac{5}{2} \phi \right) \quad (2.1)$$

où  $\phi$  est la fraction volumique des particules.

Taylor (1932,1934) a étendu les travaux d'Einstein et a développé une expression théorique pour exprimer la viscosité effective de deux fluides newtoniens. Il a développé une expression pour la viscosité de l'émulsion tenant compte de la fraction volumique des inclusions mais aussi de la viscosité des phases :

$$\eta = \eta_M \left( 1 + \frac{5k+2}{2k+2} \phi \right) \quad (2.2)$$

où  $\eta_M$  est la viscosité de la matrice,  $k = \eta_1 / \eta_M$  représente le rapport de viscosité entre la phase dispersée et la matrice, et  $\phi$  la concentration en inclusions dans cette émulsion. Comme dans le cas développé par Einstein, la solution est supposée diluée de façon à négliger les interactions particule-particule. Quand  $k \rightarrow \infty$ , c'est-à-dire pour des suspensions de particules solides, on retrouve l'expression développée par Einstein (Eq. 2.1). Cette expression obtenue par Taylor reste valable tant que la tension de surface est suffisamment grande pour conserver la particule dispersée sous forme sphérique et que les déformations sont faibles.

Une des étapes du développement de la rhéologie des systèmes multiphasés est issue des travaux de Fröhlich et Sack (1946). Ces auteurs ont développé une équation pour prédire le comportement d'une suspension dans un écoulement dépendant du temps et ont montré qu'une émulsion diluée de sphères élastiques suspendues dans un liquide newtonien présentait un comportement viscoélastique. Fröhlich et Sack ont obtenu l'équation suivante pour décrire le comportement rhéologique de ces émulsions :

$$\left(1 + \lambda_1 \frac{d}{dt}\right) \underline{\underline{\sigma}} = \eta \left(1 + \lambda_2 \frac{d}{dt}\right) \underline{\underline{\dot{\gamma}}} \quad (2.3)$$

$$\text{avec } \eta = \eta_0 \left(1 + \frac{5}{2} \phi\right) \quad (2.4)$$

$$\lambda_1 = \left(\frac{3\eta_0}{2G}\right) \left(1 + \frac{5}{3} \phi\right) \quad (2.5)$$

$$\lambda_2 = \left(\frac{3\eta_0}{2G}\right) \left(1 - \frac{5}{2} \phi\right) \quad (2.6)$$

$\underline{\underline{\sigma}}$  est le tenseur des contraintes,  $\underline{\underline{\dot{\gamma}}}$  le tenseur vitesse de déformation et  $G$  est le module des

particules sphériques obéissant à la loi de Hooke. A noter que l'équation (2.3) constitue la première approche viscoélastique des émulsions. Cependant, dans ce modèle n'intervient pas la tension interfaciale. Le comportement viscoélastique de l'émulsion provient du caractère élastique des sphères qui après déformation retournent vers une forme d'équilibre sphérique.

Oldroyd (1953) a développé une expression similaire à celle de Fröhlich et Sack pour décrire le comportement rhéologique d'une émulsion constituée de deux liquides newtoniens incompressibles. Cependant, dans l'expression d'Oldroyd interviennent les dérivées de Jaumann permettant à l'équation de répondre aux propriétés d'invariance. L'équation décrivant les propriétés de l'émulsion comporte trois paramètres : un temps de relaxation  $\lambda_1$ , un temps de retard  $\lambda_2$  et une viscosité limite  $\eta$  qui peuvent être représentés par :

$$\eta = \eta_0 \left[ 1 + \left( \frac{5k+2}{2k+2} \right) \phi + \frac{(5k+2)^2}{10(k+1)^2} \phi^2 \right] \quad (2.7)$$

$$\lambda_1 = \frac{(19k+16)(2k+3)}{40(k+1)} \left( \frac{\eta_0 R}{\alpha} \right) \left[ 1 + \frac{19k+16}{5(k+1)(2k+3)} \phi \right] \quad (2.8)$$

$$\lambda_2 = \frac{(19k+16)(2k+3)}{40(k+1)} \left( \frac{\eta_0 R}{\alpha} \right) \left[ 1 - \frac{3(19k+16)}{10(k+1)(2k+3)} \phi \right] \quad (2.9)$$

$k = \eta_i / \eta_M$  représente le rapport de viscosité entre la phase dispersée et la matrice,  $\alpha$  la tension interfaciale et  $\phi$  la fraction volumique des inclusions. En 1955, Oldroyd améliore son modèle en tenant compte de la variation de la tension interfaciale en fonction de la déformation de la particule. Dans ce cas de figure, les propriétés rhéologiques se trouvent décrites par deux temps de relaxation, deux temps de retard et une viscosité limite. Oldroyd montre aussi que l'effet de l'ajout d'un compatibilisant ayant un comportement visqueux, associé à la présence d'un film à l'interface et d'un glissement à l'interface, ne modifie pas la loi de comportement. Seules les valeurs des constantes rhéologiques  $\eta$ ,  $\lambda_1$  et  $\lambda_2$  se

trouvent modifiées. Quand le film à l'interface présente un caractère élastique, il faut tenir compte des dérivées d'ordre supérieure par rapport à la contrainte et au gradient de vitesse de déformation. Pour de faibles déformations (Oldroyd, 1953), l'émulsion est décrite par :

$$\underline{\sigma} = \eta^* \underline{\dot{\gamma}} \quad (2.10)$$

La viscosité complexe de l'émulsion s'exprime alors par :

$$\eta^* = \eta_0 \frac{1 + \lambda_2 \Delta + \nu_2 \Delta^2 + \dots}{1 + \lambda_1 \Delta + \nu_1 \Delta^2 + \dots} \quad (2.11)$$

Le numérateur de l'équation (2.11) s'applique au tenseur de déformation tandis que le dénominateur est appliqué au tenseur des contraintes (cf. Eq. 2.10). Les constantes  $\eta_0$ ,  $\lambda_1$ ,  $\lambda_2$ ,  $\nu_1$  et  $\nu_2$  peuvent être déterminées en fonction des propriétés de l'émulsion et  $\Delta = d/dt$ . Avec les hypothèses d'une interface infiniment mince et d'une tension interfaciale  $\alpha$  constante,

$$\frac{\eta^*}{\eta_M} = \frac{40(\eta_M + \eta_I)\alpha + R(3\eta_M + 2\eta_I)(16\eta_M + 19\eta_I)\Delta + 3\phi[4(2\eta_M + 5\eta_I)\alpha - R(\eta_M - \eta_I)(16\eta_M + 19\eta_I)\Delta]}{40(\eta_M + \eta_I)\alpha + R(3\eta_M + 2\eta_I)(16\eta_M + 19\eta_I)\Delta - 2\phi[4(2\eta_M + 5\eta_I)\alpha - R(\eta_M - \eta_I)(16\eta_M + 19\eta_I)\Delta]} \quad (2.12)$$

Pour un cisaillement oscillatoire à faible amplitude, l'opérateur  $\Delta$  est équivalent à une multiplication de l'expression par  $i\omega$ . L'équation (2.12) peut s'exprimer par :

$$\eta^* = \eta_M^* \left( \frac{1 + 3\phi H}{1 - 2\phi H} \right) \quad (2.13)$$

$$\text{avec } H = \frac{4\alpha/R(2+5k) + i\omega\eta_M(k-1)(16+19k)}{40\alpha/R(1+k) + i\omega\eta_M(3+2k)(16+19k)} \quad (2.14)$$

L'équation (2.13) est valable tant que l'on se situe dans le domaine des faibles déformations.

Plusieurs cas limites se présentent. Quand  $H=1/2$ , c'est-à-dire pour une suspension de particules rigides dans un liquide newtonien, on retrouve l'expression (2.1) développée par Einstein. Quand  $\omega \rightarrow 0$ , l'équation (2.14) se simplifie et

$$\eta^* = \eta_M \left( \frac{1+3\phi H}{1-2\phi H} \right) \quad (2.15)$$

$$\text{avec } H = \frac{1+5/2k}{5(1+k)} \quad (2.16)$$

Un développement limité à l'ordre 2 par rapport à  $\phi$ , la fraction volumique en inclusion, permet alors d'accéder aux paramètres de l'émulsion décrits par les équations (2.7, 2.8, 2.9).

Dans l'analyse de Fröhlich et Sack, comme dans celle d'Oldroyd, à la fois les effets d'inertie et les interactions hydrodynamiques sont négligés. Il existe tout de même une différence entre les deux approches. Les propriétés viscoélastiques de l'émulsion résultent, dans le modèle développé par Fröhlich et Sack, du caractère hookien des sphères introduites. Dans le cas du modèle d'Oldroyd, le caractère élastique de l'émulsion provient de la tension interfaciale entre les deux fluides newtoniens, tension interfaciale qui fournit les forces à la particule déformée pour retrouver sa position d'équilibre sphérique. Ceci implique que le modèle est restreint à de faibles déformations. Il faut noter que le modèle d'Oldroyd prédit que la viscosité de l'émulsion dépend uniquement de la fraction volumique des particules et des viscosités des deux composantes. Le temps de relaxation et le temps de retard varient directement avec le rayon de la goutte et inversement proportionnel avec la tension interfaciale. Ceci signifie que les relaxations aux basses fréquences sont dues à la déformation des particules et au retour de celles-ci vers leur position d'équilibre sphérique qui tend à minimiser l'aire interfaciale.

En 1967, Goddard et Miller ont développé une équation d'état pour déterminer les effets de la déformation induite par cisaillement sur le comportement global d'une

suspension diluée de particules de caractère hookien dans un fluide newtonien. Cependant, ces auteurs n'ont pas considéré les effets de la tension interfaciale. Tous ces modèles ont été développés pour des systèmes dilués, c'est-à-dire que le volume des sphères est petit comparé au volume de la substance les englobant. En se basant sur des modèles de cellules, Choi et Schowalter (1975) ont développé une équation d'état qui prend en considération les interactions hydrodynamiques et qui tient compte de l'effet de la déformation des particules. Sous sa forme simplifiée, cette équation est similaire à celle d'Oldroyd et s'exprime par :

$$(1 + \lambda_1 D/Dt) \underline{\underline{\sigma}} = \eta (1 + \lambda_2 D/Dt) \dot{\underline{\underline{\gamma}}} \quad (2.17)$$

avec  $D$  la dérivée de Jaumann,  $\eta$  une viscosité limite et  $\lambda_1, \lambda_2$ , deux temps caractéristiques:

$$\eta = \eta_0 \left[ 1 + \left( \frac{5k+2}{2k+2} \right) \phi + \frac{5(5k+2)^2}{8(k+1)^2} \phi^2 \right] \quad (2.18)$$

$$\lambda_1 = \frac{(19k+16)(2k+3)}{40(k+1)} \left( \frac{\eta_0 R}{\alpha} \right) \left[ 1 + \frac{5(19k+16)}{4(k+1)(2k+3)} \phi \right] \quad (2.19)$$

$$\lambda_2 = \frac{(19k+16)(2k+3)}{40(k+1)} \left( \frac{\eta_0 R}{\alpha} \right) \left[ 1 + \frac{3(19k+16)}{4(k+1)(2k+3)} \phi \right] \quad (2.20)$$

L'utilisation des modèles exposés précédemment est limitée par plusieurs facteurs. Dans la grande majorité des cas, les deux fluides considérés sont newtoniens et les modèles ne s'appliquent que pour des systèmes dilués soumis à des déformations de faible amplitude. Dans les modèles tels que ceux de Fröhlich et Sack ou Oldroyd, pour parvenir aux lois de comportement, les auteurs considèrent l'inclusion seule, entourée par une matrice jusqu'à une distance finie, le tout inclu dans un milieu possédant les propriétés de l'émulsion. Par analogie avec un formalisme électrique, Paliarne (1990, 1991) a développé un modèle pour prédire, dans le cadre d'un cisaillement oscillatoire de faibles amplitudes, le comportement d'une émulsion de deux fluides viscoélastiques incompressibles prenant en compte la

polydispersité, la tension interfaciale de même que les interactions hydrodynamiques. Aucune hypothèse n'est imposée sur la concentration de particules, mais, comme les interactions sont assimilées à celles du type dipôle-dipôle et que les effets s'annulent en moyenne, dès que les particules ne sont plus assez éloignées le modèle est déficient limitant ainsi son application à des concentrations modérées. Ce modèle a été utilisé dans cette étude et est présenté en détail dans le chapitre 4. Il a été mentionné en introduction qu'il était essentiel de pouvoir relier les propriétés rhéologiques des mélanges à leur état de dispersion. Avoir une meilleure compréhension des mécanismes de rupture de particules apparaît donc très important pour pouvoir optimiser les procédés de transformation. Néanmoins, aucune des relations introduites dans ce chapitre ne permet de remplir cette fonction.

### **2.2.3) Rhéologie et développement de morphologie**

Le but principal des travaux de recherche, aussi bien expérimentaux que théoriques, qui ont été effectués dans le domaine de la morphologie, est de comprendre comment un écoulement donné peut modifier des domaines et générer ainsi un nouvel état de dispersion. Différents mécanismes, tels que rupture, coalescence, retraction, instabilités capillaires, vont participer à l'élaboration d'une émulsion caractérisée par une rhéologie bien spécifique. Comprendre et prévoir ces changements d'états se révèlent d'un profond intérêt aussi bien pour le design d'appareils de mélange que pour un contrôle accru lors de la mise en forme. Le nombre de publications ayant trait au développement d'une morphologie étant exhaustif, quelques résultats généraux, qui constituent des bases, seront simplement présentés et permettront ainsi de souligner les questions auxquelles la recherche est encore confrontée aujourd'hui. Une synthèse importante des différents avancements dans ce domaine peut être obtenue dans les revues de Han (1981), Rallison (1984) ou Utracki et Shi (1992). Les études les plus récentes n'y sont évidemment pas abordées mais elles n'entrent pas dans le cadre du travail effectué ici.

Les premiers travaux de Taylor (1934) sur les systèmes newtoniens ont montré que

les mécanismes de rupture des particules étaient conditionnés par le rapport de viscosité entre les deux phases et par le nombre capillaire qui représente le rapport des forces visqueuses aux forces interfaciales. Lorsque ce nombre capillaire atteint une valeur proche de 0.5, la rupture de la goutte se produit. Taylor a aussi mis en évidence l'importance de l'écoulement. En effet, dans le cas d'un cisaillement simple, la rupture des particules est favorisée pour des rapports de viscosité compris entre 0.1 et 1 et une limite supérieure est atteinte pour un rapport d'environ 3.5. En revanche, la rupture des particules est plus facile dans un écoulement élongationnel et ce quelque soit le rapport de viscosité. La formation d'une morphologie demeure malgré tout un processus transitoire. En utilisant une technique de perturbations, Barthél-Biesel et Acrivos (1973) ont obtenu une solution en terme de paramètres de perturbation pour décrire la forme d'une goutte dans un écoulement en cisaillement dépendant du temps. Les équations sont cependant lourdes à manipuler. Lorsque les phases sont viscoélastiques, la littérature est assez pauvre en information quantitative. Néanmoins, les quelques études menées sur des systèmes où l'une des phases est viscoélastique font apparaître que l'élasticité stabilise la morphologie car le nombre capillaire critique est plus élevé (Elmendorp et Maalcke, 1985). L'influence de l'élasticité demeure à ce jour encore très mal comprise. La littérature s'accorde à dire que la taille finale des domaines résulte d'un équilibre entre les phénomènes de rupture et de coalescence. Pourtant ces sujets sont moins traités, pas nécessairement mieux compris, et restreints à de faibles concentrations (Elmendorp et Van der Vegt, 1986; Fortelný et Živný, 1995, Søndergaard et Lyngaae-Jørgensen, 1996).

Même si les problèmes et les mécanismes reliés à la dispersion de fluides newtoniens sont abondamment traités, beaucoup sont limités à l'étude de la déformation et de la rupture d'une goutte ou d'un fil dans un écoulement parfaitement contrôlé. Or, dans la pratique, les concentrations en phase dispersée s'avèrent généralement beaucoup trop élevées pour pouvoir considérer les domaines isolés les uns des autres. De plus, selon les caractéristiques rhéologiques des phases, l'écoulement favorise préférentiellement la rupture ou la coalescence des domaines. Ces contraintes, ainsi que la nécessité d'inclure une dynamique



dans l'établissement de la morphologie ont conduit Doi et Ohta (1991) à introduire de nouveaux concepts pour visualiser un système hétérogène dans un écoulement en tenant compte des effets combinés dus à la rupture et à la coalescence des domaines. Leur modèle a été étendu par Lee et Park (1994) et a fait l'objet d'intenses recherches ces dernières années. Parallèlement, Grmela et Ait-Kadi (1994) ont proposé une voie moins phénoménologique pour déterminer et adapter ces équations d'évolution. Cette nouvelle approche laisse entrevoir un potentiel intéressant de recherche dans le domaine de la rhéologie des mélanges de polymères immiscibles soumis à de fortes déformations. Ces équations constitutives ont donc été utilisées pour ce travail de doctorat et sont largement discutées dans les chapitres 4, 5 et 6.

#### **2.2.4) Conclusion**

Alors que les modèles de type émulsion ont déjà pu être confronté à l'expérience et validé, notamment celui de Palieme (1990,1991), que le modèle de Doi et Ohta (1991) a été testé dans de nombreuses situations au cours des toutes dernières années, les prédictions du modèle de Lee et Park n'ont pas été étudiées. Comme nous le verrons dans les chapitres ultérieurs, plusieurs questions subsistent quant au champ d'application de ce modèle. Il n'en demeure pas moins que cette approche est celle qui tente le plus de se rapprocher de la réalité et que même si la description des phénomènes était grossière, ceci constitue la seule relation qui serait capable de prévoir l'évolution d'une morphologie considérant à la fois les phénomènes de rupture, de coalescence et de modification de la morphologie dans un mélange par action de l'écoulement.

### CHAPITRE 3 - PRESENTATION DES ARTICLES

Il est mentionné dans la revue bibliographique, que le modèle de Lee et Park (1994), élaboré à partir de la théorie de Doi et Ohta (1991), constitue une équation d'état susceptible de décrire le comportement rhéologique des mélanges immiscibles dans un écoulement à fortes déformations, et ce, en incluant les évolutions de la morphologie. Les auteurs ont validé leur modèle sur un mélange polystyrène / polyéthylène (PS/PE) uniquement dans le domaine de la viscoélasticité linéaire. Ils n'ont cependant pas confronté les prédictions de leur relation avec d'autres modèles (tel que celui de Paliarne (1990)) et n'ont pas analysé le comportement de cette nouvelle équation constitutive dans le cas de fortes déformations. Etudier les prédictions d'un modèle dans le domaine de la viscoélasticité linéaire, zone dans laquelle la morphologie du mélange n'évolue pas, constitue la première étape dans la validation d'une équation d'état. Néanmoins, il importe de s'assurer que les résultats obtenus pour un mélange soient généralisables à d'autres systèmes. Par conséquent, le premier article (chapitre 4) est constitué d'une étude comparative dans le domaine des faibles déformations entre les modèles de Paliarne (1990) et de Lee et Park (1994). Différents mélanges de polymères immiscibles ont été étudiés et les limites de chacun des deux modèles analysés ont été soulignées. Finalement, une relation semi-empirique a été proposée afin d'obtenir une meilleure description des données rhéologiques et satisfaire certains cas limites. Ceci représente la première étape avant d'évaluer les possibilités dans le domaine des larges déformations de cette nouvelle équation d'état ainsi que du modèle de Lee et Park.

Le deuxième article (chapitre 5) est donc consacré à l'étude de différents modèles dans le domaine de la viscoélasticité non linéaire. Le modèle de Grmela et Ait-Kadi (1994) est modifié et étendu de façon à retrouver à partir de considérations thermodynamiques des équations initialement développées sur les bases d'une analyse dimensionnelle. Ces relations sont utilisées pour prédire les changements de morphologie se produisant au cours d'un cisaillement simple. L'étude effectuée sur un mélange polypropylène (PP) / éthylène vinyl acétate (EVA)-éthylène méthylacrylate (EMA) montre que de relativement faibles

déformations peuvent influencer grandement la morphologie du mélange non stabilisé au niveau de la rupture et de la coalescence des domaines. Certains des modèles étudiés sont aptes à prédire qualitativement, et dans certains cas quantitativement, ces changements de morphologie induits par cisaillement.

Afin d'évaluer si les équations constitutives utilisées dans le chapitre 5 peuvent être appliquées dans un cadre général, les relations entre les propriétés rhéologiques et la morphologie induite par cisaillement simple ont été étudiées sur un système PS/PE. Des déficiences entre les prédictions des diverses relations et l'expérience sont observées. Les limitations des modèles analysés sont alors présentées. Ceci constitue la première partie du troisième article (chapitre 6). La seconde partie de ce chapitre traite des relations entre les propriétés rhéologiques et la morphologie induite dans des écoulements préférentiellement élongationnels. Cette étude est menée pour deux types de mélange afin d'évaluer, dans un écoulement majoritairement élongationnel, l'influence du rapport de viscosité sur la morphologie du matériau. Les données de viscosité extensionnelle, nécessaires à l'utilisation des modèles, ont été déterminées à partir de la perte de pression dans une filière convergente hyperbolique. Les modèles étudiés décrivent alors uniquement de façon qualitative les changements de morphologie qui s'opèrent dans l'écoulement. D'un point de vue pratique, ces modifications de morphologie majeures mettent en relief l'importance du type d'écoulement considéré.

#### Remarques sur les articles déjà publiés :

Dans le chapitre 4, la définition proposée dans l'équation 4.29a est basée sur le fait que pour un régime sinusoïdal à faibles déformations,  $Q$  ne varie presque pas avec le temps. Dans le chapitre 5, le terme  $C_1$  a été choisi par Grmela et Ait-Kadi de part la définition de la tension interfaciale et non par analogie avec la théorie de Doi-Ohta. Enfin, si les particules se déforment dans un premier temps avant de coalescer et que cette étape est significative, une légère augmentation de  $Q/Q_0$  devrait être observée. Un changement du pas de temps pour l'intégration des équations pourrait alors permettre d'observer ce phénomène.

## **CHAPITRE 4**

### **Linear viscoelastic behavior of molten polymer blends: A comparative study of the Palierne and Lee and Park models**

**C. Lacroix, M. Aressy and P.J. Carreau\***

Centre de Recherche Appliquée sur les Polymères, CRASP,  
Department of Chemical Engineering, Ecole Polytechnique,  
P.O. Box 6079, Stn Centre-Ville, Montréal, QC, H3C 3A7, Canada

\* corresponding author

Cet article est publié dans *Rheologica Acta*, **36**, 416-428 (1997).

#### 4.1) Abstract

The linear viscoelastic properties of several molten blends with immiscible components of different viscosity ratio have been investigated. All the blends show a morphology of emulsion type. At low frequencies, the behaviors of these blends are essentially governed by the interface. The Palieme (1990) model is shown to predict well the linear behavior of all the blends. The Lee and Park model (1994), developed to take into account the relationships between the rheological behavior and morphological changes under large strain flows, is also shown to describe well the storage and loss moduli of the blends by adjusting a single fitting parameter. Based on the weighted relaxation spectra, a comparison of both model predictions is made focussing on the time associated to the interface. An approximate method is then proposed to evaluate the interface parameter introduced in the Lee and Park model. At high frequency, discrepancies are observed for the Lee and Park predictions when the viscoelastic properties of both components are considerably different. The description of the bulk properties of the blend, i.e, the mixing rule used by Lee and Park, is modified to get a better description of the high frequency data.

**Keywords :** blends, linear viscoelasticity, emulsion models.

## 4.2) Introduction

The development of new polymer blends of specific properties is intimately related to the nature of the phases and to the control of the morphology. The rheology of multi-phase systems is very complex mainly due to the flow history dependence of the morphology. Rheological models can be a powerful tool to relate microscopic and macroscopic quantities. Nevertheless considerable efforts need to be devoted to take into account the viscoelastic nature of the polymers under the different types of flow generally encountered in processing. In the case of small amplitude oscillatory flow, the Palierne Model (1990) has been shown to be very useful for predicting the rheological behavior of the immiscible blends (Brahimi et al., 1991; Graebbling et al., 1990, 1993; Bousmina and Muller, 1993; Carreau et al., 1994; Germain et al., 1994; Bousmina et al., 1995). Satisfactory predictions are obtained up to relatively high concentrations of the dispersed phase. Estimation of unknown interfacial tension (Graebbling et al., 1993, 1994; Lacroix et al., 1996), determination of particle size distribution (Friedrich et al., 1995), and analysis of the deformation of droplets under elongational flow (Delaby et al., 1994) have also been successfully carried out, using the Palierne model.

Recently, Lee and Park (1994) have developed a new model for multiphase systems based on the Doi and Ohta theory (1991). The model is not restricted to dilute or semi-dilute concentrations of the dispersed phase and accounts for coalescence and breakup phenomena. In principle, it is able to describe the rheological behavior of polymer blends for any type of flow, especially for small amplitude oscillatory flow, assuming that the Cox-Merz rule is valid for the blend components.

More recently, Guenther and Baird (1996) have applied the Doi-Ohta theory (1991) to a PET/PA blend, of which the components exhibited almost a Newtonian behavior. The theory could be used to qualitatively describe the effects of the interfacial tension on the steady shear viscosity and primary normal stress difference. Overshoots and undershoots

observed experimentally during transient experiments could not be described by the Doi-Ohta theory. The Doi and Ohta (1991) theory has also been used to relate the morphology of blends to steady state normal stress data (Vinckier et al., 1996). In this case, several blends of nearly inelastic polymers with various concentrations and viscosity ratios have been analyzed with the Doi and Ohta theory.

As far as we know, except for Lee and Park who have compared and validated their model predictions to experimental data of a PS/PE system over a wide range of composition, no attempt has been made to show that the Lee and Park model (or the Doi-Ohta model) can adequately describe the linear viscoelastic properties of immiscible blends. The aim of this paper is to compare the predictions of the Palierne and the Lee and Park models in the linear viscoelastic domain. This is the first step needed before assessing the Lee-Park model for large deformation flows. The experimental data of these different polymer blends, covering a wide range of viscoelastic properties are used for the assessment of the models. The limitations of the two models are underlined and in light of experimental results, a modification of the Lee and Park model is proposed.

### 4.3) Theoretical Background

Since both Palierne and Lee and Park models are based on two completely different approaches, the major assumptions are recalled and limitations of the results are also discussed.

#### Palierne model (1990, 1991)

By analogy with an electric formalism, Palierne derived an equation for predicting the complex modulus of molten (emulsion type) blends,  $G_b^*$ , as a function of the complex moduli of both phases,  $G_M^*$  (for the matrix) and  $G_I^*$  (for the inclusions or dispersed phase) taking into account several important features of a multiphase system. The viscoelasticity of

both phases, the hydrodynamics interactions, the droplets size and size distribution and the interfacial tension are indeed included in this formulation. Neglecting the effects of gravity and inertia,  $G_B^*$  can be expressed as function of volume fractions  $\phi_i$  of droplets of radius  $R_i$  by :

$$G_B^*(\omega) = \frac{1+3\sum_i \phi_i H_i^*(\omega)}{1-2\sum_i \phi_i H_i^*(\omega)} G_M^*(\omega) \quad (4.1)$$

with  $H_i^*$  given by :

$$H_i^*(\omega) = \frac{4\left(\frac{\alpha}{R_i}\right)\left[2G_M^*(\omega)+5G_I^*(\omega)\right]+\left[G_I^*(\omega)-G_M^*(\omega)\right]\left[16G_M^*(\omega)+19G_I^*(\omega)\right]}{40\left(\frac{\alpha}{R_i}\right)\left[G_M^*(\omega)+G_I^*(\omega)\right]+\left[2G_I^*(\omega)+3G_M^*(\omega)\right]\left[16G_M^*(\omega)+19G_I^*(\omega)\right]} \quad (4.2)$$

where  $\alpha$  is the interfacial tension between the two polymer blend components. Equation (4.1) is restricted to linear viscoelasticity, that is : the case of small amplitude oscillatory shear flow. Therefore morphological changes during the flow, such as breakup or coalescence cannot be predicted by the model. Theoretically, a general behavior of the interface was considered by Paliarne (1990) by introducing two parameters:  $\beta'(\omega)$  which expresses the dependence of the interfacial tension  $\alpha$  on local changes of the interfacial area,  $\beta''(\omega)$  which describes the effect of local shear. Since these parameters are virtually impossible to determine experimentally, they are usually set equal to zero (Bousmina and Muller, 1993), as it is the case for Eqs (4.1 and 4.2). Recently, Friedrich et al. (1996) have empirically made use of  $\beta'$  and  $\beta''$  to account for the effect of adding a copolymer as a compatibilizer.

The rheological properties of an emulsion are strongly dependent on the morphology.



The behavior of an emulsion may also be affected by steric interactions or anisotropic effects which occur often in concentrated systems. In such cases, failures have been reported (Bousmina and Muller, 1993; Carreau et al., 1994) limiting the use of the Palierne model to moderate concentrations. Nevertheless, the Palierne model very well describes emulsions of viscoelastic fluids up to relatively high concentrations under small amplitude oscillatory flow. For a polydispersity of the droplet size  $d/d_n$  (ratio of the volume and number average diameter respectively) less than 2, it has been shown that the model predictions can be calculated assuming monodispersed droplets and using the volume average diameter (Graebbling et al., 1993; Bousmina et al., 1995). For a monodisperse droplet size distribution and for Newtonian components the Oldroyd expression (1953,1955) is retrieved. Because the symmetry, the dipole-dipole interactions included in the Palierne approach do not contribute to the deviatoric stress tensor. Several others relations, such as the Einstein equation can be retrieved as special cases. Another particular case is obtained by setting  $\alpha = 0$ . The Palierne model then yields to the following expression :

$$G_B^* = \left( \frac{1+3/2H^*}{1-H^*} \right) G_M^* \quad (4.3)$$

with  $H^*$  given by

$$H^* = \sum_i \phi_i \frac{2(G_I^*(\omega) - G_M^*(\omega))}{2G_I^*(\omega) + 3G_M^*(\omega)} \quad (4.4)$$

This result justifies the generalization to viscoelastic components of Dickie's results (1973) obtained from the work of Kerner for a dispersion of Hookean inclusions dispersed in a Hookean matrix. Equation (4.3) reduces to Einstein's expression for rigid inclusions in a Newtonian matrix.

### Lee and Park model (1994)

The model proposed by Lee and Park is based on the theory developed by Doi and Ohta to predict the rheology of texture fluids. Lee and Park modified the Doi-Ohta theory (1991), originally developed for an equal mixture of two immiscible fluids with the same viscosity and density undergoing flows at low Reynolds number, to account for a mismatch in the viscosities of the polymers. They started from the general expression of the stress tensor for an emulsion given by Mellema and Willemse (1983) and references cited therein:

$$\sigma_{ij} = \eta_M \dot{\gamma}_{ij} + \lim_{V \rightarrow \infty} \frac{1}{V} (\eta_I - \eta_M) \int (u_i n_j - n_i u_j) dS + \lim_{V \rightarrow \infty} \frac{1}{V} \int \alpha \left( \frac{1}{3} \delta_{ij} - n_i n_j \right) dS - P \delta_{ij} \quad (4.5)$$

where  $\dot{\gamma}_{ij} = \kappa_{ij} + \kappa_{ji}$  are the components of the rate of deformation tensor and  $\kappa_{ij}$  are the components of the velocity gradient tensor. The integrals are over the entire area of the interface  $S$ ,  $\delta_{ij}$  is the Kronecker delta,  $\mathbf{n}$  the unit vector normal to the interface,  $\mathbf{u}$  the velocity vector,  $\eta_M$  and  $\eta_I$  are the viscosities of the matrix and the inclusion respectively. Lee and Park associated the third term on the right of Eq. (4.5) as the anisotropy tensor term in Doi-Ohta theory, and as Doi and Ohta, Lee and Park used the interface tensor  $\mathbf{q}$  defined by Onuki (1987):

$$q_{ij} = \lim_{V \rightarrow \infty} \frac{1}{V} \int \left( n_i n_j - \frac{1}{3} \delta_{ij} \right) dS \quad (4.6)$$

Thus Eq. (4.5) only differs from that of Doi-Ohta by its second right term (called the viscosity ratio term). Considering almost spherical particles ( $\alpha \rightarrow \infty$ ), a pure straining motion, and first order volume fractions, Schowalter et al. (1968) expressed this viscosity ratio term as a function of the volume fraction of inclusions  $\phi$ , and of matrix and inclusion viscosities by :

$$\lim_{V \rightarrow \infty} \frac{1}{V} (\eta_I - \eta_M) \int (u_i n_j - n_i u_j) dS = \frac{6}{10} \left( \frac{\eta_I - \eta_M}{\eta_I + \eta_M} \right) \eta_M \Phi \dot{\gamma}_{ij} \quad (4.7)$$

Replacing Eq. (4.6) and (4.7) in Eq. (4.5) leads for constant  $\alpha$  to :

$$\sigma_{ij} = \left( 1 + \frac{6(\eta_I - \eta_M)}{10(\eta_I + \eta_M)} \Phi \right) \eta_M \dot{\gamma}_{ij} - \alpha q_{ij} - P \delta_{ij} \quad (4.8)$$

The interface tensor is assumed to be determined by two factors: the flow which enlarges and orients the interface, and the interfacial tension which opposes the effects of the flow. These effects are accounted for separately :

$$\frac{dq_{ij}}{dt} = \left( \frac{dq_{ij}}{dt} \right)_{flow} + \left( \frac{dq_{ij}}{dt} \right)_{interfacial \ tension} \quad (4.9)$$

Lee and Park have considered the same flow terms as those derived by Doi-Ohta for a 50/50 mixture of two immiscible Newtonian fluids with the same viscosity and assuming affine deformation. The evolution equation for the tensor  $q$  for the flow contribution is then given by :

$$\left( \frac{dq_{ij}}{dt} \right)_{flow} = -q_{ik} \kappa_{kj} - q_{jk} \kappa_{ki} + \frac{2}{3} \delta_{ij} \kappa_{lm} q_{lm} - \frac{Q}{3} \dot{\gamma}_{ij} + \left( \frac{q_{lm} \kappa_{lm}}{Q} \right) q_{ij} \quad (4.10)$$

where the first three terms represent the lower convected derivative and  $Q$  is the area of the interface per unit volume. The variation of  $Q$  with time under the effects of the flow is given by :

$$\left( \frac{dQ}{dt} \right)_{flow} = -\kappa_{ij} q_{ij} \quad (4.11)$$

Lee and Park considered three different mechanisms of relaxation : coalescence, shape relaxation, and break up by interfacial tension (the relaxation mechanisms by interfacial tension proposed by Doi-Ohta did not account explicitly for the break-up phenomena ). The relaxation rates are assumed to be controlled by  $\alpha$ ,  $Q$ , and  $\eta_M(\dot{\gamma})$  only, and a dimensional analysis leads to the following kinetics equations for the relaxation of the interfacial area  $Q$ , and its anisotropy  $q_{ij}/Q$  :

$$\left( \frac{dQ}{dt} \right)_{interfacial\ tension} = -c_1 \frac{\alpha}{\eta_M} Q^2 - c_3 \frac{\alpha}{\eta_M} q_{ij} q_{ij} \quad (4.12)$$

$$\frac{d}{dt} \left( \frac{q_{ij}}{Q} \right)_{interfacial\ tension} = -c_2 \frac{\alpha Q}{\eta_M} \left( \frac{q_{ij}}{Q} \right) \quad (4.13)$$

where  $c_1$ ,  $c_2$ ,  $c_3$  are dimensionless parameters which may depend on the volume fraction of the inclusions  $\phi$ . Equations (4.12) and (4.13) can be rearranged to get :

$$\left( \frac{dq_{ij}}{dt} \right)_{interfacial\ tension} = -d_1 \frac{\alpha}{\eta_M} Q q_{ij} - d_1 d_3 \frac{\alpha}{\eta_M} \left( \frac{q_{lm} q_{lm}}{Q} \right) q_{ij} \quad (4.14)$$

$$\left( \frac{dQ}{dt} \right)_{interfacial\ tension} = -d_1 d_2 \frac{\alpha}{\eta_M} Q^2 - d_1 d_3 \frac{\alpha}{\eta_M} q_{ij} q_{ij} \quad (4.15)$$

where  $d_1 = c_1 + c_2$ ,  $d_2 = c_1 / (c_1 + c_2)$  and  $d_3 = c_2 / (c_1 + c_2)$ , respectively  $\lambda$ ,  $\mu$  and  $\nu$  in the Lee and Park paper, and denoted to as degrees of total relaxation, size relaxation, and break up and shape relaxation respectively. The time evolution of the interface tensor under the opposite effects of the flow and of the relaxation by interfacial tension is found by substituting Eqs. (4.10) and (4.14) in Eq. (4.9) :

$$\frac{dq_{ij}}{dt} = -q_{ik}\kappa_{kj} - q_{jk}\kappa_{ki} + \frac{2}{3}\delta_{ij}\kappa_{lm}q_{lm} - \frac{Q}{3}\dot{\gamma}_{ij} + \left(\frac{q_{lm}\kappa_{lm}}{Q}\right)q_{ij} - d_1\frac{\alpha}{\eta_M}Qq_{ij} - d_1d_3\frac{\alpha}{\eta_M}\left(\frac{q_{lm}q_{lm}}{Q}\right)q_{ij} \quad (4.16)$$

and the time evolution of interfacial area per unit volume  $Q$  is given by :

$$\frac{dQ}{dt} = -\kappa_{ij}q_{ij} - d_1d_2\frac{\alpha}{\eta_M}Q^2 - d_1d_3\frac{\alpha}{\eta_M}q_{ij}q_{ij} \quad (4.17)$$

For a given velocity gradient tensor component  $\kappa_{ij}$  and for initial values of interfacial area per unit volume  $Q(0)$  and its anisotropy  $q_{ij}(0)$ , the stresses occurring in a blend are calculated using Eqs. (4.8), (4.16) and (4.17). Lee and Park obtained the following results for oscillatory shear flow of a viscoelastic blend by applying the Cox-Merz rule to the pure components. Equation (4.8) becomes :

$$G_B^* = \left(1 + \frac{6(G_I^* - G_M^*)}{10(G_M^* + G_I^*)}\phi\right) G_M^* + G_{interface}^* \quad (4.18)$$

where  $G_{interface}^*$  is the contribution of the interface to the complex modulus. The transformation of Eq. (4.8) using the Cox-Merz rule constitutes also a point of discussion. Lee and Park assumed that the Cox-Merz rule is valid for the pure components and that the evolution with time of the anisotropy tensor  $q$  is expressed here as the special case of oscillatory shear flow. This approach is empirical since the original evolution equations for

$q$  and  $Q$  have been developed considering the viscosities of both components to be similar so that the interface is affected only by the interfacial tension. Clearly the Cox-Merz rule does not apply to the blend, mainly because of the morphology evolution during shear flow (Han et al., 1995; Bousmina and Muller, 1996) and also, because of the non linearity of the contributions of the bulk properties and interfacial effect. Applying the set of Eqs. (4.16) and (4.17) for a polymer blend of different viscosities constitutes a crude approximation which can be probably overcome by using a fitting parameter. Such an empiricism is nevertheless quite useful for describing the blend morphology under large deformation flow.

For an imposed small amplitude shear strain  $\gamma(\omega) = \gamma^0 \sin(\omega t)$ , the resulting stress due to the interface,  $-\alpha q_{12}(\omega)$ , will also vary sinusoidally with the stress amplitude  $\sigma_{interface}$  but will be out of phase with respect to the strain.  $\sigma_{interface}$  and its phase lag  $\delta_{interface}$  are calculated by solving Eqs. (4.16) and (4.17) with initial values  $Q(0)$  and  $q_{ij}(0)$ . The interfacial moduli are then calculated by using the following definitions exactly like in the work of Lee and Park:

$$G'_{interface} = \frac{\sigma_{interface}}{\gamma^0} \cos(\delta_{interface}) \quad (4.19)$$

$$G''_{interface} = \frac{\sigma_{interface}}{\gamma^0} \sin(\delta_{interface}) \quad (4.20)$$

#### 4.4) Experimental

Three different types of blends were studied : polystyrene, polyethylene (PS/PE), polyethylene terephthalate glycol, ethylene vinyl acetate (PETG/EVA) and polypropylene (PP)/EVA blends. These blends have been chosen for comparing the predictions of the models because of their wide range of the zero-shear viscosity ratio ( $\eta_{10} / \eta_{100}$ ) varying from

0.1 to 1. The experimental procedure concerning the PETG/EVA system has already been discussed elsewhere (Lacroix et al., 1996). For the other two systems, the commercial polymers were a PP (PP3020GN3) and an EVA (EVATANE 2805) supplied by Elf-Atochem while a PS (Styron D685) and a PE (LLDPE Tuflin) products were obtained from Dow Chemical and Union Carbide respectively.

### Blending procedure

For each type of blends, as well as for the unblended components, the following blending procedures have also been applied, so that the thermomechanical history of the blends and of the components would be the same.

#### PS/PE blends :

The blends were prepared using a Brabender internal mixer under nitrogen atmosphere at 200°C and 50 rpm during 300 s, time long enough to reach a constant torque value. The samples extracted from the chamber were compression molded at 200°C during 6 min, the pressure load progressively was increased from 200 kPa to 1.1 MPa. Blends of composition by volume of 90/10, 80/20 were prepared.

#### PP/EVA blends :

The pellets were first dry-blended and melted in the Brabender at a set temperature of 200°C and with a rotor speed of 20 rpm. Then, once all the pellets were loaded and melted, the speed was increased to 40 rpm and the components were mixed during 200 s. This time was sufficient to reach a constant torque value. The melt processing was carried out under nitrogen atmosphere to prevent degradation. The samples were extracted from the chamber and quenched in cold water. Samples for rheological measurements were then compression molded at 200°C during 7 min. The pressure load was progressively increased

from 200 kPa to 1.4MPa. The samples were then quenched in cold water. Blends of composition by weight percent of 90/10, 80/20, 70/30 and 65/35 (corresponding to particles volume concentrations of 0.095, 0.19, 0.285 and 0.332) were investigated.

#### Scanning electron microscope :

The morphological stability of the blends was checked by extracting from the rheometer the samples at different times. The morphologies were frozen with dry air, which allows the temperature inside the samples to decrease by about 150°C in 2 min. The blend morphologies were determined by using a Jeol JSM-840 scanning electron microscope, for fractured samples in liquid nitrogen and coated with 50/50 gold palladium to avoid charging. To account for the fact that the observation plane does not necessarily cut through the particles at their equator, the Scharwz-Saltikhov (1967) corrections were applied, using the program developed by Lavallée (1990). The number and volume average diameters  $d_n$  and  $d_v$  were determined from the surface analysis of at least 300 particles with a digitalizing device . Our estimate of the accuracy of the measurements is at best  $\pm 10 \%$ .

#### Rheological measurements :

The linear viscoelastic properties of the molten blends were measured as a function of frequency using a Bohlin CSM rheometer with a concentric disk geometry. The diameter of the plates was 25 mm and the gap about 1.5 mm. The measurements were carried out under nitrogen at a set temperature of 200°C except for the PETG/EVA blends for which the temperature was 210°C and the frequency range investigated was 0.001-10 Hz. The samples were found to be stable with time by running repeated frequency sweep experiments or experiments at a low constant frequency for periods of over 1 h. To keep the response in the viscoelastic linear domain, the applied stress was controlled to keep the total deformation at around 0.05, except for very low frequencies where larger stresses input were used to increase the sensitivity.



#### 4.5) Results and discussions

Figures 4.1 to 4.6 report the linear viscoelastic data for the three different blends. The PETG/EVA, PP/EVA and PS/PE blends exhibit the typical rheological behavior observed for blends with an emulsion type morphology. For the three systems investigated, the viscosity ratio ( $\eta_i / \eta_M$ ) is lower than 1 over almost the whole frequency range. For relatively low concentrations of the dispersed phase (10% and 20%), the loss modulus of the blends coincide almost with that of the matrix. By increasing the amount of the dispersed phase of lower viscosity, the loss modulus tends to decrease progressively compared to that of the major phase. The storage modulus is characterized by a shoulder in the low frequency region compared to that of the matrix (dashed line in Figure 4.1). The shoulder is quite visible in Figs. 4.3, 4.4. This increase in elasticity in the terminal zone of the matrix has been attributed to the deformability of the suspended droplets (Bousmina et al., 1995; Carreau et al., 1994, Bousmina and Muller, 1993; Graebbling et al., 1993; Graebbling and Muller, 1990; Scholtz et al., 1989). It results that the terminal zone of the blends is shifted towards lower frequencies compared to that of the matrix. In order to observe such effects, measurements have to be carried out at sufficiently low frequencies, for which the oscillation period is long enough to observe the relaxation of the deformable droplets. We report also in the figures the predictions of the Palierne and Lee-Park models. The comparison is discussed in the following section and limitations of these two models are underlined. The models are also used to estimate the relaxation times associated with the droplet deformation.

PS/PE blends :

From the knowledge of the rheological behavior of the components and from the determination of the particle size distribution and the interfacial tension, the behavior of the blends can be predicted by using Eq. (4.1) and this, without adjustable parameters.

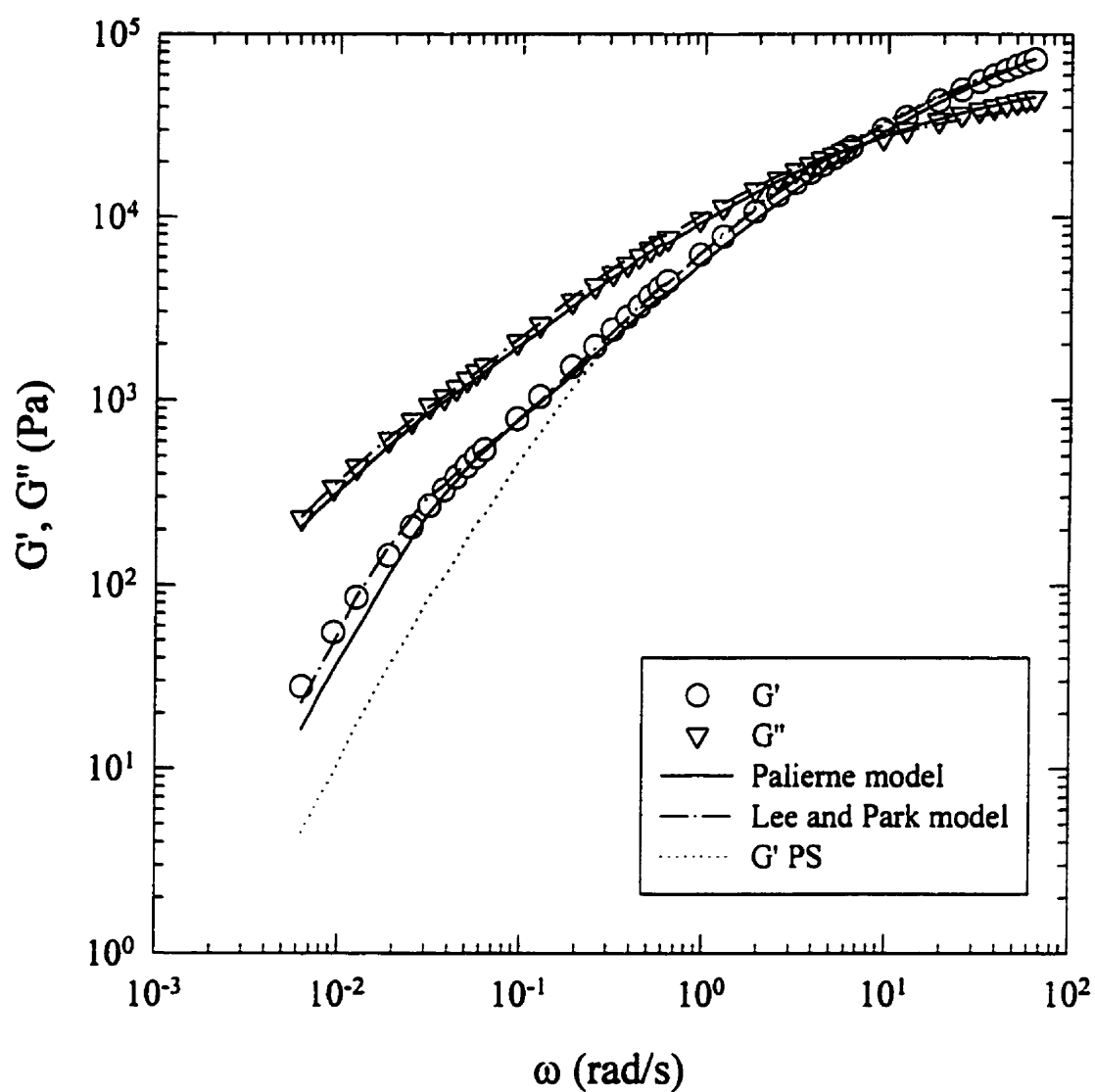


Figure 4.1 : Comparison between experimental data and model predictions for the 80/20 PS/PE blend;  $T=200^{\circ}\text{C}$ .

On the other hand, if unknown, the interfacial tension can be determined by fitting the theoretical predictions to the experimental data. For the PS/PE blends as well as the two others blends (PETG/EVA and PP/EVA) considered later, the polydispersity in size ( $d_v/d_n$ ) of the inclusions did not exceed 2 so that we could consider the system as monodisperse in particle size and use the volume average diameter for calculating the model predictions (Graebing et al., 1993; Bousmina et al., 1995). The morphology was checked during the measurements and the stabilized values of the volume average diameter were used (see Table 4.1). Recall that the Palierne model implicitly assumes no coalescence and that the droplets remain almost spherical.

Table 4.1 : Morphological data, interfacial tension and parameters used for predicting the rheological behavior.

Blends	$\phi$	$R_v$ ( $\mu\text{m}$ )	$\alpha$ (mN/m)	$d_1$	$d_2$	$d_3$
PS/PE	0.1	1.15	$5.0 \pm 0.5$	1.3	0	0.9
@ 200°C	0.2	2.4	$5.0 \pm 0.5$	0.6	0	0.8
PETG/EVA	0.1	0.55	$4.0 \pm 0.5$	1.5	0	0.9
@ 210°C	0.2	1.23	$4.0 \pm 0.5$	0.6	0	0.8
PP/EVA	0.095	0.3	$1.0 \pm 0.2$	2	0	0.905
@ 200°C	0.19	1.4	$1.0 \pm 0.2$	1.2	0	0.81
	0.285	2.8	$1.0 \pm 0.2$	0.5-0.7	0	0.715
	0.332	4.1	$1.0 \pm 0.2$ (0.6)	0.6	0	0.668

Even if the Lee and Park model is fundamentally different, especially regarding the treatment of the interface, it can be used to describe the linear rheological behavior of polymer blends. The anisotropy tensor as well as the interfacial area variations with time are

required to assess the interfacial contribution in the Lee-Park model. The evolution with time of the quantities characterizing the interface ( $q_i$  and  $Q$ ) is obtained from the solution of the non linear set of coupled Eqs. (4.16) and (4.17). In small amplitude oscillatory flow, (for sufficiently low deformations) coalescence is negligible. So, as done in the analysis done by Lee and Park,  $d_i$  associated to coalescence is set equal to zero and  $d_j$ ,  $v$  in the original Lee and Park article, associated to simultaneous shape relaxation and break-up is set equal to  $1-\phi$ . We assume that the system is initially isotropic, so we set  $q_i(0)$  equal to zero.  $Q(0)$  is determined from the quantitative analysis of the morphology, the interfacial stress and the phase lag ( $\sigma_{interface}$  and  $\delta_{interface}$ ) can be estimated from the established solution of the governing interface equations.  $G'_{interface}$  and  $G''_{interface}$  are then calculated by using Eqs. (4.19) and (4.20). The complex modulus of the blend is finally obtained from Eq (4.18). The parameter  $d_i$  is adjusted to give the best fit between the model predictions and the experimental data in the low frequency region because as we will show in a following section, the relaxation time associated to the interface in the blend is dependent on the  $d_i$  value.

Figure 4.1 compares both model predictions to the data for a 80/20 PS/PE blend. For the Palierne model we assume the interfacial tension to be equal to 5.0 mN/m (Wu, 1982) and use the morphological data given in Table 4.1. Without any fitting parameter, the data can be well predicted by the Palierne model as shown in the figure. A slightly better fit of the lower frequency data could be obtained by using a lower value of the interfacial tension. Also reported on the figure are the  $G'$  data for the matrix (dashed line). The parameters used to calculate the predictions of the Lee-Park model are presented in Table 4.1. The results of both Lee-Park and Palierne models are very similar and, over the whole frequency range, the experimental data are correctly described by both Palierne and Lee-Park models.

All predictions of the Lee-Park model were obtained in the same way. A single fitting parameter was used ( $d_i$ ) and adjusted to get the best fit in the low frequency region. The relaxation mechanism induced by the interfacial tension indeed becomes predominant

at low frequencies. The influence of the parameter  $d_i$  is shown in Figure 4.2 for the 80/20 PS/PE blend. In the low frequency region, the model predictions are quite sensitive to  $d_i$ , which is shown in Table 4.1 to depend on the volume fraction of the dispersed phase as well as on the viscosity ratio. A decrease of  $d_i$  corresponds to an increase in elasticity and to a shift of the terminal zone towards lower frequencies for the blend.

#### PETG/EVA blends :

The interfacial tension between these two polymers was initially unknown. A very good agreement between the model predictions and the experimental data had been found for values of  $\alpha$  around 4.0 mN/m using the Palierne model (Lacroix et al., 1996) and this, for the two compositions investigated at 210°C. This previously determined interfacial tension value of 4 mN/m was used to test the Lee-Park model. Figure 4.3 compares the predictions of both models for the 80/20 PETG/EVA blend. Both models gives a good description of the data over the whole frequency range and the increase in elasticity in the low frequency region is well described. We must nevertheless keep in mind that if the interfacial tension is known the Palierne model does not contain any adjustable parameter. Table 4.1 summarizes the values of  $d_i$  used to obtain the best fits of the Lee-Park model for the 90/10 and 80/20 PETG/EVA blends.

#### PP/EVA blends :

The two previous blends investigated have shown that the Lee-Park model leads to a good description of the linear viscoelastic properties. For the third system analyzed in this study, the differences of the rheological behavior of both components are much more pronounced. The zero-shear viscosity ratio is lower ( $\eta_{l0}/\eta_{h0}$  is around 0.1 instead of 0.3 for the PS/PE blends and around 0.7 for the PETG/EVA blends) and, over the whole frequency range the viscosity ratio between the components is lower compared to the PS/PE and PETG/EVA blends.

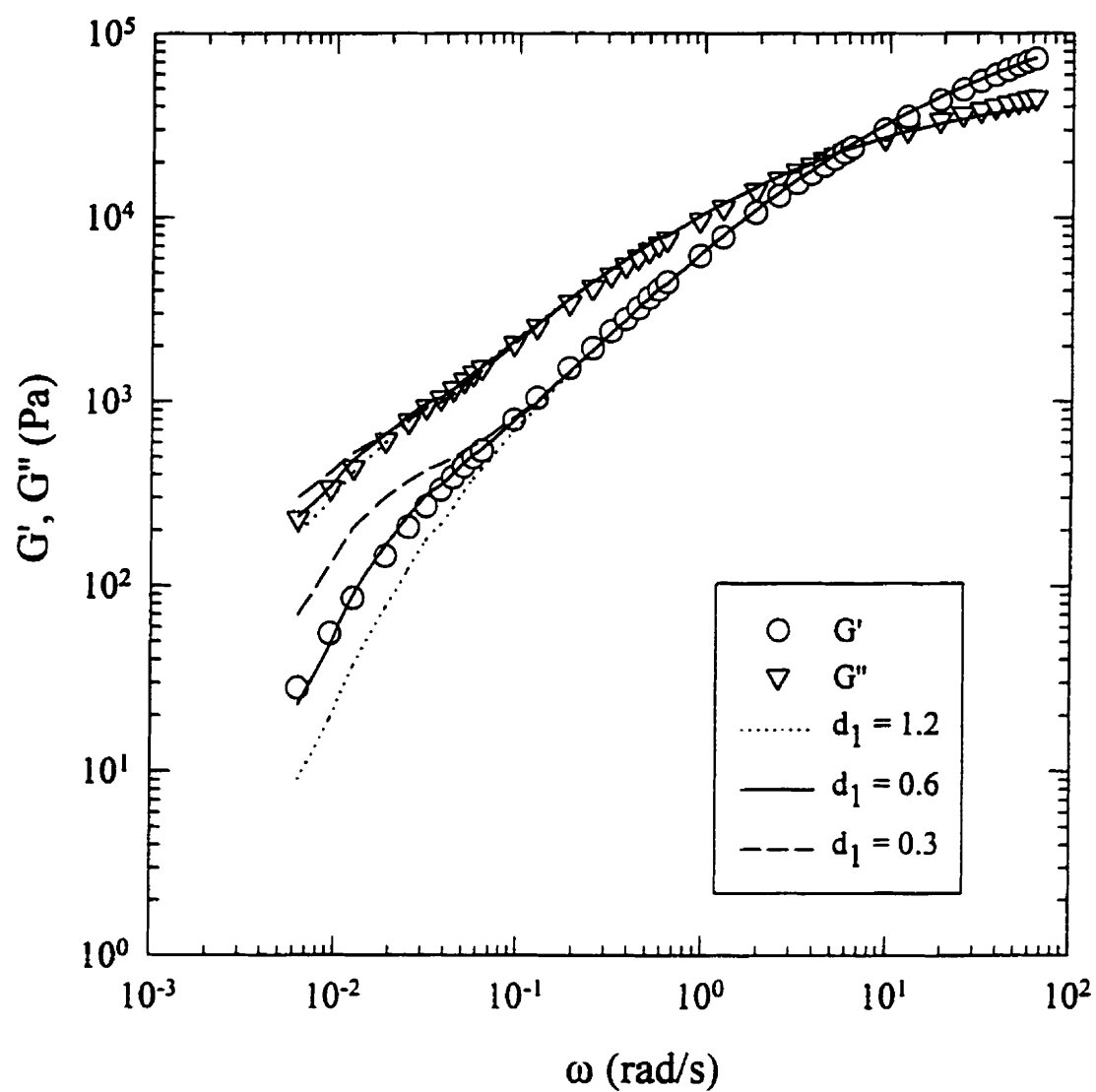


Figure 4.2 : Influence of the parameter  $d_1$  on the predictions of the Lee and Park model for the 80/20 PS/PE blend;  $T=200^\circ\text{C}$ .

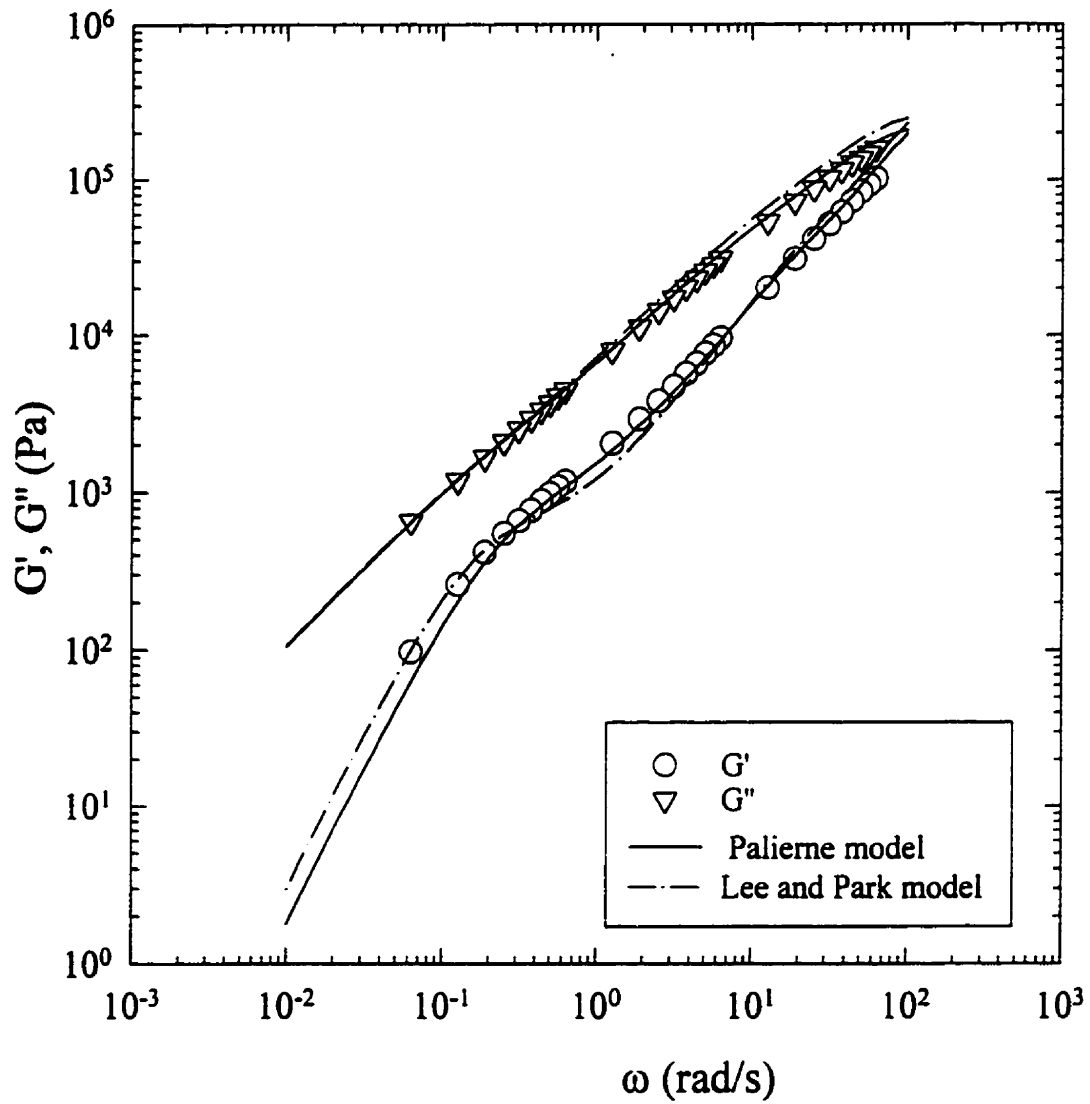


Figure 4.3 : Comparison between experimental data and model predictions for the 80/20 PETG/EVA blend;  $T=210^{\circ}\text{C}$ .

Figure 4.4 compares the predictions of both models for the 70/30 and 65/35 PP/EVA blends. The Palierne model predictions were determined by adjusting the interfacial tension to fit the experimental data. For almost all the compositions, the rheological behavior over the whole frequency range, as well as the increase in elasticity at low frequencies, are well predicted by the model. Slight discrepancies between the Palierne model and the 80/20 PP/EVA data occurred for the low frequency region (not shown in the figure). Nevertheless, the values of the interfacial tension found by adjusting the model predictions to the data are in agreement with the value obtained using the harmonic mean equation, 1.2 mN/m, except for the 65/35 PP/EVA blend where a best fit of the rheological data is obtained for  $\alpha = 0.6$  mN/m (Fig. 4.5). With increasing concentration of the dispersed phase up to 30% by weight of EVA, the terminal zone of the emulsion is shifted towards the low frequency region and the magnitude of the shoulder associated with the presence of the interface is increased.

The sensitivity of  $\alpha$  on the Palierne model predictions is shown in Figure 4.5 for the 65/35 PP/EVA blend. Using the lower value,  $\alpha = 0.6$  mN/m, an overall better fit of the experimental data is observed, but the lowest frequency data for this blend are still not very well predicted. At this concentration, steric interaction as well as partial miscibility are not to be excluded, and this may explain the lower elastic modulus at low frequencies compared to the model predictions. Moreover, the experimental data at very low frequencies are not necessarily very accurate.

Figure 4.4 shows also that the loss and storage moduli are overpredicted by the Lee and Park model in the high frequency region. It can also be noted that these discrepancies are more significant for the larger concentration of dispersed EVA phase. Nevertheless the behavior in the low frequency region, and related to the interface is correctly described. The low frequency  $G'$  data for the 80/20 PP/EVA blend are better described by the Lee-Park model (not shown here), and globally the deviations are reasonable.



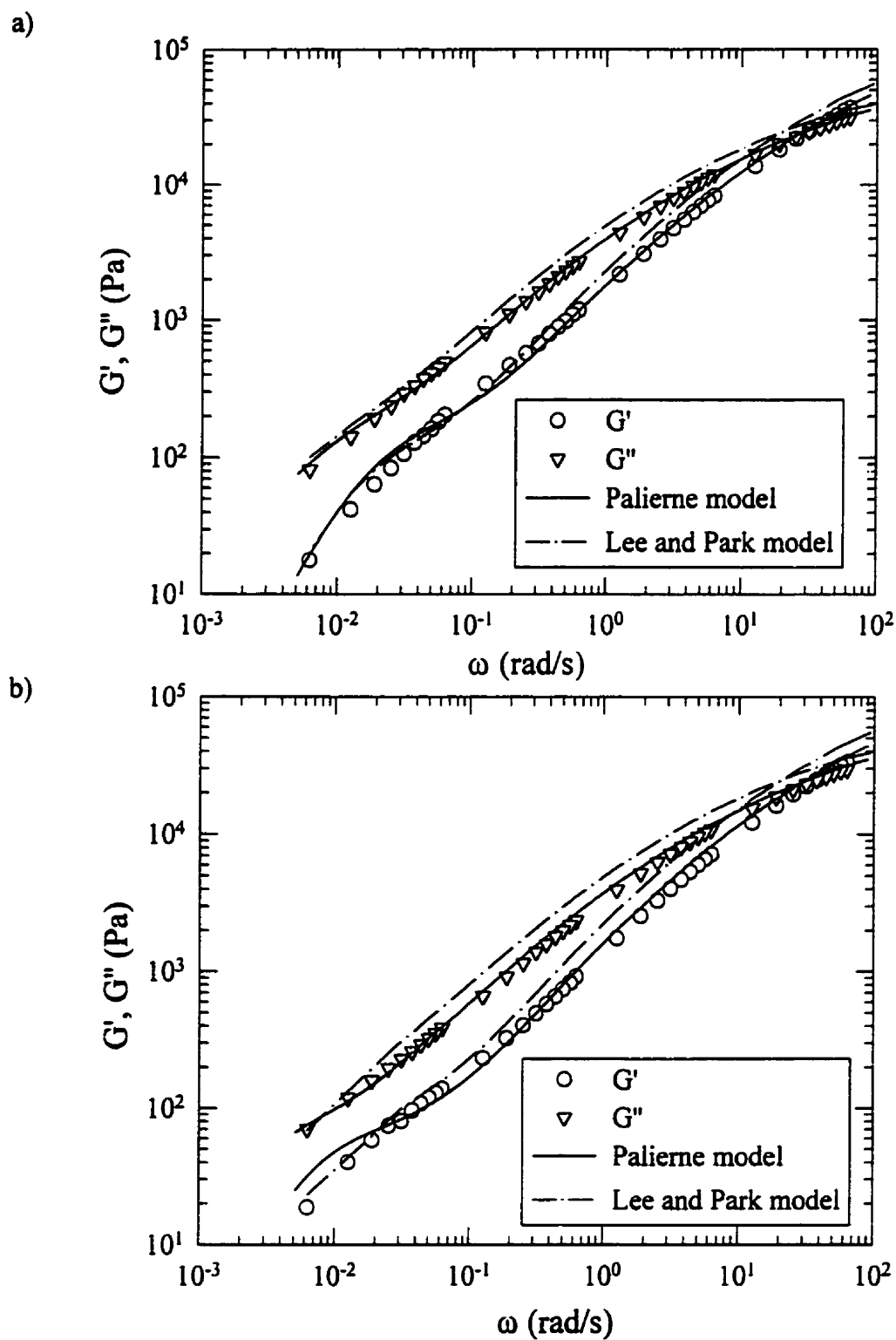


Figure 4.4 : Comparison between experimental data and model predictions for two PP/EVA blends: a) 70/30 PP/EVA, b) 65/35 PP/EVA;  $T=200^\circ\text{C}$ .

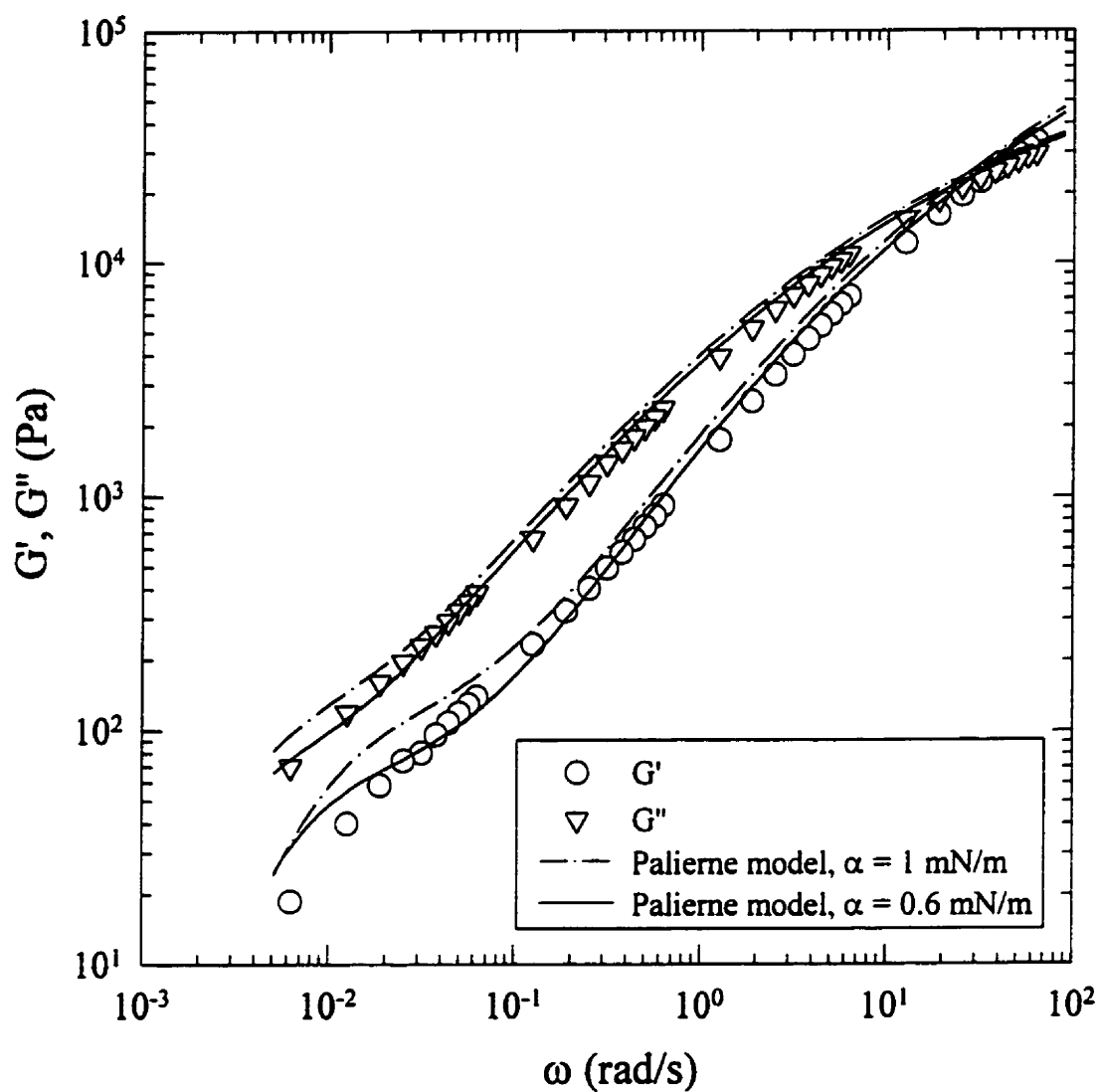


Figure 4.5 : Comparison between experimental data and the Palierne emulsion model predictions for the 65/35 PP/EVA blend; influence of the interfacial tension value on the model predictions;  $T=200^\circ\text{C}$ .

In the high frequency region, where discrepancies between the Lee-Park model predictions and the data are observed for the PP/EVA blends, the contribution of the interface is negligible compared to those of the bulk properties of both phases (mixing rule). In the Lee and Park model, the behavior of the blend at high frequencies is dominated by the first term of Eq. (4.18). This viscoelastic term comes from an extension of the work of Schowalter et al. (1968), initially developed for a mixture of Newtonian fluids in which the particles are kept almost spherical ( $\alpha \rightarrow \infty$ ), and applying the Cox-Merz rule to both components. Assuming that the interfacial tension contribution is negligible (this is clearly valid at high frequency), the limiting case of this model can be written as follows :

$$G_B^* = \left( 1 + \frac{6(G_I^* - G_M^*)}{10(G_M^* + G_I^*)} \phi \right) G_M^* \quad (4.21)$$

As shown in the previous paragraphs, the Palieme model is able to predict very well the behavior of the blends over the whole frequency range. By setting  $\alpha = 0$  in the Palieme model, Dickie's results (1973) are then retrieved and can be expressed as follows :

$$G_B^* = \left( \frac{1 + 3/2 H^*}{1 - H^*} \right) G_M^* \quad (4.22)$$

with

$$H^* = \phi \frac{2(G_I^*(\omega) - G_M^*(\omega))}{2G_I^*(\omega) + 3G_M^*(\omega)} \quad (4.23)$$

This corresponds to the Palieme model predictions in the limit of high frequency where the interfacial effects become negligible. Although the two high frequency limits are different (Eqs (4.21) and (4.22)), the behavior of the PS/PE and the PETG/EVA blends are correctly

described by both models because the viscoelastic properties of the two components for these blends are not much different. For the 80/20 PETG/EVA blend, a slight overestimation of the loss modulus can be detected at very high frequencies. For the PP/EVA blends which show the lower viscosity ratio over the whole frequency range, more significant discrepancies are observed.

Considering that the Palierne model leads to a good descriptions of the high frequency data, we choose to modify Eq. (4.18) as follows :

$$G_B^* = \left( \frac{1+3/2H^*}{1-H^*} \right) G_M^* + G_{interface}^* \quad (4.24)$$

with  $H^*$  given by Eq. (4.23).  $G_{interface}^*$  is calculated according to the same procedure as described in the case of the Lee-Park model.

The use of the Lee and Park model (Eq. (4.18)) as well as of the modified model (Eq. (4.24)) requires further comments. In developing Eq. (4.18), Lee and Park have associated the anisotropy tensor term,  $-aq_y$ , to the limit of the morphology-dependent term (Mellema and Willemse, 1983) by assuming a constant interfacial tension. If one considers the limit of non deformable spheres,  $q_y$  is equal to zero and then Eq. (4.18) does not reduce to the well known Einstein formula. In such a case, the limit of the morphology-dependent term will differ from that implicit in Schowalter et al. (1968) and derived by Mellema and Willemse (1983). The modified Lee and Park model (Eq. (4.24)) correctly reduces to the Einstein expression for rigid inclusions in Newtonian fluids. On the other hand, as indicated by one of the reviewers, the viscosity ratio term and the morphology-dependent term were obtained by Schowalter and Mellema and Willemse for almost spherical non deformable spheres at low volume fractions. Adding the limits of these two terms leads to the following form of the Eq. (4.18) :

$$G_B^* = \left(1 + \frac{5k+2}{2k+2}\phi\right) G_M^* + G_{interface}^* \quad (4.25)$$

which is a generalized Taylor equation. We have tested this form (Eq (4.25)) and found considerable disagreement with our data at high frequencies. Note this result is considerably different from that of Palierne at high frequencies where the contribution of  $G_{interface}^*$  becomes negligible. However this form may prove to be more appropriate for other conditions.

Figure 4.6 compares the predictions of both the Lee-Park and modified (Eq. (4.24)) models for the 70/30 and 65/35 PP/EVA blends. The results have been obtained by using the same value of  $d_f$  as previously determined (Table 4.1). The figure shows that the modification significantly improves the predictions at high frequencies and, as expected, both the modified Lee and Park and the Palierne models are equivalent at high frequencies. It is therefore believed that the mixing rule for the bulk properties embedded in the Palierne model is more appropriate. For the other blends, good agreement is also found with this modified model, but no significant differences could be observed.

For high concentrations of the dispersed phase, the empirically modified Lee-Park model with an adjustable parameter  $d_f$  is more flexible than the Palierne model. Comparing Figs. 4.5 and 4.6, it is clear that a better fit of the low frequency data is obtained with the modified Lee-Park model for this 65/35 PP/EVA blend. The original Lee-Park model can account for particle-particle interactions, coalescence and breakup under large strain flows through adjustable parameters. These features could be of major interest in relation to the processing of polymer blends. This parameter  $d_f$  is related to the shape relaxation of the deformed droplets in the relaxation mechanism of Lee and Park. By adjusting its value, the anisotropy relaxation rate is modified (see Eq. (4.13)). The relaxation time associated to the interface in the blend is then dependent on the  $d_f$  value.

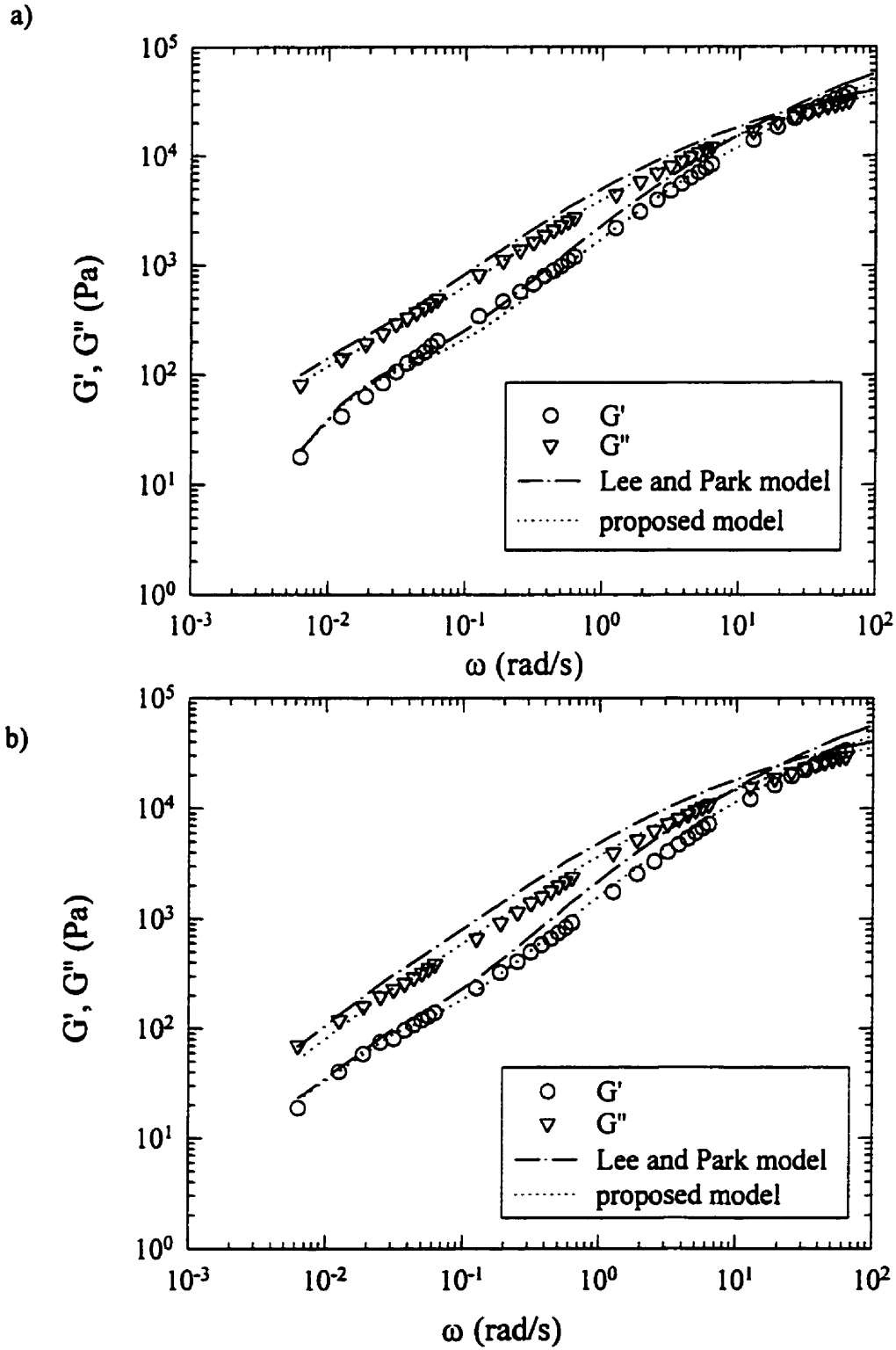


Figure 4.6 : Comparison between the Lee-Park and modified Lee-Park model predictions for two PP/EVA blends : a) 70/30 PP/EVA, b) 65/35 PP/EVA;  $T=200^{\circ}\text{C}$ .

Based on this observation, Guenther and Baird (1996) have chosen another way of determining the parameter related to the anisotropy relaxation rate in the Doi-Ohta model, equivalent to the parameter  $d_i$  in this case. We will discuss this approach in the following section in light of the relaxation times determined from the weighted spectra.

Interface relaxation times :

The comparison of the plots of the weighted relaxation spectra  $\lambda H(\lambda)$  as a function of  $\log(\lambda)$  for the blend and the components is an efficient way to show the additional relaxation mechanism associated with interfacial tension (Gramespacher and Meissner (1992)). The relaxation spectrum  $H(\lambda)$  is related with  $G'$  and  $G''$  by :

$$G'(\omega) = \int_{-\infty}^{\infty} H(\lambda) \frac{\omega^2 \lambda^2}{1 + \omega^2 \lambda^2} d \ln \lambda \quad (4.26)$$

$$G''(\omega) = \int_{-\infty}^{\infty} H(\lambda) \frac{\omega \lambda}{1 + \omega^2 \lambda^2} d \ln \lambda \quad (4.27)$$

We have applied a modified Tikhonov regularization method (Weese (1993), Honerkamp and Weese (1993)) to calculate the spectra. The weighted relaxation spectra of the PS, PE and 80/20 PS/PE blend are given in Fig. 4.7. The blend spectrum exhibits two maxima. The first one coincides with that of the matrix, suggesting that the matrix governs the rheological behavior of the blend at high frequency. The second peak detected at longer relaxation times is associated with the shape relaxation of the droplets. The same features are observed for the PP/EVA blends in Fig 4.8 for different concentrations of the dispersed phase. As the dispersed phase concentration is increased, we observe a shift of the additional peak towards longer times ( i.e. an increase of the relaxation time, characteristic of the interface). Similar results observed for the PETG/EVA blends are not illustrated here.

Expressions for the characteristic time associated with the relaxation of the shape of the interface can be obtained from the Palierne and Lee and Park models. Graebling et al. (1993) reported the time associated with the droplets deformation for the emulsion model of Palierne. They pointed out that if a secondary plateau in  $G'$  associated with the shape relaxation of the droplets exists for a blend of viscoelastic polymers, it occurs in a frequency range where  $G_M^* \sim i\omega\eta_M$  and  $G_I^* \sim i\omega\eta_I$ . They considered that the contribution to the storage modulus of the emulsion arising from the relaxation of the droplets can be calculated as if the phases were Newtonian liquids. Assuming that the droplets are monodispersed ( $R_I = R$ ) they showed that the Palierne model is analogous to a Jeffreys model. The following expression for the time associated with the relaxation of the shape of the droplets is then obtained :

$$\lambda_1 = \frac{R\eta_M (19k+16)(2k+3-2\phi(k-1))}{4\alpha (10(k+1)-2\phi(5k+2))} \quad (4.28)$$

where  $k = \eta_I/\eta_M$ .

For the Lee and Park model, the relaxation of the anisotropy of the interface under the effect of the interfacial tension is described by Eq (4.13). It is a first order kinetic equation and the inverse of the relaxation rate gives a relaxation time  $\lambda_2$  expressed as :

$$\lambda_2 = \frac{\eta_M}{\alpha Q d_1} \quad (4.29a)$$



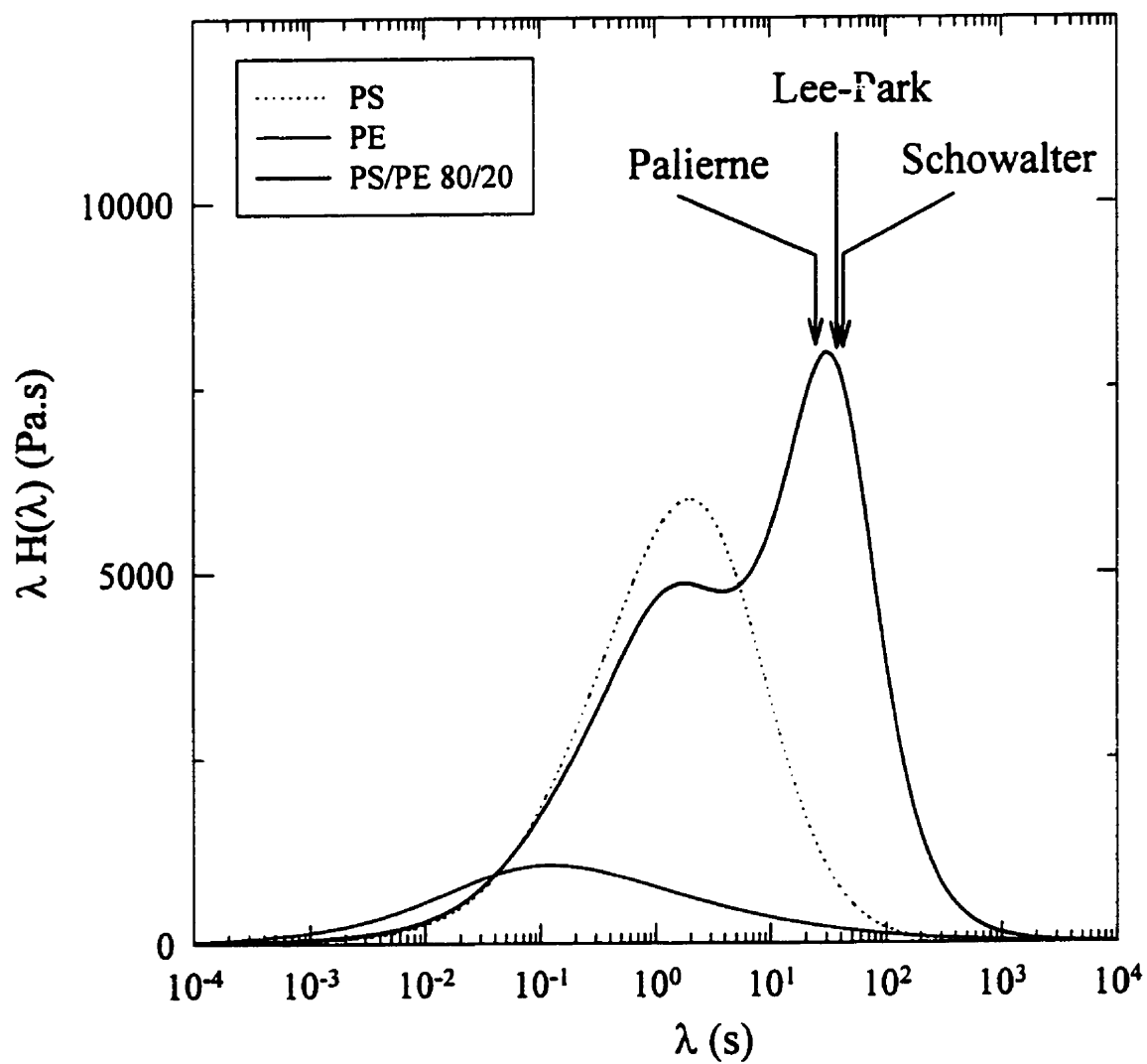


Figure 4.7 : Weighted relaxation spectra for the PS, PE and the 80/20 PS/PE blend;  
 $T=200^{\circ}\text{C}$ .

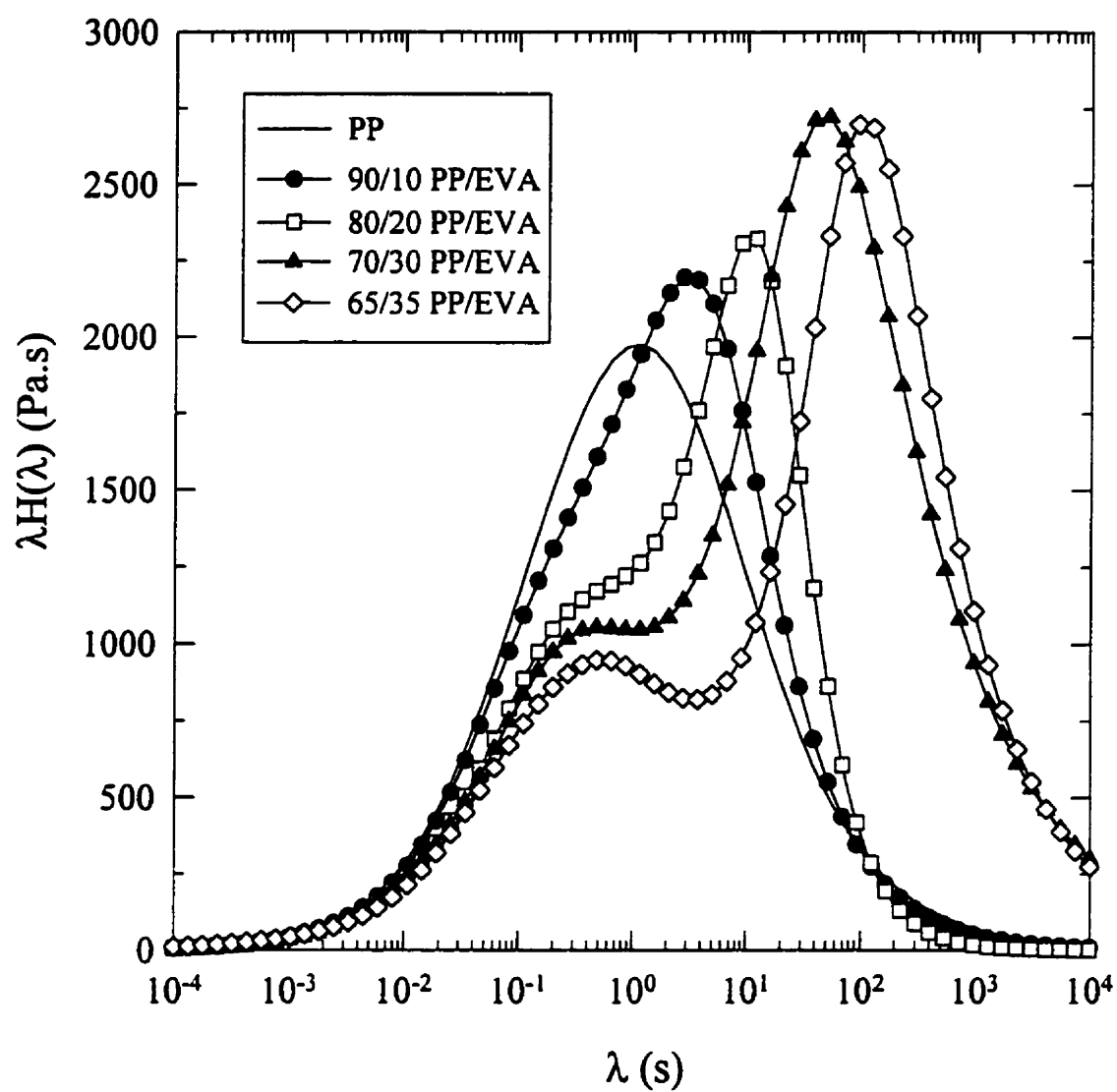


Figure 4.8 : Weighted relaxation spectra for the PP and the PP/EVA blends for various compositions of EVA;  $T=200^{\circ}\text{C}$ .

which reduces in the case of spherical monodisperse droplets of radius  $R$  to :

$$\lambda_2 = \frac{R\eta_M}{\alpha} \frac{1}{3\phi d_1} \quad (4.29b)$$

The expressions for the time constants (Eq (4.28) and (4.29b)) are quite similar and, by taking  $\lambda_1 = \lambda_2$  the Lee and Park parameter  $d_1$  can be calculated from physical parameters. Identification of the characteristic times associated with the relaxation of the interface was also considered by Guenther and Baird (1996). They identified the characteristic time equivalent to  $\lambda_2$  in the Doi-Ohta theory with the relaxation time derived by Choi and Schowalter (1975). In this constitutive equation developed for semi diluted emulsions of two Newtonian fluids the expression for the relaxation time  $\lambda_3$ , associated with interfacial tension, can be expressed as:

$$\lambda_3 = \lambda_0 \left( 1 + \frac{5\phi(19k+16)}{4(k+1)(2k+3)} \right) \quad (4.30.a)$$

with :

$$\lambda_0 = \frac{R\eta_M}{4\alpha} \frac{(19k+16)(2k+3)}{10(k+1)} \quad (4.30.b)$$

The Guenther and Baird approach was partly based on the results presented by Gramespacher and Meissner (1992). For PMMA/PS blends, they found that the relaxation time  $\lambda_3$  calculated using Eqs. (4.30a) and (4.30b) was equal to the experimentally obtained value, corresponding to the peak in the weighted relaxation spectra associated with the interfacial tension.

Table 4.2 lists the relaxation times associated with the interface for the Paliere, Lee

and Park, and Choi and Schowalter models, and those determined from the second peak of the weighted relaxation spectra as shown in Figs. 4.7 and 4.8.

Table 4.2 : Comparison of different interface relaxation times

Blends	Composition	$\lambda_1$ (s)	$\lambda_2$ (s)	$\lambda_3$ (s)	$\lambda_{peak}$ (s)
PS/PE	90/10	10,4	16	15	8
	80/20	24	37	43	30
PETG/EVA	90/10	2,2	2,4	3	0,8
	80/20	5,4	6,6	9	4,8
PP/EVA	90/10	5,5	6,8	7,8	2,8
	80/20	27	26	50	12
	70/30	60	70	128	51,8
	65/35	93	85	207	92,9

When considering the whole time scale under investigation, the times associated with the different models are found, for any given blend, to fall in the same range of values. Discrepancies between the times are, however, observed. They can be important (up to 100%), and they vary from one system to another. For the PP/EVA and PETG/EVA blends the Palierne and the Lee and Park characteristic times are quite similar (the differences do not exceed 20 %), but the times obtained from the Choi and Schowalter equation are 50% to 100 % higher. By contrast, for the PS/PE blends, the Choi and Schowalter and the Lee and Park characteristic times are quite similar, while the times associated with the Palierne model are now about 50% lower. The characteristic times determined from the models are roughly consistent with the estimation from the weighted relaxation spectra using the peak associated with interfacial tension. The time corresponding to this peak is, however, generally lower,

specially at low dispersed phase concentrations where the distinction of the peaks associated with the matrix and the interface is difficult. Coupling effects between the peaks could then made the determination of the characteristic time associated with the interface less reliable.

The Lee and Park model predictions for the PS/PE blends (systems for which the discrepancies between the Palierne and Lee and Park characteristic times are the largest), using the parameter  $d_i$  calculated by taking  $\lambda_1 = \lambda_2$ , are reported in Fig. 4.9 and compared to the data for two concentrations of the dispersed phase. Also shown by the solids lines are the best fits obtained by adjusting  $d_i$ . The model with  $d_i$  given by Eq. (4.29) is found to underestimate the storage modulus of the blend in the low frequency range. The global agreement is, however, satisfactorily, so that setting the interface characteristic time of the Lee and Park model equal to the characteristic time of the Palierne model is believed to be a simple way of determining an approximate value of  $d_i$ .

Finally, in calculating the Lee and Park model predictions presented so far the parameter  $d_i$  had been taken equal to  $1 - \phi$ . In the case of the PS/PE blends and when  $d_i$  is calculated by taking  $\lambda_1 = \lambda_2$ , the adjustment of  $d_i$  did not make it possible to improve the fit between the model predictions and the experimental data. For small amplitude oscillatory flow the predictions of the model are almost insensitive to the value of this parameter.

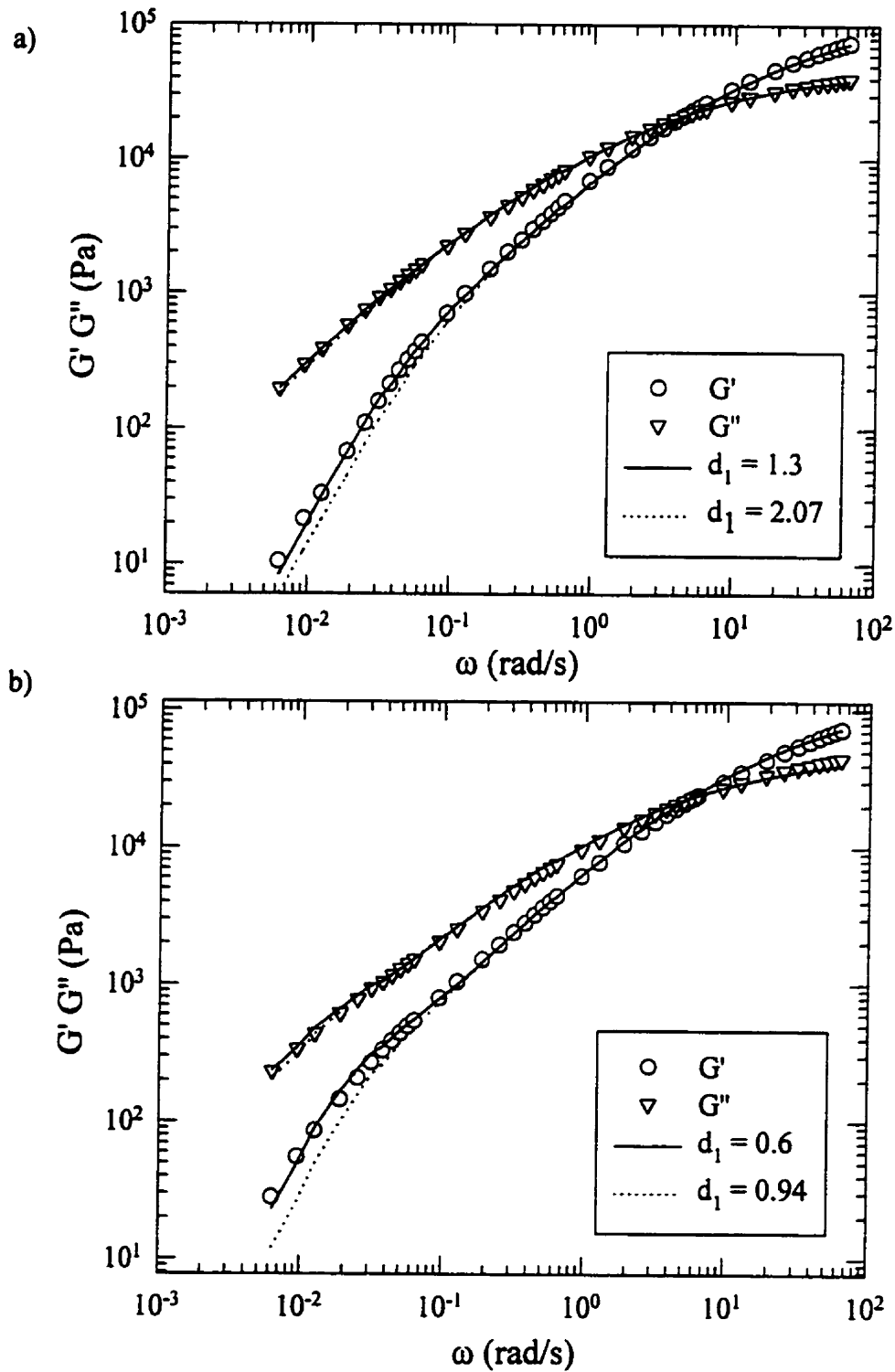


Figure 4.9 : Comparison between experimental data and the Lee and Park model predictions for two PS/PE blends : a) PS/PE 90/10, b) PS/PE 80/20; — best fits; ..... using  $d_1$  calculated from Eq (4.24).

#### 4.6) Conclusions

We have confirmed for three different systems the ability of the Palierne model to predict the linear viscoelastic behavior of immiscible blends. The linear viscoelastic data of the same blends could also be relatively well described by the Lee-Park model using a single fitting parameter related to the relaxation of the interface. For the more concentrated emulsions, when particle-particle interactions become important, the Lee-Park model with an adjustable parameter appears to be more flexible than the Palierne model to describe the low frequency behavior although some empiricism remains in the development of such an equation. The times associated with the relaxation of the shape of the interface derived from Lee and Park and Palierne models were found to be of similar magnitude and in relative agreement with the characteristic time determined from the peak of the weighted relaxation spectra. As a first approximation, the parameter  $d$ , associated with the interface relaxation in the Lee-Park model can be estimated using the characteristic time derived from the Palierne equation. For a blend with a relatively different viscosity ratio between the components, the Lee and Park model overestimates the data in the high frequency range. So, in light of these experimental results, a modification of the Lee-Park model is proposed to get a better description of the linear viscoelastic data. This modified model reduces to the Palierne equation for high frequencies and the Einstein equation is recovered for the case of rigid spheres diluted in a Newtonian fluid.

#### Acknowledgments

The authors are thankful to Prof. D. Maier for providing the NLREG program. We also acknowledge financial support received from ELF-ATOCHEM and from NSERC (grant STR0163362).

#### 4.7) References

- Bousmina M, Muller R (1993) Linear Viscoelasticity in the Melt of Impact PMMA. Influence of Concentration and Aggregation of Dispersed Rubber Particles. *J Rheol* 37: 663-679
- Bousmina M, Muller R (1996) Rheology/morphology/flow conditions relationship for polymethylmetacrylate/rubber blend. *Rheol Acta* 35 : 369-381
- Bousmina M, Bataille P, Sapieha S, Schreiber HP (1995) Comparing the Effect of Corona Treatment and Block Copolymer Addition on Rheological Properties of Polystyrene/Polyethylene Blends. *J Rheol* 39: 499-517
- Brahimi B, Ait-Kadi A, Ajji A, Jérôme R, Fayt R (1991) Rheological Properties of Copolymer modified Polyethylene/Polystyrene blends. *J Rheol* 35 : 1069-1091
- Carreau PJ, Bousmina M, Ajji A (1994) Rheological Properties of Blends : Facts and Challenges. In : Ghiggin KP (ed) *Progress in Pacific Polymer Science-3*. Springer-Verlag, New-York, pp 25-40
- Choi SJ, Schowalter WR (1975) Rheological Properties of Nondilute Suspensions of Deformable Particles. *Phys Fluids* 18 : 420-427
- Delaby I, Ernst B, Germain Y, Muller R (1994) Droplet deformation in polymer blends during uniaxial elongational flow. Influence of viscosity ratio for large capillary number. *J Rheol* 38 : 1705-1720
- Dickie RA (1973) Heterogeneous Polymer-Polymer Composites I Theory of Viscoelastic properties and Equivalent Mechanical Model. *J Appl Polym Sci* 17 : 45-63
- Doi M, Ohta T (1991) Dynamics and Rheology of Complex Interfaces. I. *J Chem Phys* 95 : 1242-1248
- Friedrich Ch, Gleinser W, Korat E, Maier D, Weese J (1995) Comparison of Sphere-Size Distribution obtained from Rheology and Transmission Electron Microscopy in PMMA/PS Blends. *J Rheol* 39 : 1411-1425



- Friedrich Ch, Riemann RE, Maier D, Korat E (1996) Influence of interfacial rheological properties of a PMMA-PS polymer blend. Proc. XII th Int. Congr. On Rheology, Quebec, Canada, p143
- Germain Y, Ernst B, Genelot O, Dhamani L (1994) Rheological and Morphological Analysis of compatibilized PP/PA Blends. J Rheol 38 : 681-697
- Graebbling D, Muller R (1990) Rheological Behavior of Polydimethylsiloxane/ Polyoxyethylene Blend in the Melt. Emulsion Model of two Viscoelastic Liquids. J Rheol 34 : 193-205
- Graebbling D, Muller R, Palierne JF (1993) Linear Viscoelastic Behavior of Some Incompatible Polymer Blends in the Melt. Interpretation of Data with a Model of Emulsion of Viscoelastic Liquids. Macromolecules 26 :320-329
- Graebbling D, Benkira A, Gallot Y, Muller R (1994) Dynamic Viscoelastic Behavior of Polymer blends in the Melt. Experimental Results for PDMS-POE, PS/PMMA and PS/PEMA blends. Eur Polym J 30 : 301-308
- Guenther GK, Baird DG (1996) An Evaluation of the Doi-Ohta Theory for an Immiscible Polymer Blend. J Rheol 40 : 1-20
- Han JH, Feng CC, Li DJ, Han CD (1995) Effect of flow geometry on the rheology of dispersed two phase blends of polystyrene and polymethylmethacrylate. Polym 36 : 2451-2463
- Honerkamp J, Weese J (1993) A Non Linear Regularization Method for the Calculation of Relaxation Spectra. Rheol Acta. 32 : 65-73
- Lacroix C, Bousmina M, Carreau PJ, Favis BD, Michel A (1996) Properties of PETG/EVA Blends : Viscoelastic, Morphological and Interfacial Properties, Part I. Polymer 37 : 2939-2947
- Lavallée C (1990) Stéréologie appliquée aux alliages polymères. CNRC, IMI, Boucherville, Qc, Canada
- Lee HM, Park OO (1994) Rheology and dynamics of Immiscible Polymer Blends. J Rheol 38 : 1405-1425

- Mellema J, Willemse MWM (1983) Effective Viscosity of Dispersions Approached by a Statistical Continuum Method. *Physica* 122A : 286-312
- Oldroyd JG (1953) The Elastic and Viscous Properties of Emulsions and Suspensions. *Proc R Soc London Ser A* 218 : 122-132
- Oldroyd JG (1955) The Effect of Interfacial stabilizing Films on the Elastic and Viscous Properties of Emulsions. *Proc Roy Soc A* 232 : 567-577
- Onuki A. (1987) Viscosity enhancement by Domains in Phase -Separating Fluids near the Critical Point : Proposal of Critical Rheology. *Phys Rev A* 35 : 5149-5155.
- Palierne JF (1990) Linear Rheology of Viscoelastic Emulsions with Interfacial Tension. *Rheol Acta* 29 : 204-214; (1991) 30 : 497
- Saltikov S A (1967) The Determination of the Size Distribution of particles in an Opaque Material from a Measurement of the Size Distribution of their Section. In : Elias H (ed) *Stereology Proc Second Int Cong for Stereology*, Springer Verlag NY, pp 163-173
- Scholz P, Froelich D, Muller R (1989) Viscoelastic Properties and Morphology of Two-Phase Polypropylene/Polyamide 6 blends in the Melt. Interpretation of Results with an Emulsion Model. *J Rheol* 33 : 481-499
- Schowalter WR, Chaffey CE, Brenner H (1968) Rheological Behavior of a dilute Emulsion. *J Colloid Interface Sci* 26 : 152-160
- Vinckier I, Moldenaers P, Mewis J (1996) Relationship between Rheology and Morphology of Model Blends in Steady Shear Flow. *J Rheol* 40 : 613-631
- Weese J (1993) A Regularization Method for Non Linear Ill Posed Problems. *Comput Phys Commun* 77 : 429-440
- Wu S (1982) *Polymer interface and adhesion*. Dekker, New York

**CHAPITRE 5**

**Relationships between rheology and morphology  
for immiscible molten blends  
of polypropylene and ethylene copolymers under shear flow**

**C. Lacroix, M. Grmela and P.J. Carreau\***

Centre de Recherche Appliquée sur les Polymères, CRASP,  
Department of Chemical Engineering, Ecole Polytechnique,  
P.O. Box 6079, Stn Centre-Ville, Montréal, QC, H3C 3A7, Canada

\* corresponding author

Cet article est publié dans *Journal of Rheology*, 42 41-62 (1998)

### 5.1) Synopsis

The linear and nonlinear viscoelastic properties of immiscible polymer blends polypropylene/ethylene vinylacetate-ethylene methylacrylate [PP/(EVA-EMA)] have been investigated. The transient shear flow experiments reflect the structural changes of the blends during the flow. Overshoots in stress growth experiments are observed when the dispersed phase is deformable. In this case, a good description of these transient rheological data is obtained using modified versions of the Lee and Park [J. Rheol. **38**, 1405 (1994)] and the Grmela and Ait-Kadi [J. Non-Newtonian Fluid Mech. **55**, 191 (1994)] models. Predictions of the morphological evolution of the blend under transient shear flows were calculated from the modified models which are shown to describe the breakup and coalescence phenomena under moderately large deformation shear flow. When the dispersed phase is undeformable, these models, which are either based on the original Doi and Ohta [J. Chem. Phys. **95**, 1242 (1991)] theory or derived to retrieve an extension of the Doi-Ohta theory [Lee and Park, J. Rheol. **38**, 1405 (1994)] predict phase separation in contrast to the experimental evidence of stable emulsion. The Palierne emulsion model [Rheol. Acta **29**, 201 (1990)] is used to characterize the linear viscoelastic properties of the blend before and after the transient shear experiments.

**Keywords :** modelling, polymer blends, morphology, creep, stress growth

## 5.2) Introduction

For the last 60 years, considerable efforts have been devoted to the study of the relationships between rheology and morphology of emulsions from the theoretical as well as experimental point of view. The subject is of prime importance because the blending of immiscible polymers produces generally a two phase morphology. This microstructure then governs the final properties of the material. In order to find the key parameters controlling the development of the morphology for optimizing the manufacture of new blends, it is essential to provide a relationship between the flow conditions and the morphology. This is a fascinating but also a very complex task. The main question that arises is how rheological models can be used to describe the morphology and eventually predict quantitatively the structural changes occurring during flow?

Under an applied flow, the complex structure of an immiscible molten blend changes and this in turn affects the rheology of the fluid. A large amount of work has been carried out on immiscible blends subjected to small amplitude oscillatory flow [Scholtz et al. (1989); Graebbling and Muller (1990); Brahim et al. (1991); Graebbling et al. (1990), (1993); Bousmina and Muller (1993); Carreau et al. (1994); Germain et al. (1994); Bousmina et al. (1995); Friedrich et al. (1995); Lacroix et al. (1996), (1997)]. The linear viscoelastic properties can be then used to describe the microscopic structure as long as the morphology is stable and no degradation occurs. In the case of small amplitude oscillatory flow, the major characteristic of the response of the blends is an increase in elasticity at low frequencies. Several emulsion models have been developed to describe or predict this long relaxation time process. This has been associated to the deformability of the suspended particles and their recovery to their equilibrium shape under the effects of the interfacial tension. The Paliarne model (1990), (1991) is the most widely used model to describe the linear properties of emulsion type polymer blends. The agreement between the Paliarne model predictions and the data is generally excellent. Nevertheless, this type of model is restricted to small amplitude oscillatory flow and cannot be used for large deformation flows

where the dispersed phase is highly deformed.

In blending and in processing operations, coalescence and breakup phenomena take place, which may affect the rheological properties depending on the composition and on the strain. In this case, the measured rheological properties are no more representative of a given morphology but reflect the morphological changes induced by the flow. The necessity to provide a description for this dynamics of the morphology occurring during the flow had led Doi and Ohta (1991) to introduce new constitutive equations for complex interfaces that take into account also coalescence and breakup phenomena. The theory was originally developed for an equal mixture of Newtonian fluids with similar viscosities and viscoelastic behavior is brought about by an additional stress due to the interfacial tension in the deformations generated during the flow. The theory predicts that the shear stress and the first normal stress difference are proportional to the shear rate. These scaling relations were investigated experimentally by Takahashi et al. (1994a), (1994b) who showed that the relations hold for mixtures of immiscible fluids having the same viscosity and different compositions. However, observed undershoots and overshoots after stepping up and stepping down the shear rate were not predicted by the Doi-Ohta theory. The same conclusions were made by Guenther and Baird (1996) who studied a blend of nearly Newtonian (PET/PA) fluids. More recently, the Doi and Ohta theory has been used with several blends of nearly inelastic polymers at various concentrations and viscosity ratios [Vinckier et al., (1996)]. The normal stress due to the interfacial contribution has been related to the morphology of the blends under steady state and the specific interfacial area was found to be proportional to the ratio of the interfacial tension over the shear stress.

Lee and Park (1994) have extended the Doi-Ohta theory and have proposed a modification of the stress tensor to take into account the mismatch of viscosities in polymer blends. They have introduced, based on the work of Schowalter et al. (1968) and Mellema and Willemse (1983), a viscosity ratio term and they have also proposed a modified relaxation mechanism. Assuming the Cox-Merz rule to be valid for the pure components,

they compared their model predictions to experimental data for a polystyrene/polyethylene (PS/PE) system over a wide range of compositions in the case of small amplitude oscillatory flows. We have recently done a detailed comparison of both the Lee and Park and Paliarne models for various types of blends in the linear viscoelastic domain [Lacroix et al., (1997)]. The limitations of the Lee and Park model have been underlined and we have proposed a modification of the mixing rule included in the Lee and Park model and obtained a better description of our experimental linear viscoelastic data. At high frequency, this modified model reduces to the Dickie's results (1973) which are retrieved when setting the interfacial tension to zero in the Paliarne model. This was the first step before assessing the Lee and Park model for large deformation flows. As far as we know, no steady shear nor transient measurements have been compared with their model predictions.

Most of the experimental studies in the literature make use of the Doi-Ohta theory for immiscible polymer blends [Takahashi et al. (1994a), (1994b), (1995); Guenther and Baird (1996); Vinckier et al. (1996), (1997)]. Using a thermodynamic approach, Grmela and Ait-Kadi (1994) have developed a set of equations that extends the model of Doi and Ohta (1991). The objective of this work is to evaluate the ability of the modified Lee and Park model [Lacroix et al. (1997)] and of a modified Grmela and Ait-Kadi model for predicting the rheological properties and the morphological changes occurring during simple shear flow. Before presenting the results, we will first recall the major assumptions leading to the development of the Lee and Park model, of its modification, and then we will introduce the proposed modification of the Grmela and Ait-Kadi model. These two models are shown to predict either qualitatively or quantitatively the morphological evolution of polypropylene/ethylenevinylacetate-ethylenemethylacrylate PP/(EVA-EMA) blend during shear flow and after cessation of the flow, using only a few parameters.

### 5.3) Rheological models

#### 5.3.1) Lee and Park model (1994)

The Lee and Park model is based on the Doi and Ohta theory (1991),(1993). This theory is now relatively well documented and has been investigated with different kinds of systems [Takahashi et al. (1994a), (1994b), (1995); Guenther and Baird (1996); Vinckier et al. (1996), (1997); Lacroix et al. (1997)]. Lee and Park have considered three different mechanisms of relaxation, introducing an additional term on the time evolution equations of Doi and Ohta. They also modified the stress equation to take into account the mismatch of viscosities of the different polymers. This results in the following set of coupled equations relating the evolution with the time of the anisotropy tensor  $q$ , the evolution with the time of the interfacial area per unit of volume  $Q$ , to the extra stress tensor (we use the summation convention, i.e. summation over the repeated indices) :

$$\frac{dq_{ij}}{dt} = -q_{ik}\kappa_{kj} - q_{jk}\kappa_{ki} + \frac{2}{3}\delta_{ij}\kappa_{lm}q_{lm} - \frac{Q}{3}\dot{\gamma}_{ij} + \left(\frac{q_{lm}\kappa_{lm}}{Q}\right)q_{ij} - d_1\frac{\alpha}{\eta_M}Qq_{ij} - d_1d_3\frac{\alpha}{\eta_M}\left(\frac{q_{lm}q_{lm}}{Q}\right)q_{ij} \quad (5.1)$$

$$\frac{dQ}{dt} = -\kappa_{ij}q_{ij} - d_1d_2\frac{\alpha}{\eta_M}Q^2 - d_1d_3\frac{\alpha}{\eta_M}q_{ij}q_{ij} \quad (5.2)$$

$$\sigma_{ij} = \left(1 + \frac{6(\eta_I - \eta_M)}{10(\eta_I + \eta_M)}\phi\right)\eta_M\dot{\gamma}_{ij} - \alpha q_{ij} - P\delta_{ij} \quad (5.3)$$

where  $\alpha$  is the interfacial tension,  $\eta_M$  and  $\eta_I$  the viscosities of the matrix and of the inclusions respectively,  $\phi$  the volume fraction of the dispersed phase,  $\dot{\gamma}_{ij} = \kappa_{ij} + \kappa_{ji}$  are the components of the rate of deformation tensor, and  $\kappa_{ij}$  are the components of the velocity gradient tensor,



$\delta$  is the Kronecker symbol,  $P$  the pressure and  $d_1, d_2, d_3$  ( $\lambda, \mu, \nu$  respectively in Lee and Park) are denoted to as degrees of total relaxation, of size relaxation and of breakup and shape relaxation [Lee and Park, (1994)]. Some questions remain about the use of Eq. (5.3). For dilute suspensions of rigid spheres, the well-known Einstein result is not retrieved. Since the particles are non deformable, no contribution comes from the interface. This model has been used by Lee and Park in the case of small amplitude oscillatory flow by assuming that the Cox-Merz rule was only valid for the pure components. Depending on the rheological properties of the components, the Lee and Park equation could lead to an overestimation of the small amplitude oscillatory flow data at high frequencies [Lacroix et al. (1997)]. We have therefore proposed another mixing rule to retrieve as a limiting case Einstein's result and to better describe our experimental data [a more complete expression is developed in Grmela and Ait-Kadi (1994) and is presented in the next section]. This empirical relation is expressed as :

$$G_B^* = \left( \frac{1+3/2H^*}{1-H^*} \right) G_M^* \quad (5.4)$$

with

$$H^* = \phi \frac{2(G_I^*(\omega) - G_M^*(\omega))}{2G_I^*(\omega) + 3G_M^*(\omega)} \quad (5.5)$$

where  $G_B^*$  is the complex modulus of the blend,  $G_I^*$  and  $G_M^*$  are the complex moduli of the dispersed phase (inclusions) and of the matrix and  $\phi$  is the volume fraction of inclusions. If we assume the Cox-Merz rule to be valid for the pure components, the extra stress tensor for the blend can be expressed by :

$$\sigma_{ij} = \eta_M \left( \frac{1+3/2H}{1-H} \right) \dot{\gamma}_{ij} - \alpha q_{ij} \quad (5.6)$$

with  $H$  given by :

$$H = \phi \frac{2(\eta_I - \eta_M)}{2\eta_I + 3\eta_M} \quad (5.7)$$

The transformation of Eq. (5.4) raises exactly the same question than the development of the Lee and Park equation for small amplitude oscillatory flow. We have already discussed this point in our previous article but we think it should be briefly recalled. One could think that the derivation of Eq. (5.6) from Eq. (5.4) implies necessarily that the Cox-Merz rule is considered to be valid for the blend. This is not the case. Experimental studies [ Han et al. (1995); Bousmina and Muller (1996)] show that the morphological changes induced by the flow will modify the rheological properties of the blend. Therefore the Cox-Merz rule will be no longer valid. On the other hand, the following analysis can be made : the extra stress tensor for the blend is the result of the bulk properties of the components, i.e. the mixing rule, added to a contribution due to the interface evolution. By assuming the Cox-Merz rule to be valid for the pure components and because the interface evolution can be expressed for various types of flow, this legitimizes the transformation of Eq. (5.4). By using this argument, the viscosity of the blend can be calculated from Eq. (5.6) by simply dividing the shear stress by the shear rate. One must also keep in mind that the interface evolution equations of  $q$  and  $Q$  [Eqs. (5.1) and (5.2)] have been originally developed for a blend with components of similar Newtonian viscosities in a ratio 1:1. The use of such a set of equations for molten polymer blends of different viscosities and elastic properties constitutes a crude approximation. It is clearly understandable that the viscosity ratio as well as the elastic ratio should influence the interface during the flow. For blends with components of different viscosities, this model, with the modified Grmela and Ait-Kadi model presented below are the only semi-theoretical models available for describing the anisotropy tensor as well as the interface area evolution under large strain flows taking into account breakup and coalescence phenomena. This approach is essential if one wishes to predict the morphological evolution of a blend under typical processing conditions.

### 5.3.2) Grmela and Ait-Kadi model (1994)

Grmela and Ait-Kadi have developed a set of equations governing the evolution with time of the two quantities of interest,  $q$  and  $Q$ , as well as the extra stress tensor ( $\sigma_{ij}$ ) expressed in terms of  $q$  and  $Q$  :

$$\begin{aligned} \frac{\partial q_{ij}}{\partial t} = & -q_{kj} \frac{\partial}{\partial r_k} \left( \frac{\partial \Phi}{\partial u_i} \right) - q_{ki} \frac{\partial}{\partial r_k} \left( \frac{\partial \Phi}{\partial u_j} \right) + \frac{2}{3} \delta_{ij} q_{lk} \frac{\partial}{\partial r_k} \left( \frac{\partial \Phi}{\partial u_l} \right) - \frac{Q}{3} \left( \frac{\partial}{\partial r_i} \left( \frac{\partial \Phi}{\partial u_j} \right) + \frac{\partial}{\partial r_j} \left( \frac{\partial \Phi}{\partial u_i} \right) \right) \\ & + \frac{q_{km} q_{ij}}{Q} \frac{\partial}{\partial r_k} \left( \frac{\partial \Phi}{\partial u_m} \right) - \frac{\partial \Psi}{\partial (\partial \Phi / \partial q_{ij})} \end{aligned} \quad (5.8)$$

$$\frac{\partial Q}{\partial t} = -q_{ij} \frac{\partial}{\partial r_i} \left( \frac{\partial \Phi}{\partial u_j} \right) - \frac{\partial \Psi}{\partial \left( \frac{\partial \Phi}{\partial Q} \right)} \quad (5.9)$$

$$\sigma_{ik} = q_{ik} \frac{\partial \Phi}{\partial Q} + \frac{2}{3} Q \frac{\partial \Phi}{\partial q_{ik}} + 2 q_{kj} \frac{\partial \Phi}{\partial q_{ij}} - \frac{q_{ki} q_{ml}}{Q} \frac{\partial \Phi}{\partial q_{ml}} \quad (5.10)$$

We shall see that with an appropriate choice of the thermodynamic potential  $\Phi$  and the dissipative potential  $\Psi$ , Eqs. (5.8) and (5.9) become identical to equations (5.1) and (5.2). Expression (5.10) for the extra stress tensor contains, however, non linear terms compared to Eq. (5.3). In the original publication of Grmela and Ait-Kadi (1994), the sixth term on the right hand side of their equation (6) differs from the Doi and Ohta equation [equation (4.1) in Doi and Ohta (1991)] by the multiplicative factor 2. This is a calculation error. In the original expression of the extra stress tensor, the fourth term on the right hand side of Eq. (5.8) in Grmela and Ait-Kadi (1994) is multiplied by 2 which is also a calculation error.

Equations (5.8), (5.9) and (5.10) have been derived by Grmela and Ait-Kadi (1994) using the Poisson bracket formulation. We present here a somewhat more direct derivation. Let us consider first the non dissipative part of Eqs. (5.8) and (5.9), i.e with  $\Psi = 0$  and define a conformation tensor  $C$  that characterizes an element of surface. Its convection is governed by the lower convected derivative :

$$\frac{\delta C_{ij}}{\delta t} = \frac{\partial C_{ij}}{\partial t} + C_{kj}\kappa_{ki} + C_{ki}\kappa_{kj} = 0 \quad (5.11)$$

We assume here, as in Doi and Ohta (1991) and in Grmela and Ait-Kadi (1994), that  $C$  is uniform, i.e. independent of the position vector. If we relate the tensor  $C$  to  $q$  and  $Q$  by :

$$Qq_{ij} = C_{ij} - \frac{1}{3}Q^2\delta_{ij} \quad (5.12)$$

and with

$$\sigma_{ij} = 2C_{ik}\frac{\partial\Phi}{\partial C_{kj}} \quad (5.13)$$

we recover Eqs. (5.8), (5.9) and (5.10) with  $\Psi = 0$ . The expression for the extra stress tensor (5.13) is implied by the Poisson bracket formalism [Grmela (1988)] and also by the compatibility with thermodynamic analysis [Grmela (1985)]. In the original publication [Grmela and Ait-Kadi (1994)] the thermodynamic potential  $\Phi$  is defined by :

$$\Phi = \int dr u^2(r)/2\rho + C_1 \int dr Q(r) + C_2 \int dr q_{ij}(r)q_{ij}(r) \quad (5.14)$$

where  $\rho$  is a constant density,  $u$  is the momentum field and the dissipative potential  $\Psi$  is expressed by :

$$\Psi = \int dr K_1 \left( \frac{\partial\Phi}{\partial Q(r)} \right)^2 + \int dr K_2 \left( \frac{\partial\Phi}{\partial q_{ij}(r)} \right)^2 \quad (5.15)$$

with  $K_1 = \Lambda_1 Q^2$  and  $K_2 = \Lambda_2 Q$ ,  $\Lambda_1$  and  $\Lambda_2$  are parameters and  $r$  is a position vector. The last term on the right hand side of Eq. (5.14) represents a contribution to the thermodynamic potential due to the deformation of the interface. At equilibrium, the interface is not deformed,  $q = 0$ , and the term is thus equal to zero. The quadratic form of  $\Psi$  was chosen by Grmela and Ait-Kadi so that  $\Psi(0)=0$ ,  $\Psi$  reaches its minimum at 0, and is a convex function in a neighborhood of 0. The two extreme cases for a blend are a complete miscibility or a macroscopically phase separated state. In this original form [Eqs. (5.8), (5.9) and (5.10)], the model predicts that  $Q$  is equal to zero under no flow (equilibrium conditions) corresponding to a macroscopically phase separated state. This result is thermodynamically sound but it cannot describe the pseudo-equilibrium conditions of an emulsion type blend. Under the effects of the interfacial tension, the deformed droplets of the minor phase tend to recover their equilibrium shape. Once this process is realized, no more relaxation will occur in absence of migration and/or of coalescence of particles, and the final morphology state will be different from  $Q = 0$ . These considerations have been introduced in a modification of the relaxation rate in the Doi-Ohta theory [Doi and Ohta (1991); Doi (1993)] and exploited by Guenther and Baird (1996). To take into account this phenomenon which occurs in almost all cases for immiscible polymer blends, we have to modify the dissipative potential  $\Psi$ . Several possibilities are offered for choosing this potential. We have chosen  $\Psi$  in such a way that the relaxation modes proposed by Lee and Park (1994) can be retrieved:

$$\Psi = \Psi_0 + \Psi_1 + \Psi_2 + \Psi_3 \quad (5.16)$$

with

$$\Psi_0 = \int dr \frac{1}{2} K_0 \left( \frac{\partial \Phi}{\partial Q(r)} \right)^2 \quad (5.17)$$

$$\Psi_1 = \int dr \frac{1}{2} K \left( \frac{\partial \Phi}{\partial Q(r)} \right)^2 \quad (5.18)$$

$$\Psi_2 = \int dr \frac{1}{2} K_2 \left( \frac{\partial \Phi}{\partial q_y(r)} \right)^2 \quad (5.19)$$

$$\Psi_3 = \int dr \left( \frac{\partial \Phi}{\partial q_y(r)} \right)^2 \frac{1}{4} K_3 \left( \frac{\partial \Phi}{\partial q_{lm}(r)} \right)^2 \quad (5.20)$$

$K_2$ ,  $K_3$  are parameters whereas  $K = K_1 q_y q_{yy}$  and  $K_0 = \Lambda_1 Q^2$  with  $\Lambda_1$  also a parameter. By substituting  $\Psi$  and  $\Phi$  in Eqs. (5.8) and (5.9) we can obtain evolution equations for  $q$  and  $Q$  which reduce to the evolution equations (5.1) and (5.2) of Lee and Park. The parameters  $K_1$ ,  $K_2$ ,  $K_3$  and  $\Lambda_1$  used in the dissipative potential are related to the previous constants  $d_1$ ,  $d_2$ ,  $d_3$  so as to retrieve Eqs. (5.1) and (5.2). In this case, the only difference between the Lee and Park model and this model comes from the expression of the stress tensor. In the case of the Lee and Park model, the contribution due to the interface to the extra stress tensor is expressed by  $-\alpha q_y$ , whereas the theory of Grmela and Ait-Kadi leads to an equation involving non linear terms [see Eq. (10)]. Two constants  $C_1$  and  $C_2$  are introduced in the derivatives of  $\Phi$ ,  $\partial \Phi / \partial Q$  and  $\partial \Phi / \partial q_y$  [see Eq. (14)]. By analogy with the Doi and Ohta theory,  $C_1$  can be set equal to  $-\alpha$ . The parameter  $C_2$  is new with respect to the Doi-Ohta theory.

#### 5.4) Experimental

The blends investigated in this study are mixtures of polypropylene (PP), ethylene vinylacetate (EVA) and ethylenemethylacrylate (EMA). Since EVA and EMA are miscible, binary blends of PP and (EVA-EMA) are then obtained. The commercial polymers, PP3020GN3 (PP,  $M_w = 337\,000 \text{ g.mol}^{-1}$  with a polydispersity index  $PI=5.3$ ), EVATANE 2805 (EVA,  $M_w = 53\,000 \text{ g.mol}^{-1}$ ,  $PI=3.0$ ) and LOTRYL 28MA07 (EMA,  $M_w = 81\,300 \text{ g.mol}^{-1}$ ,

PI=5.1), were supplied by ELF-ATOCHEM.

#### **5.4.1) Blending procedure**

For each type of blends, as well as for the unblended components, the following blending procedures have also been applied, so that the thermomechanical history of the blends and of the components would be the same.

The pellets were first dry-blended and melted in the Brabender at a set temperature of 200°C and with a rotor speed of 20 rpm. Then, once all the pellets were loaded and melted, the speed was increased to 40 rpm and the components were mixed during 200 s. This time was sufficient to reach a constant torque value. The melt processing was carried out under nitrogen atmosphere to prevent degradation. The samples were extracted from the chamber and quenched in cold water. Samples for rheological measurements were then compression molded at 200°C during 7 min. The pressure load was progressively increased from 200 kPa to 1.4MPa. The samples were then quenched in cold water. Blends of composition by weight percent of 70/30 (corresponding to a volume concentration of 0.285 of the dispersed phase) and 30/70 were investigated. This specific composition of 70/30 PP/(EVA/EMA) has been chosen so that morphological evolutions can be detected using rheological measurements. Compositions of 90/10 and 80/20 PP/(EVA/EMA) have been investigated but they did not lead to interesting results considering the relative small range of shear rates that could be covered in rheometry. A small amount of antioxidant (Irganox B225 from CIBA-GEIGY) was added to prevent the degradation of the PP.

#### **5.4.2) Rheological measurements**

Various experiments have been carried out either on a controlled stress rheometer (Bohlin CSM) or on a controlled strain rheometer (Bohlin VOR). A cone-and-plate geometry was chosen in order to avoid complication with non uniform shear rate. The

diameter of the plates were either 25 mm in the case of the CSM with an angle of  $2.5^\circ$  or 40 mm for the VOR with an angle of  $2^\circ$ . The measurements were carried out under nitrogen atmosphere at a set temperature of  $200^\circ\text{C}$  for both rheometers. The range of shear rates investigated was restricted because at relatively moderate shear rates the sample were ejected from the cone and plate geometry. Transient shear experiments were carried out using both types of apparatus, and the linear viscoelastic properties of the molten blends were investigated in a frequency range of 0.001 Hz - 10 Hz using the CSM. In that case the applied stress was controlled to keep the total deformation at around 0.05. In all cases, the linear as well as the non linear viscoelastic data of the blends have been reproduced several times and this with different batches of polymers. The reproducibility of the data is estimated to be  $\pm 10\%$ .

#### 5.4.3) Scanning electron microscope

The morphologies of the sheared and non sheared samples were frozen and compared in order to study the morphological evolution induced in the imposed simple shear flow experiments carried out on the VOR. After the blends reached a quasi-steady state morphology (a balance between breakup and coalescence), the flow was stopped and the sheared samples were allowed to relax. The time scale of this process could be deduced from the evolution with time of the anisotropy tensor  $q$ . Recall that  $q_{ii} = 0$  corresponds to an isotropic state. It could be of the order of few seconds to few minutes depending on the shear rate. But in all cases we let the sample relax much longer than the time predicted by the model. Then the geometry was put into cold water and the samples were frozen in few seconds. This procedure is very important because the extracted samples cooled with dry air showed completely different morphologies due to crystallization effects in the PP phase. Indeed the PP begins to crystallize whereas the EVA-EMA phase is still in the molten state. Hence we believe that the morphologies determined from these quenched samples are more representative of "the molten state". The extracted blend morphologies were determined using a Jeol JSM-840 scanning electron microscope, for fractured samples in liquid nitrogen



and coated with 50/50 gold palladium to avoid charging. To account for the fact that the observation plane does not necessarily cut through the particles at their equator, the Scharwz-Saltikhov (1967) corrections were applied, using the program developed by Lavallée (1990). The number and volume average diameters  $d_n$  and  $d_v$  were determined from the surface analysis of at least 300 particles with a digitalizing device. Our estimate of the accuracy of the measurements is at best  $\pm 10\%$ .

## 5.5) Results and discussion

Measurements in the linear regime as well as in the non linear region have been carried out. We will first present the linear viscoelastic data, then discuss the non linear viscoelastic data before reconsidering dynamic data upon cessation of flow.

### 5.5.1) Linear viscoelasticity

As already mentioned, measurements under small amplitude oscillatory flow constitute a powerful tool for describing the microscopic state of the blend. Figure 5.1(a) shows the dynamic moduli of the pure components so as their viscosities whereas Fig. 5.1(b) reports the  $G'$  and  $G''$  data for the unsheared 70/30 PP/ (EVA-EMA) blend. For comparison, the elastic modulus of the matrix is also shown in Fig. 5.1(b). The blend exhibits an increase in elasticity at low frequencies, characteristic of the deformability of the suspended droplets [ Bousmina et al. (1995); Carreau et al. (1994), Bousmina and Muller (1993); Graebbling et al. (1993); Graebbling and Muller (1990); Scholtz et al. (1989)]. This is now relatively well known and it can be predicted by the Palierne model (1990) or described by the Lee and Park model (1994) or by its modified version [Lacroix et al. (1997)]. If the interfacial tension, the volume average diameter of the particles and the rheological behavior of the components are known, the linear viscoelastic behavior of the blend can be predicted by the Palierne model without using any adjustable parameters. On the other hand the use of the Lee and Park model requires the determination of a fitting parameter.

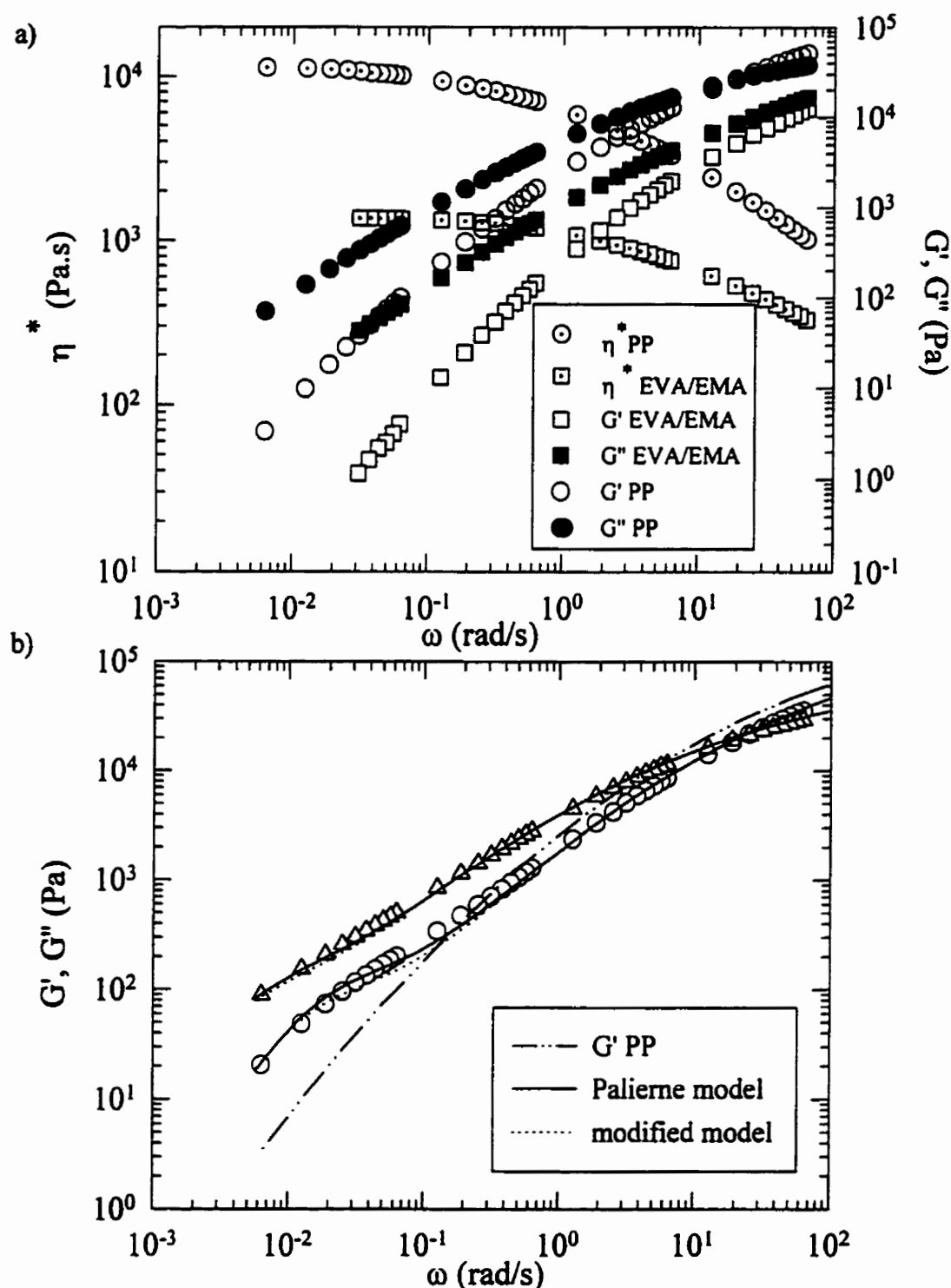


Figure 5.1 : Linear viscoelastic properties of the PP, EVA-EMA and 70/30 PP/(EVA-EMA) blend at  $T=200^\circ\text{C}$  : (a) Complex viscosities and dynamic moduli of the PP and EVA-EMA components. (b) Comparison between linear data and model predictions for the 70/30 PP/(EVA-EMA) blend.

The Palierne model predictions were calculated using the volume average diameter determined from the morphological analysis ( $R_v = 3.75 \mu\text{m}$ ) and the interfacial tension value,  $\alpha = 1.2 \text{ mN/m}$ , obtained via the harmonic mean equation. The Palierne model was used in his simplest form, assuming constant interfacial tension and particles monodisperse in size with a radius  $R_v$  [the polydispersity did not exceed 2, Graebling et al. (1990); Bousmina et al. (1995)]. The agreement between the Palierne model predictions and the data is excellent as shown in Fig. 5.1(b).

We observed that the Lee and Park model led to an overestimation of the high frequency data for the PP/(EVA-EMA) blend as well as for the PP/EVA blends [Lacroix et al. (1997)]. So, in Fig. 5.1(b) we report the model predictions obtained by using the modified mixing rule introduced in Eq. (5.4) combined to the relaxation mechanism proposed by Lee and Park. We consider that no coalescence takes place and we set  $d_2$  equal to zero and  $d_1$  equal to  $1-\phi$ , as done by Lee and Park. We have proposed [Lacroix et al. (1997)] an approximate method to determine the parameter  $d_1$ ; this method leads to a value of around 0.65, but a slightly better fit at low frequencies is obtained with  $d_1$  equal to 0.5 when using the Lee and Park model (not shown here). Notice that we have used exactly the same value of  $d_1$  for the modified model. Both model predictions are in agreement with the experimental data but as stated previously, the Palierne model is restricted to small amplitude oscillatory flow. In the following section, we will discuss non linear viscoelastic data.

### 5.5.2) Non linear viscoelasticity

To study the morphological evolution of the blends under flow, three types of experiments have been carried out using either the controlled stress rheometer or the controlled strain rheometer. First in transient creep experiments, the samples have been subjected to stresses of different magnitude varying from 100 Pa up to 1500 Pa. It was not possible to use higher stresses because, as already mentioned, the samples were ejected rapidly from the geometry. Figure 5.2 reports the variation with time for the different applied

stresses of the 70/30 PP/(EVA-EMA) blend viscosity. This is of course not a viscosity at equilibrium for a constant shear rate. This is an instantaneous viscosity calculated using an average “local” shear rate. For the lowest stresses, a large decrease of the viscosity is first observed and then an equilibrium value is reached. At a moderate stress (750 Pa), the effects are not as much pronounced whereas at a higher stress (1500 Pa) a small increase of the viscosity is observed. Neither the matrix nor the dispersed phase alone could explain such an unusual behavior. We can attribute these evolutions to the morphological changes occurring during simple shear. This assumption is the most plausible and the final quasi steady state value of the viscosity would correspond to a stabilized structure, that means a balance between the breakup and coalescence phenomena. A steady shear rate is associated with the equilibrium evolution reached for each of the different stresses investigated. To verify the validity of our assumption, two more types of experiments have been carried out. The first set of experiments consisted of start-up experiments at a constant shear rate corresponding to the equilibrium values reached in the constant stress of experiments of Fig. 5.2. Such transient experiments are useful to test the ability of Lee-Park model and of the modified Grmela and Ait-Kadi (1994) model for predicting the morphological evolution of the blend. After the viscosity reached a constant value or before the sample would be ejected, the flow was stopped and the samples were allowed to relax. During this process, the deformed particles would recover their equilibrium shape under the effects of the interfacial tension. The second set of experiments consisted of dynamic measurements at small amplitude, carried out following a complete relaxation of the stresses, and this with the objective of comparing the linear viscoelastic properties of the blends before and after shearing.

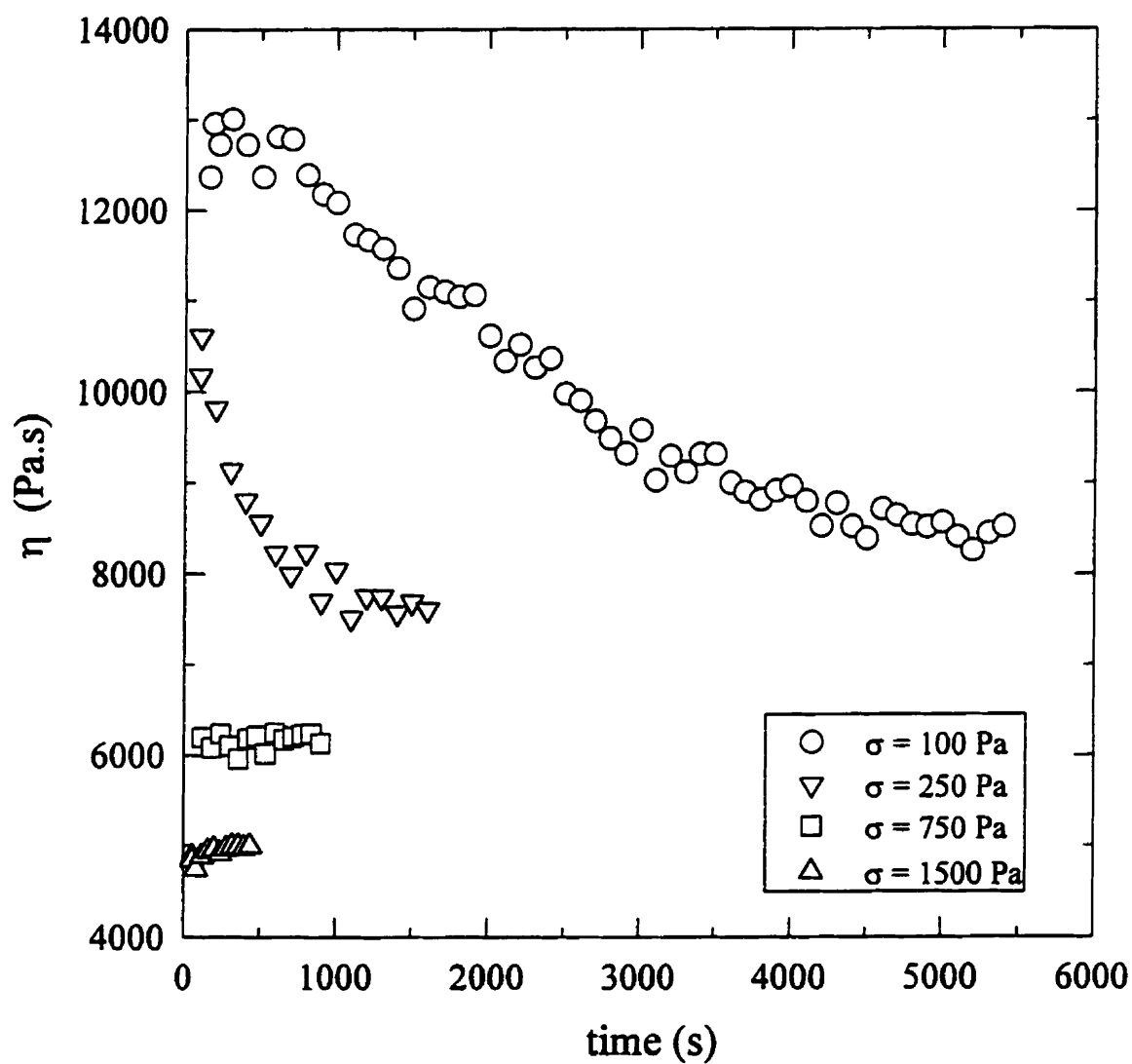


Figure 5.2 : Transient viscosity in creep as a function of time for a 70/30 PP/(EVA-EMA) blend;  $T=200^{\circ}\text{C}$ .

### 5.5.3) Stress growth results

The shear viscosity at the onset of a steady shear rate of the 70/30 PP/(EVA-EMA) blend is shown in Fig. 5.3 for four different shear rates ( $0.0126 \text{ s}^{-1}$ ,  $0.0317 \text{ s}^{-1}$ ,  $0.126 \text{ s}^{-1}$  and  $0.318 \text{ s}^{-1}$ ). Except for the lowest shear rate [Fig. 5.3(a)], an overshoot is observed at a very short time (at small deformations) and then the viscosity reaches an equilibrium value after a very long time. At larger imposed shear rates [Fig. 5.3(d)], the overshoot is then followed by an undershoot before the viscosity reaches a constant value. It must be mentioned that the corresponding stresses at the equilibrium are almost the same (the difference is around 10%) as those imposed on the controlled stress rheometer. Both “pure” components did not exhibit any measurable overshoot at the start up. For comparison, Fig. 5.3(d) reports also the growth shear viscosity of the PP matrix, for the highest shear rate. It is not to be excluded that overshoots could be observed for the pure components at higher shear rates. But in our case, the maximum shear rate investigated is relatively small. These overshoots are therefore the result of blending and are similar to those observed for thermotropic liquid crystal polymer, TLCP [Guskey and Winter (1991)], and blends of polyetherimide (PEI) with TLCP [Nobile et al. (1990)]. But the TLCPs already have their own anisotropy. It is therefore difficult to draw an analogy between the two systems.

We compare now the model predictions with the growth shear viscosity data. In order to avoid repetitive designation, we will call the modified Lee and Park model [Lacroix et al. (1997)] the LPL model and the modified model of Grmela and Ait-Kadi (1994) combined to the mixing rule included in Eq. (5.4) the LGC model. The original Lee and Park model, as well as other modified Lee and Park and Grmela and Ait-Kadi models using an additive mixing rule were found to be unsatisfactory. The descriptions of the transient data were obtained as follows. For the LPL and LGC models, the three parameters,  $d_1$ ,  $d_2$  and  $d_3$ , have to be fitted in order to follow the evolution with time of the anisotropy tensor and that of the interfacial area.

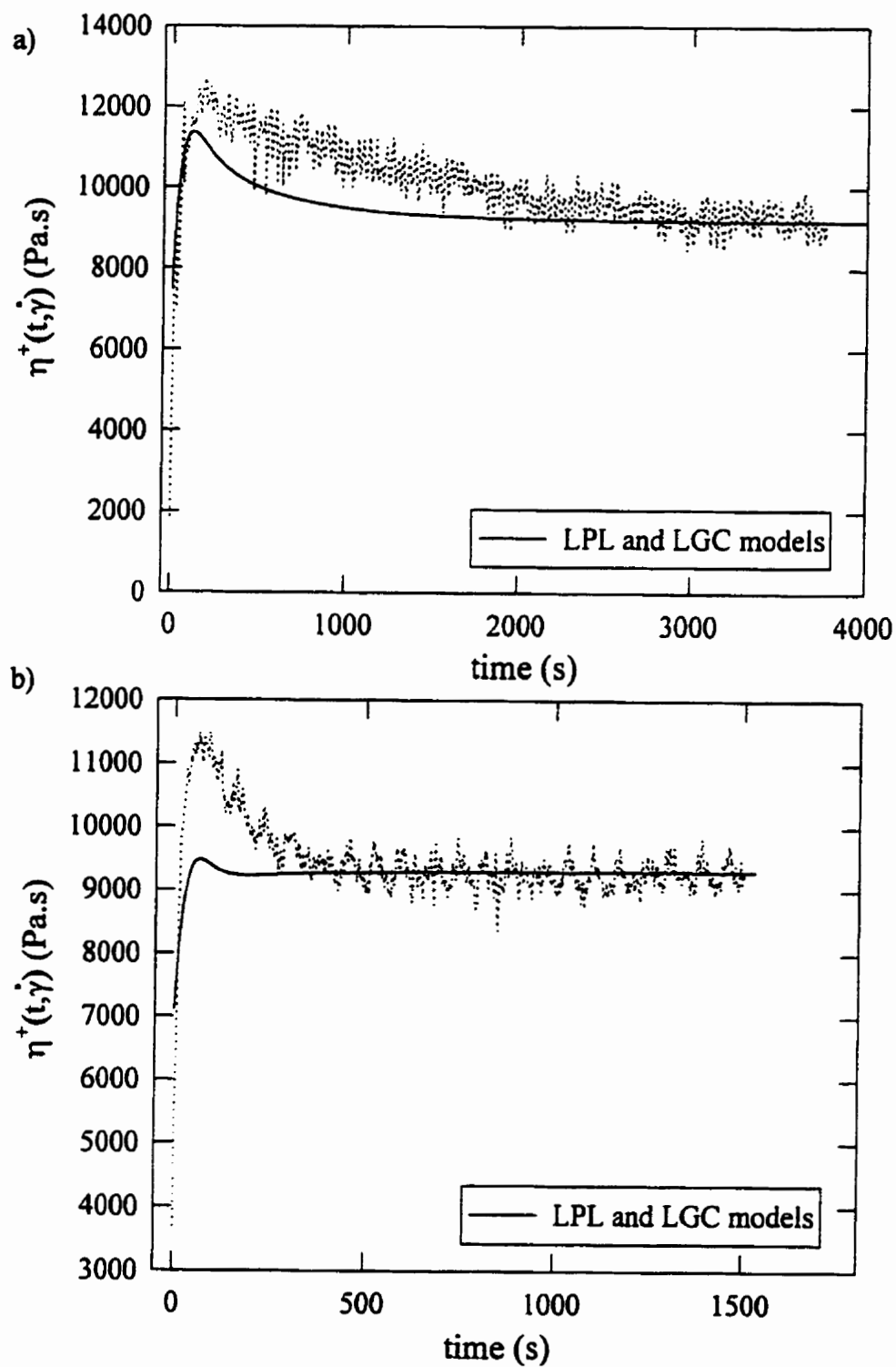


Figure 5.3 : Comparison between stress growth viscosity data and models predictions for the 70/30 PP/(EVA- EMA) blend at  $T=200^{\circ}\text{C}$  : (a)  $\dot{\gamma} = 0.0126 \text{ s}^{-1}$ , (b)  $\dot{\gamma} = 0.0317 \text{ s}^{-1}$ , (c)  $\dot{\gamma} = 0.126 \text{ s}^{-1}$ , (d)  $\dot{\gamma} = 0.318 \text{ s}^{-1}$ .

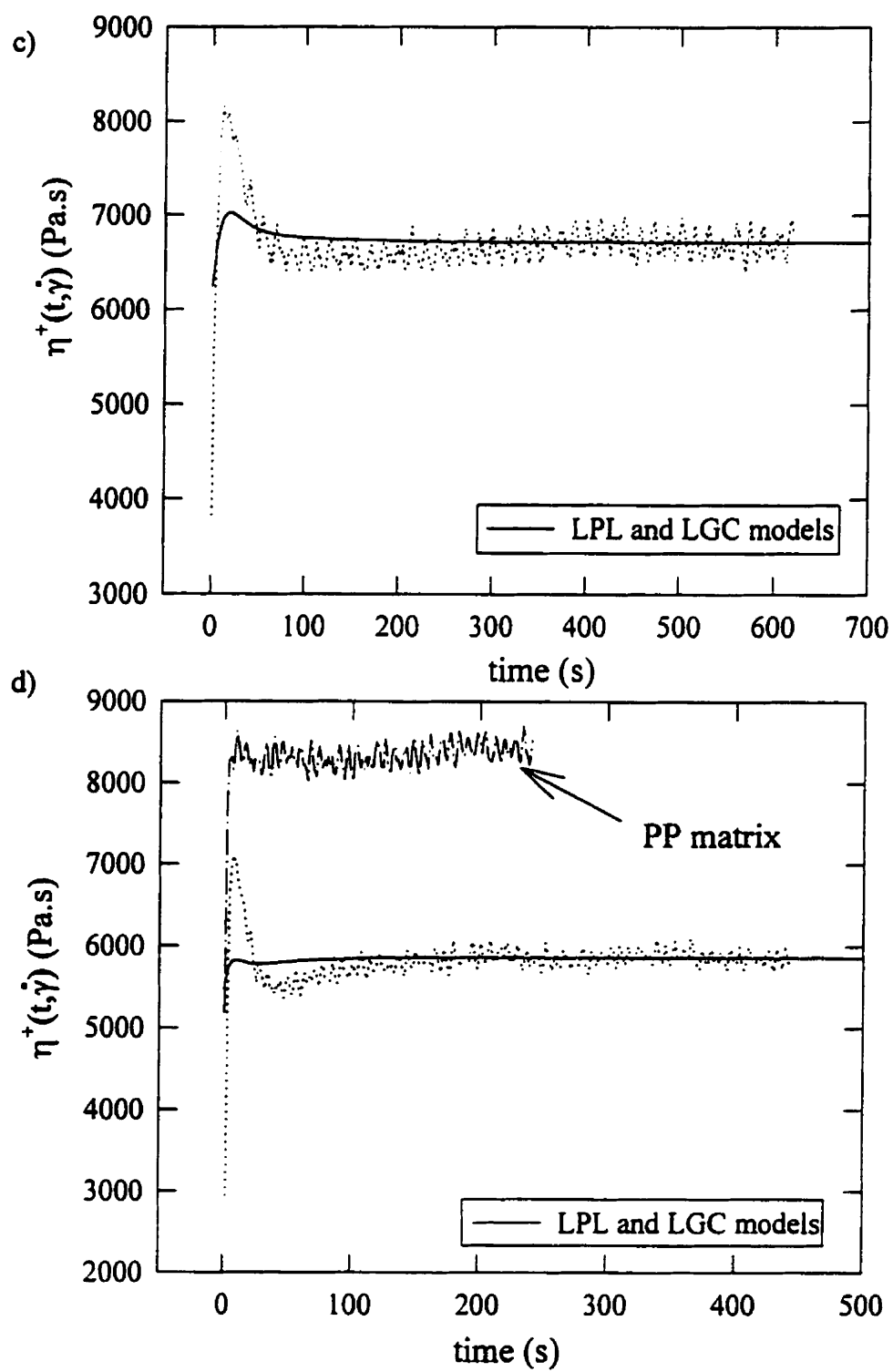


Figure 5.3 (suite)



We have shown that choosing  $d_3$  equal to  $1-\phi$  and fitting  $d_1$  gave a good description of the linear viscoelastic data at low frequencies [Lacroix et al. (1997)]. For the particular case of small amplitude oscillatory flow  $d_2$  was set equal to zero. For the non linear predictions  $d_2$  was fitted from the stress growth data as discussed below, we chose to keep  $d_3$  equal to  $1-\phi$  as done by Lee and Park (1994) and  $d_1$  equal to the value previously determined from linear viscoelastic data ( $d_1 = 0.5$ ). This last choice may appear to be arbitrary and questionable since we use dynamic data at small deformation to predict the rheological behavior of the blend under steady shear flow. We assume, however, that  $d_1$ , related to the kinetics of the relaxation of the interfacial area  $Q$  and its anisotropy  $q_y/Q$  under the effects of the interfacial tension, is not affected by the shear rate. To calculate the contribution of the bulk properties (the mixing rule) during stress growth, we further assume that the unblended components reach their equilibrium viscosity almost instantaneously. The Carreau-Yasuda model was used to calculate the viscosity of the pure components from the dynamic measurements, assuming that the Cox-Merz rule is valid for both pure components. Finally, parameter  $d_2$  was fitted to obtain the best agreement between the model predictions and the stabilized value of the viscosity. When using the LPL and the LGC models, we chose to fit the data essentially based on the quasi-steady state value for the viscosity. Better fits of the overshoots could be predicted by adjusting  $d_2$ , but then, a poorer description of the steady viscosity value was obtained. Some discrepancies between the model predictions and the overshoots can be observed in Fig. 5.3. For the highest shear rate, the models do not predict any undershoots [Fig. 5.3(d)].

When using the relaxation mechanism of Grmela and Ait-Kadi (1994) in the LGC model, two constants, resulting from the derivatives of the thermodynamic potential [Eq. (5.14)], have to be determined to estimate the contribution of the interface to the extra stress tensor. The first one  $C_1$  was set equal to  $-\alpha$  to retrieve exactly the same contribution as in the case of the Doi and Ohta theory (1991). The second constant  $C_2$  is a factor of the non linear terms and was adjusted along with  $d_2$  to describe the quasi-steady state viscosity. The model parameters are presented in Table 5.1.

Table 5.1 : Parameters used for predicting the transient rheological behavior of the blend with the LPL and LGC models; comparison between predicted radii values and experimentally 70/30 PP/(EVA-EMA) determined values

shear rate ( $s^{-1}$ )	$d_i=0.5, d_j=0.715$ and $-C_i=1.2$ mN/m			$R_{v, initial} = 3.75$ $\mu m$ , Calculated radii, $R_v$ ( $\mu m$ )		
	$d_2$ LPL	$d_2$ LGC	$C_2$ (N)	LPL model	LGC model	morphology
0.0126	0.30	0.30	$10^{-11}$	10.8	10.8	6.0
0.0317	0.22	0.22	$10^{-11}$	3.3	3.3	4.4
0.126	0.60	0.60	$10^{-11}$	3.2	3.2	3.0
0.318	0.60	0.60	$10^{-11}$	1.5	1.5	1.5

The predictions for both LPL and LGC models are essentially the same. Adding the contribution of the non linear terms did not improve, in this case, the quality of the fit for the various shear rates investigated. Slightly different predictions for the LGC model could be obtained by varying the parameter  $C_2$ . But it was not possible to get better predictions of the overshoots (Fig. 5.3). Therefore, considering the noise in the data we chose  $C_2$  to obtain the same fit for the viscosity as with the LPL model. Otherwise, both the LPL and the LGC models are able to predict qualitatively the overshoots.

We must first recall that in these models the stresses are constituted of a sum of two contributions : the bulk, i.e the mixing rule, plus a contribution related to the interface. When fitting the models to the transient data, one can observe that the predictions of the viscosity are highly sensitive to the choice of the mixing rule which constitutes the major part of the calculated value. Using a simple additive mixing rule led, for example, to completely different results and, for some values of the shear rate it was even impossible to fit the data. Therefore, we think that the mixing rule represents a major source of difficulties and that coupling effects between the bulk properties and interfacial properties (the orientation tensor) should be considered in the development of a more appropriate set of evolution equations. Second, the interface is treated as surrounded by Newtonian fluids of equal viscosity. It is

clear that a mismatch of the viscosity as well as of elasticities of the components will affect the behavior of the interface. Since we are dealing with viscoelastic materials, memory effects or coupling effects of both phases are not to be excluded.

#### 5.5.4) Predictions of the morphological changes

The LPL and LGC models can be used to predict the droplet size changes occurring during flow. Vinckier et al. (1996) have related the steady normal stress data to the morphology of the blend and used this scheme to evaluate the parameter  $\mu$  in the Doi and Ohta theory. In our case, we assess the ability of the two models (LPL and LGC) to predict quantitatively the morphological changes under finite strain. Knowing the interfacial area  $Q$  and assuming that the dispersed phase is present as spherical droplets, an average diameter can be determined ( $Q = 6\phi/d_v$ ). Figure 5.4 shows the evolution of the predicted normalized interfacial area in stress growth and relaxation experiments for two different shear rates. Depending on the shear rate, an increase or decrease of the interfacial area is predicted during stress growth. An increase of  $Q$  [Fig. 5.4(b)] implies that the breakup phenomenon has occurred whereas a decrease of  $Q$  [Fig. 5.4(a)] is associated either with coalescence or with recovery of the deformed droplets. From the value of  $Q$  after relaxation, the radius has been calculated using both models assuming spherical droplets. The results are reported in Table 5.1 and are compared with the determined values from the morphological analysis. Except at the lowest shear rate, for which the predicted value is twice the morphologically measured value with the LPL and the LGC models, the agreement between the LPL and LGC model predictions and the experimental data is astonishingly good. The breakup and coalescence phenomena occurring during finite strain flow are qualitatively and even quantitatively predicted by both models. For the lowest imposed shear rate, coalescence takes place as evidenced by the much larger droplet diameter after relaxation and in this case, the model predictions are only in qualitative agreement compared to the situation where breakup occurs. In contrast, for the highest shear rate a significant decrease of the particle size is observed (see Table 5.1).

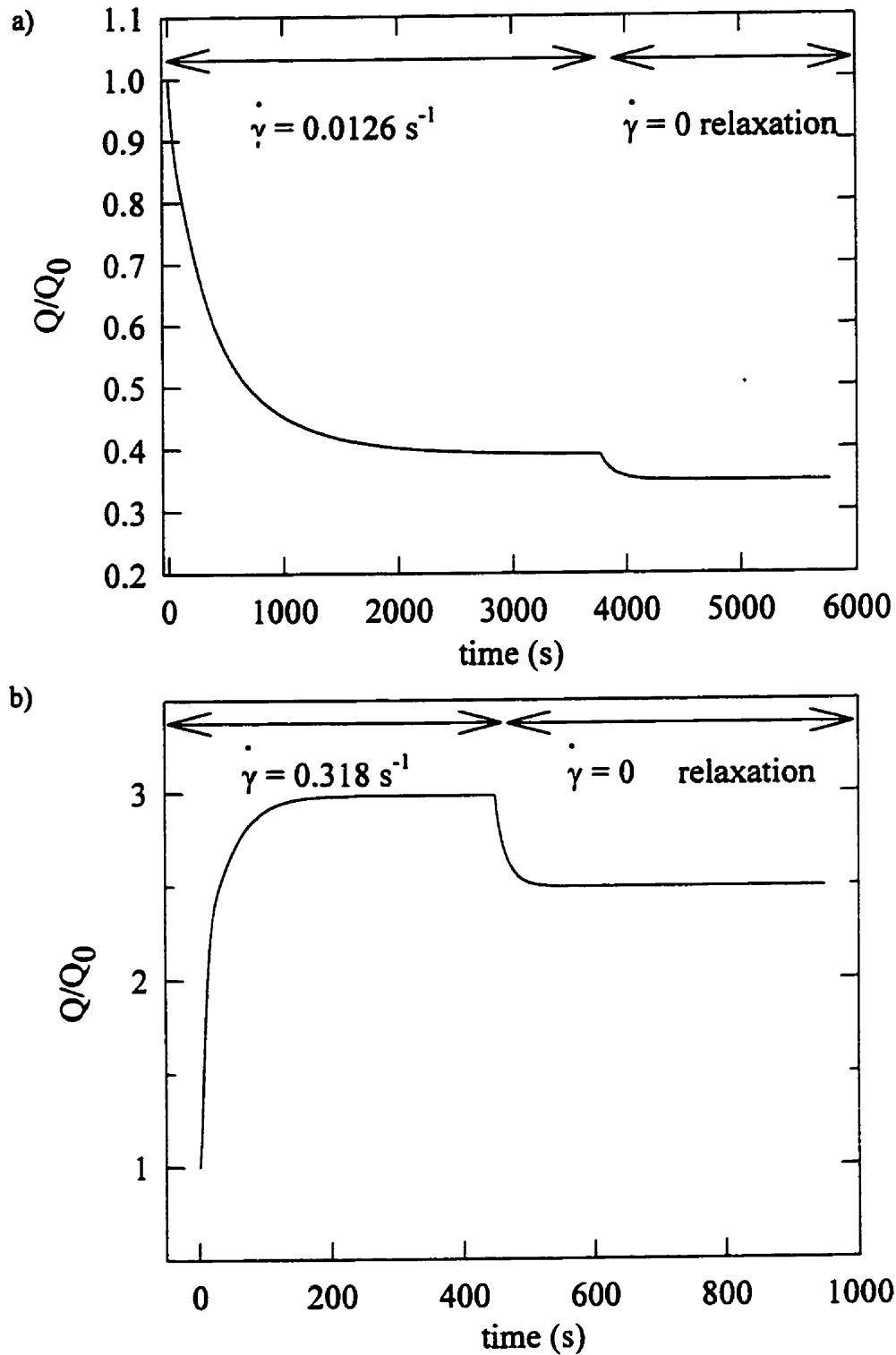


Figure 5.4 : Evolution with time of the normalized interfacial area predicted for the LGC model for the 70/30 PP/(EVA-EMA) blend in stress growth and relaxation experiment at  $T=200^\circ\text{C}$ : (a) imposed shear rate of  $\dot{\gamma} = 0.0126 \text{ s}^{-1}$ ; (b) imposed shear rate of  $\dot{\gamma} = 0.318 \text{ s}^{-1}$

The droplet diameter does not obey the proportionality relation with shear rate embedded in the Doi and Ohta theory as verified by Vinckier et al. (1996) for nearly inelastic polymers blends. Also, it was not possible to find a scaling relation between the interfacial area and the ratio of the interfacial tension over the shear stress as proposed by Vinckier et al. (1996). We found, however, semi-log relationships between the measured volume average radius and shear rate, and between the volume average radius and the ratio  $\alpha/\sigma$ . These results have a physical meaning since it is generally observed that the particle size decrease with increasing shear rate until a plateau is reached.

To confirm the above results, the dynamic data obtained following stress relaxation were compared with the Palierne model (1990) predictions calculated using the  $R_v$  values determined via the LPL and LGC models (see Table 5.1) or from the morphological analysis. As no adjustable parameters have to be fitted, the Palierne model allow a direct comparison of the results with the experimental data. These are shown in Fig. 5.5 for all the different applied shear rates. The agreement is excellent, except for the lowest shear rate [Fig. 5.5(a)] where the Palierne model predictions cannot discriminate between the diameter determined via the LPL and LGC models and that obtained from the morphological analysis. Recall that for all the droplet diameter determination using either the LPL model or the LGC model, we kept the value of parameter  $d_i$  constant and equal to 0.5. In order to verify this assumption, we have compared the LPL model predictions with the small amplitude oscillatory shear data after stress growth and relaxation using  $d_i = 0.5$  and using the diameter obtained from the morphological analysis. The agreement between the LPL model predictions and the data was found to be quite good (data not reported here). We have also verified that the LGC model was able to predict an evolution of the orientation tensor which is physically sound. For the initially dispersed spherical particles,  $q_{ij} = 0$ , and  $q_{ij}$  returns to zero corresponding to an isotropic state, following a stress growth and relaxation experiment. Figures 5.6 and 5.7 show the predicted evolution of  $q_{12}$  with time calculated for the LGC model for stress growth followed by stress relaxation.

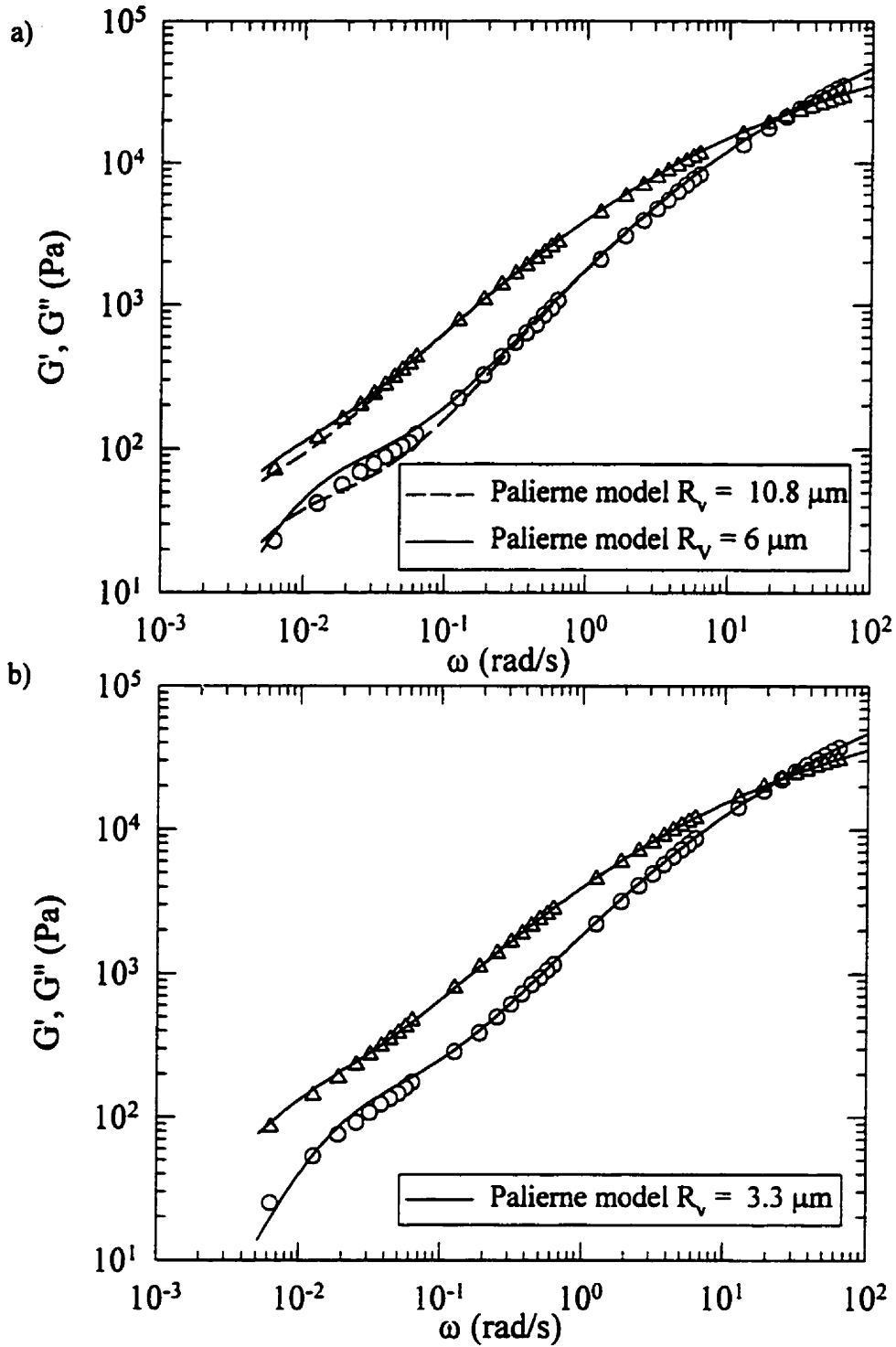


Figure 5.5 : Comparison between linear data after relaxation and Palierne model predictions for the 70/30 PP/(EVA-EMA)blend at  $T=200^{\circ}\text{C}$  using the radius values determined following relaxation after stress growth experiment at : (a)  $\dot{\gamma} = 0.0126 \text{ s}^{-1}$ , (b)  $\dot{\gamma} = 0.0317 \text{ s}^{-1}$ , (c)  $\dot{\gamma} = 0.126 \text{ s}^{-1}$ , (d)  $\dot{\gamma} = 0.318 \text{ s}^{-1}$ .

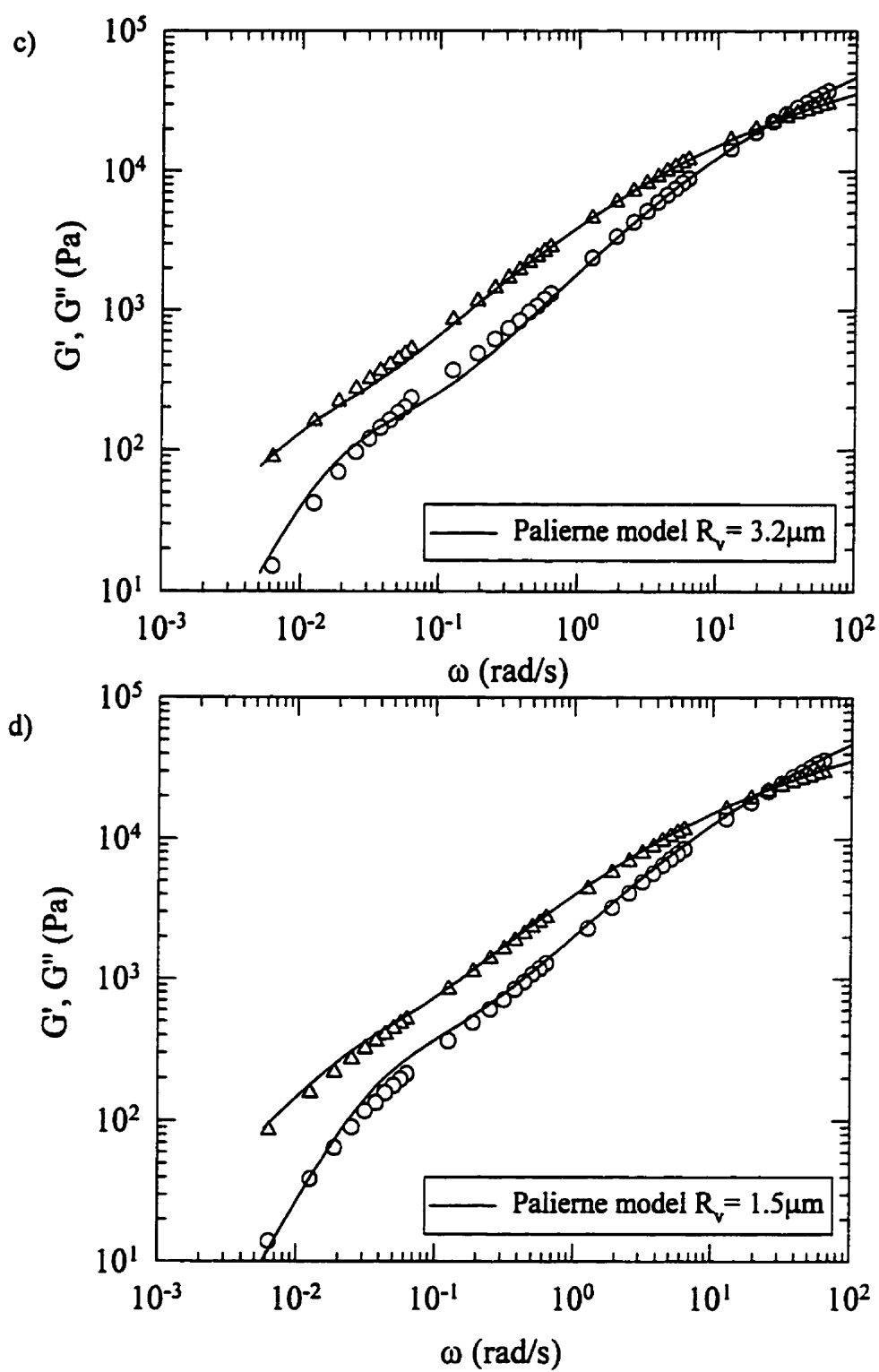
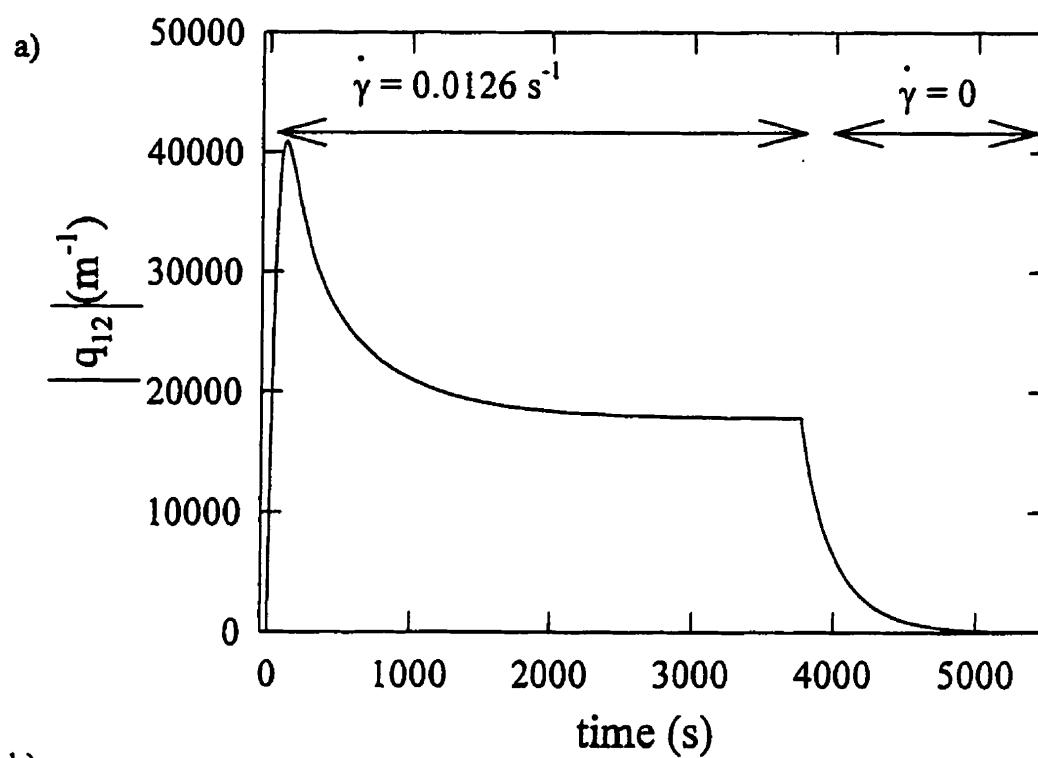


Figure 5.5 (suite)



b)

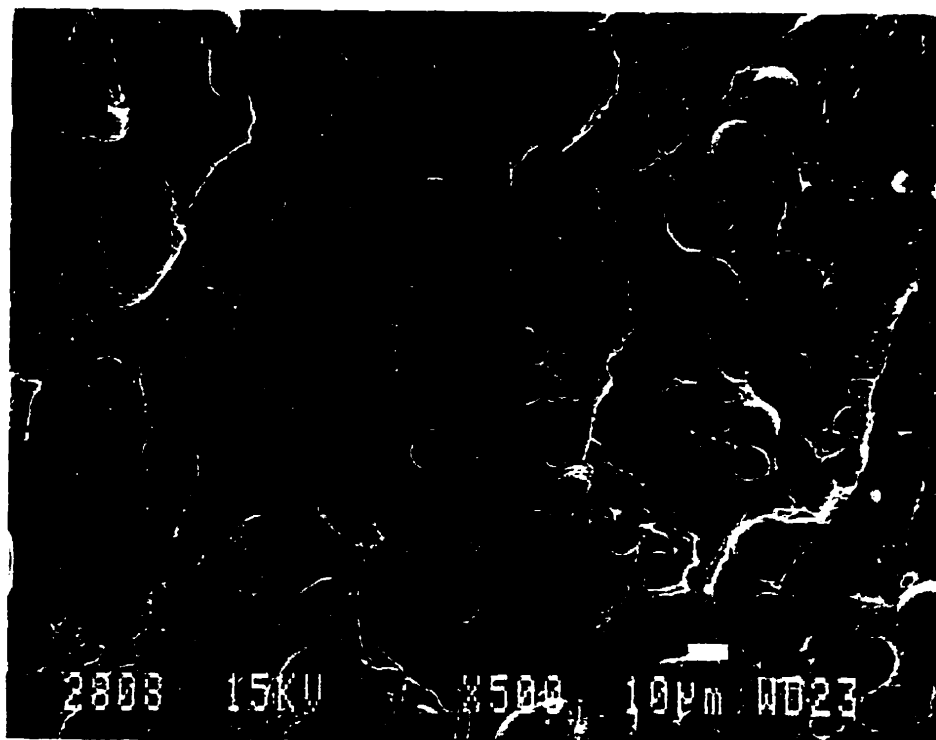
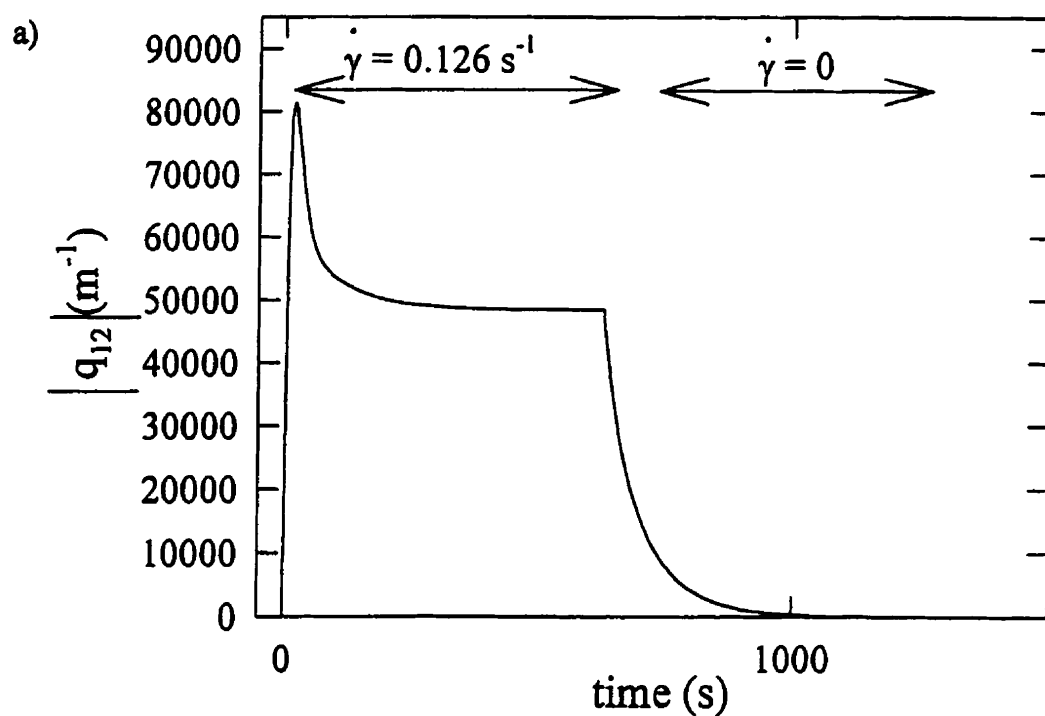


Figure 5.6 : (a) Predicted evolution with time of the anisotropy tensor component  $q_{12}$  for an imposed shear rate of  $\dot{\gamma} = 0.0126 \text{ s}^{-1}$ ; (b) scanning electron micrograph of the 70/30 PP/(EVA-EMA) blend sample after relaxation.





b)

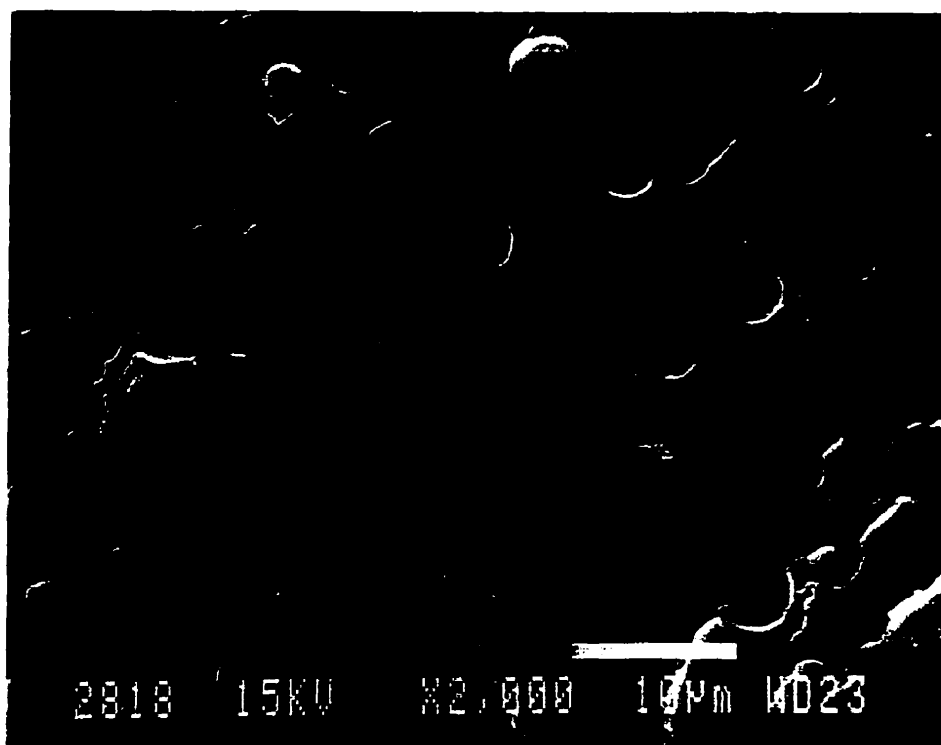


Figure 5.7 : (a) Predicted evolution with time of the anisotropy tensor component  $q_{12}$  for an imposed shear rate of  $\dot{\gamma} = 0.126 \text{ s}^{-1}$ ; (b) scanning electron micrograph of the 70/30 PP/(EVA-EMA) blend sample after relaxation.

With increasing shear rate, the time needed to reach a stabilized value of  $q_{12}$ , i.e. a constant orientation with respect to the direction of the flow, as well as the characteristic time for the relaxation process are shortened. The micrographs shown in Figs. 5.6 and 5.7 illustrate the morphological changes after complete stress relaxation for two different initially imposed shear rates. Note that the magnification of the two micrographs is different, but clearly the droplets sizes in Fig. 5.6 are considerably larger than those of Fig. 5.7 (volume average radii are reported in Table 5.1). Note that the LPL and LGC model predictions were calculated only for the stress growth and relaxation experiments and not for the creep experiments (Fig. 5.2) because the set of the governing equations which are strain-rate dependent are not easily solved for a creep (constant stress) experiment.

Let us now come back to the observed overshoots during the transient start up of shear flow. By analogy with the behavior of TLCPs, which possess their own anisotropy, these overshoots should be related to the morphological changes occurring at the beginning of the flow. A response to this question comes from the study of the inverse composition blend [30/70 PP/(EVA-EMA)]. In this case, the PP inclusions are much more viscous than the matrix (about ten times) and we expect that no deformation of the suspended particles would occur. For creep experiments, in contrast to the results shown in Fig. 5.2 for the 70/30 PP/(EVA-EMA) blend, the viscosity of the 30/70 PP/(EVA-EMA) blend is shown in Fig. 5.8 to be almost time independent for all the imposed stress values. Finally, no overshoots have been observed in stress growth experiments within the range of shear rates studied (Fig. 5.9). It is not to be excluded that higher shear rates would lead to a different behavior, but this could not be verified because of sample ejection at high shear rates. Consequently, the observed overshoots reported in Fig. 5.3 appear to be related to the deformation of the suspended droplets, as indicated by the calculated values of the  $q$  tensor (Figs. 5.6 and 5.7).

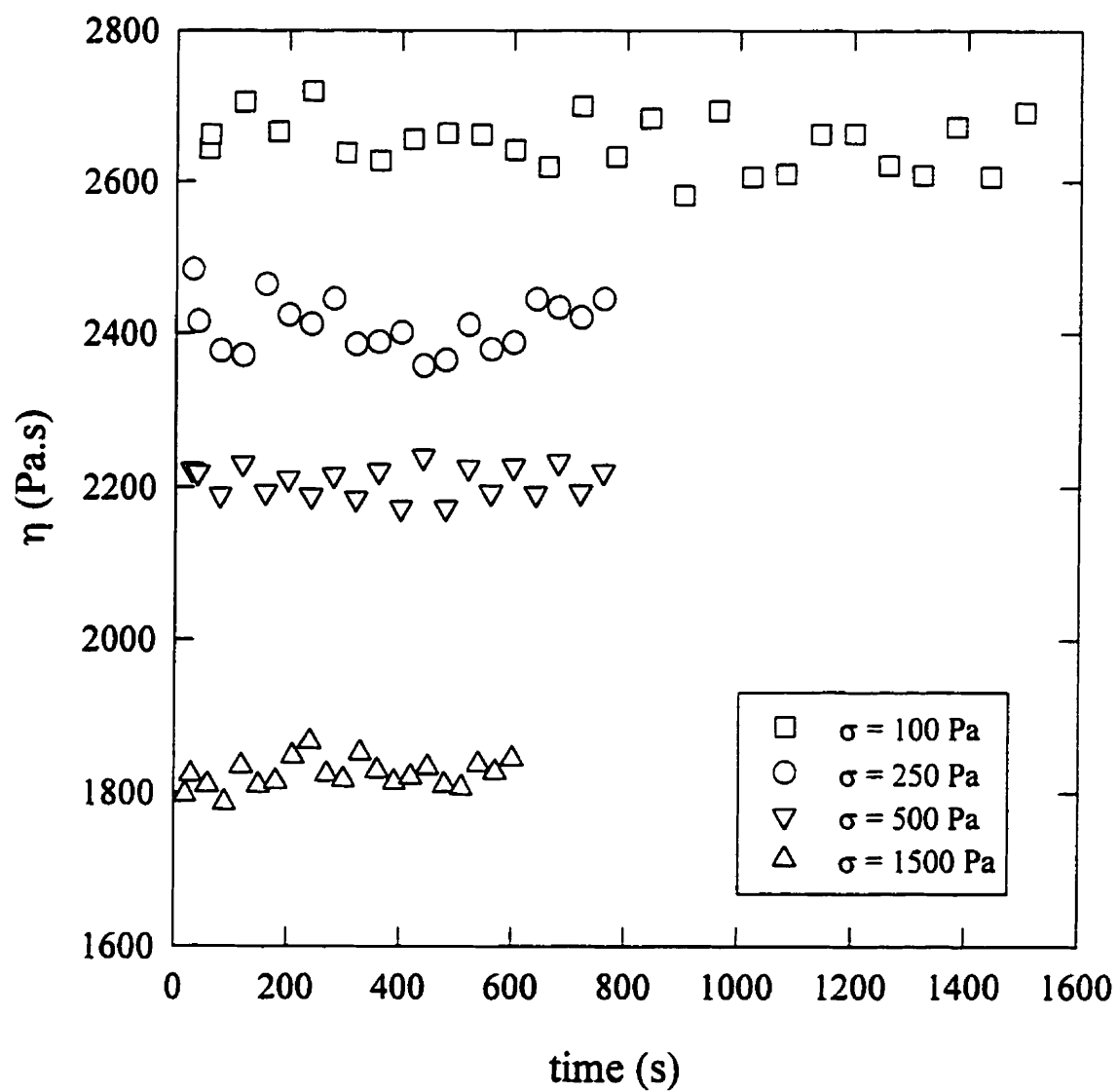


Figure 5.8 : Transient viscosity in creep as a function of time for the 30/70 PP/(EVA-EMA) blend;  $T=200^{\circ}\text{C}$ .

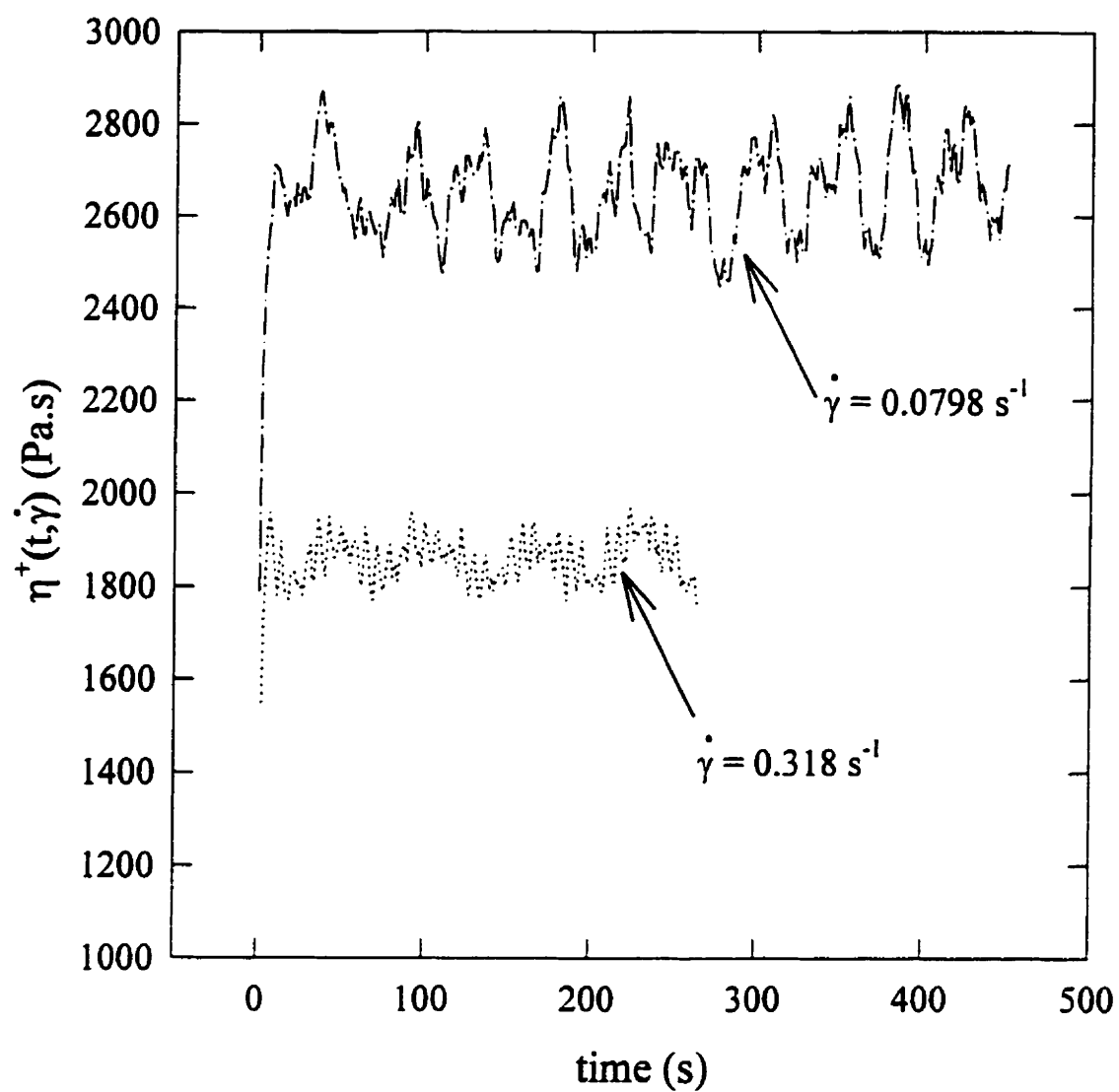


Figure 5.9 : Stress growth viscosity at two different shear rates for the 30/70 PP/(EVA-EMA) blend;  $T=200^\circ\text{C}$ .

Since the dispersed phase consists of almost undeformable particles, the initial value of the interfacial area should remain constant. The transient creep experiments carried out on the 30/70 PP/(EVA-EMA) blend confirm this assumption. But it was not possible to fit the start-up data for this blend using either the LPL or the LGC model. Discrepancies between the Doi-Ohta theory and polyisoprene/polydimethylsiloxane data for which the viscosity ratio between the dispersed phase and the matrix is equal to 4 have been observed very recently by Kitade et al. (1997). To elucidate the situation, let us consider steady state conditions and assume that the non linear terms introduced by Lee and Park (1994) in the relaxation mechanism are negligible. We are recovering in this case the evolution equations of the interface of the Doi-Ohta model. If the droplets remain spherical,  $q_{12}$  should be equal to zero. It can be deduced from the model that this particular case is fulfilled only if the parameter  $d_2$  ( $\mu$  in the Doi-Ohta model) is equal to 1. Such a value of  $d_2$  implies that  $Q = 0$ . This is not consistent with our further assumption and also with the experiment. This illustrates the limits of the relaxation mechanism when dealing with undeformable particles. When using the modified relaxation mechanism of Grmela and Ait-Kadi [Eqs. (5.16)-(5.22)] the problem is identical. We have indeed chosen  $\Psi$  so that the relaxation modes proposed by Lee and Park (extension of Doi-Ohta) can be retrieved. A possible solution would be to let  $\Lambda_1$  in Eq. (5.17) depends in  $q$  in such a way that if  $q = 0$  then  $\Lambda_1 = 0$ . This modification would eliminate from our model the relaxation of  $Q$  to its ultimate conclusion (phase separation). The governing equations of the interface would, however, involve new non linear terms that are absent in the Doi-Ohta model. In addition, one has also to keep in mind that in these models the interface dynamics is assumed to be controlled by two Newtonian fluids of similar viscosities, which is of course far from being the case in this considered limiting behavior.

## 5.6) Conclusions

The linear and non linear viscoelastic properties of immiscible blends have been investigated. The modified Lee and Park model [Lacroix et al. (1997)] is shown to be able

to describe the transient shear flow experiments for almost all the shear rates investigated. A modified version of the Grmela and Ait-Kadi model (1994) is also proposed in such a way that the relaxation modes of Lee and Park (1994) are retrieved from general considerations. This approach leads to a more complete constitutive equation. The morphological changes induced by the flow on a 70/30 PP/(EVA/EMA) blend are very important. The initial morphology of the blend is characterized by a volume average radius of  $3.75\text{ }\mu\text{m}$ . Depending on the applied shear rate, coalescence or breakup can take place. For a shear rate of  $0.0126\text{ s}^{-1}$  the final radius after relaxation is  $6\text{ }\mu\text{m}$ , whereas for a shear rate of  $0.318\text{ s}^{-1}$  the final radius after relaxation of the dispersed droplets is  $1.5\text{ }\mu\text{m}$ . Hence, at relatively moderate shear rates the morphology can be greatly affected resulting in unusual rheological properties. A large decrease of the viscosity in creep experiments is associated with coalescence whereas a slight increase occurs due to the breakup of droplets. The shear viscosity data in stress growth experiments are characterized by an overshoot when the dispersed phase of the blend is less viscous than that of the matrix. Both models predict diameter changes of the dispersed droplets occurring during flow when the inclusions are deformable and the predictions of the diameter of the dispersed droplets following stress growth and relaxation compare relatively well with the morphological data. The linear viscoelastic properties were measured after cessation of steady shear flow and the Palierne model (1990) was used to verify the particle diameters determined via the LPL and LGC models. For blends containing undeformable droplets, the LPL and LGC models as well as the Doi-Ohta model ultimately predict phase separation under any finite strain flow. Obviously, the assumptions regarding the interface dynamics are no longer valid. To improve the models, coupling effects between the bulk and interfacial properties in the governing equations describing the morphological evolution need to be included. Experimental data show indeed that relative moderate simple shear rates can affect greatly the morphology. This is bound to affect the overall or bulk rheological properties of the blend.

### **Acknowledgments**

The authors are thankful for the financial support received from ELF-ATOCHEM.

### 5.7) References

- Bousmina, M. and R. Muller, "Linear Viscoelasticity in the Melt of Impact PMMA. Influence of Concentration and Aggregation of Dispersed Rubber Particles", *J. Rheol.*, **37**, 663-679 (1993).
- Bousmina, M. and R. Muller, "Rheology/morphology/flow conditions relationship for polymethylmetacrylate/rubber blend", *Rheol. Acta*, **35**, 369-381 (1996).
- Bousmina, M., P. Bataille, S. Sapieha, and H.P. Schreiber, "Comparing the Effect of Corona Treatment and Block Copolymer Addition on Rheological Properties of Polystyrene/Polyethylene Blends", *J. Rheol.*, **39**, 499-517 (1995).
- Carreau, P.J., M. Bousmina, and A. Ajji, in "Rheological Properties of Blends : Facts and Challenges", *Progress in Pacific Polymer Science-3*, edited by K.P. Ghiggin, (Springer, New-York, 1994), pp. 25-40.
- Dickie, R.A., "Heterogeneous Polymer-Polymer Composites I Theory of Viscoelastic properties and Equivalent Mechanical Model", *J. Appl. Polym. Sci.*, **17**, 45-63 (1973).
- Doi, M., in *Rheology of Textured Materials*, edited by L. Garrido, *Complex Fluids, Lecture Notes in Physics*, (Springer, New York, 1993), p 221.
- Doi, M. and T. Ohta, "Dynamics and Rheology of Complex Interfaces. I", *J. Chem. Phys.*, **95**, 1242-1248 (1991).
- Friedrich, C., W. Gleinser, E. Korat, D. Maier and J. Weese, "Comparison of sphere-size distributions obtained from rheology and transmission electron microscopy in PMMA/PS blends", *J. Rheol.*, **36**, 1411-1425 (1995).
- Germain, Y., B. Ernst, O. Genelot, and L. Dhamani, "Rheological and Morphological Analysis of compatibilized PP/PA Blends", *J. Rheol.*, **38**, 681-697 (1994).
- Graebing, D. and R. Muller, "Rheological Behavior of Polydimethylsiloxane/Polyoxyethylene Blend in the Melt. Emulsion Model of two Viscoelastic Liquids", *J. Rheol.*, **34**, 193-205 (1990).

- Graebing, D., R. Muller, and J.F. Palierne, "Linear Viscoelastic Behavior of Some Incompatible Polymer Blends in the Melt. Interpretation of Data with a Model of Emulsion of Viscoelastic Liquids", *Macromolecules*, **26**, 320-329 (1993).
- M. Grmela, "Stress tensor in generalized hydrodynamics", *Phys. Lett. A*, **111**, 41-44 (1985).
- M. Grmela, "Hamiltonian dynamics of incompressible elastic fluids", *Phys. Lett. A*, **130**, 81-86 (1988).
- Grmela, M., and A. Ait-Kadi, "Comments on the Doi-Ohta theory of blends", *JNNFM*, **55**, 191-195 (1994).
- Guenther, G.K. and D.G. Baird, "An Evaluation of the Doi-Ohta Theory for an Immiscible Polymer Blend", *J. Rheol.*, **40**, 1-20 (1996).
- Guskey, S.M. and H.H. Winter, "Transient shear behavior of a thermotropic liquid crystalline polymer in the nematic state", *J. Rheol.*, **35**, 1191-1207 (1991).
- Han, J.H., C.C. Feng, D.J. Li, and C.D. Han, "Effect of flow geometry on the rheology of dispersed two phase blends of polystyrene and polymethylmethacrylate", *Polymer*, **36**, 2451-2463 (1995).
- Kitade, S., A. Ichikawa, N. Imura, Y. Takahashi, and I. Noda, "Rheological properties and domain structures of immiscible polymer blends under steady and oscillatory shear flows", *J. Rheol.*, **41**, 1039-1060 (1997).
- Lacroix, C., M. Bousmina, P.J. Carreau, B.D. Favis, and A. Michel, "Properties of PETG/EVA Blends : Viscoelastic, Morphological and Interfacial Properties, Part I", *Polymer*, **37**, 2939-2947 (1996).
- Lacroix, C., M. Aressy, and P.J. Carreau, "Linear viscoelastic behavior of molten polymer blends: a comparative study of the Palierne and the Lee and Park models", *Rheol Acta*, **36**, 416-428 (1997).
- Lavallée, C., "Stéréologie appliquée aux alliages polymères", CNRC, IMI, Boucherville, Qc, Canada (1990).
- Lee, H.M. and O.O. Park, "Rheology and dynamics of Immiscible Polymer Blends", *J. Rheol.*, **38**, 1405-1425 (1994).



Mellema, J. and M.W.M. Willemse, "Effective Viscosity of Dispersions Approached by a Statistical Continuum Method", *Physica* **122A**, 286-312 (1983).

Nobile, M. R., D. Acierno, L. Incarnato, and D. Nicolais, "The rheological behavior of polyetherimide and of its blends with thermotropic copolyester", *J. Rheol.*, **34**, 1181-1197 (1990).

Palierne J. F., "Linear Rheology of Viscoelastic Emulsions with Interfacial Tension", *Rheol. Acta*, **29**, 204-214 (1990); **30**, 497 (1991).

Saltikov, S.A., "The Determination of the Size Distribution of particles in an Opaque Material from a Measurement of the Size Distribution of their Section", in *Stereology*, edited by H. Elias, Proc. Second Int. Cong. for Stereology, NY (Springer, New York, 1967), pp 163-173.

Scholz, P., D. Froelich, and R. Muller, "Viscoelastic Properties and Morphology of Two-Phase Polypropylene/Polyamide 6 blends in the Melt. Interpretation of Results with an Emulsion Model", *J. Rheol.*, **33**, 481-499 (1989).

Schowalter, W.R., C.E. Chaffey, and H. Brenner, "Rheological Behavior of a dilute Emulsion", *J. Colloid. Interface Sci.*, **26**, 152-160 (1968).

Takahashi, Y., N. Kurashima, I. Noda, and M. Doi, "Experimental tests of the scaling relation for textured materials in mixtures of two immiscible fluids", *J. Rheol.*, **38**, 699-712 (1994a).

Takahashi, Y., S. Kitade, N. Kurashima, and I. Noda, "Viscoelastic properties of immiscible polymer blends under steady and transient shear flows", *Polym. J.*, **26**, 1206-1212 (1994b).

Takahashi, Y. and I. Noda, "Domain structures and viscoelastic properties of immiscible polymer blends under shear flow" in *Flow-Induced Structure in Polymers*, edited by A. Nakatani and M. D. Dadmun (Am. Chem. Soc., Washington D.C., 1995) pp 140-152.

Vinckier, I., P. Moldenaers, and J. Mewis, "Relationship between Rheology and Morphology of Model Blends in Steady Shear Flow", *J. Rheol.*, **40**, 613-631 (1996).

Vinckier, I., P. Moldenaers, and J. Mewis, "Transient rheological response and morphology evolution of immiscible polymer blends", *J. Rheol.*, **41**, 705-718 (1997).

**CHAPITRE 6****Morphological evolution of immiscible polymer blends in  
simple shear and elongational flows****C. Lacroix, M. Grmela and P.J. Carreau\***

Centre de Recherche Appliquée sur les Polymères, CRASP,  
Department of Chemical Engineering, Ecole Polytechnique,  
P.O. Box 6079, Stn Centre-Ville, Montréal, QC, H3C 3A7, Canada

\* corresponding author

Cet article est soumis à Journal of Non-Newtonian Fluid Mechanics

### 6.1) Abstract

The evolution of the morphology of the dispersed phase of immiscible polymer blends is studied in both shear and extensional flows. In the simple shear flow, predictions of the Lee and Park (J.Rheol., **38** (1994) 1405) and of the modified Lee and Park as well as the modified Grmela and Ait-Kadi (J. Non-Newtonian Fluid Mech., **55** (1994) 191) models (Lacroix et al., J.Rheol. **42** (1998) 41) are compared to stress growth data. The size of the dispersed phase is strongly affected by moderately finite strain imposed during the stress growth experiments. The morphological changes after stress relaxation are well predicted by the models for a polypropylene (PP), ethylene vinylacetate (EVA) and ethylene methylacrylate (EMA) blend (Lacroix et al., J.Rheol. **42** (1998) 41). The prediction is less satisfactory for a polystyrene (PS)/ polyethylene (PE) blend. The morphological evolution of the PP/EVA/EMA blends has also been investigated in elongation controlled flows. The morphologies of samples extracted before and after extrusion through an hyperbolic shaped (nozzle) die show that the elongational flow induces fibrillar structures. The extensional viscosity data, needed to solve the interface governing equations of the Lee and Park model, have been obtained from entrance pressure drop measurements. This set of equations allows to describe qualitatively the transition from a spherical to a fibrillar morphology.

## 6.2) Introduction

The design of new polymer blends of required properties is intimately related to the control of the morphology. In most cases, the components of the blend are immiscible and a two phase morphology is obtained. More complex situations can arise when more than two polymers are mixed together or when chemical reactions occur. In this article we will restrict our analysis to the study of binary blends. A simple way of classifying flows is to divide them in two major classes : simple shear and elongational flow. Components of both flows are encountered for instance in extrusion, injection molding, film blowing... Flow conditions can greatly affect the morphology and skin-core effects are frequently observed. To stabilize the morphology, copolymers are frequently added or generated *in situ* via chemical reactions. Therefore, predicting the evolution of the morphology under processing conditions is of major interest for optimizing the properties of new materials.

The purpose of this article is to investigate the relationships between the flow conditions and the resulting morphology for different kind of immiscible polymer blends. This study is based on theories recently developed to relate the morphological evolution of immiscible polymer blends in relation to their rheological properties (Doi and Ohta [1], Lee and Park [2], Grmela and Ait-Kadi [3], Lacroix et al. [4]). This article is divided into two main parts. The first one concerns the rheology/morphology relationships induced by simple shear flow whereas the second one focuses on the morphologies obtained in a dominant uniaxial elongational flow.

## 6.3) Relationships between rheology and morphology

In processing conditions, under an applied flow, the complex microstructure of immiscible molten blends evolves and this in turn affects the rheology of the fluid. In contrast to small amplitude oscillatory flow, large deformations can generate breakup and/or coalescence phenomena for uncompatibilized blends. This dynamics of morphological

changes induced by flows has been considered by Doi and Ohta [1]. They derived for a mixture of two Newtonian fluids new constitutive equations for describing evolution of the interface that takes into account breakup and coalescence. These interface governing equations are applicable for any type of flow.

In simple shear flow, this theory is now well documented and has been investigated with different kind of systems (Takahashi et al. [5,6,7], Guenther and Baird [8], Vinckier et al. [9,10,11], Kitade et al. [12]). Lee and Park [2] have modified the stress equation of Doi and Ohta [1] to take into account the mismatch of viscosities of the different polymers. They have also introduced additional terms regarding the evolution of the interface. This model has been discussed and analyzed by Lacroix et al [13] in the linear viscoelastic domain as well as in the non linear viscoelastic domain (Lacroix et al. [4], Vinckier et al. [11]). A modification of the mixing rule included in the Lee and Park model [2] has been proposed by Lacroix et al. [13] to better describe linear viscoelastic data for polypropylene (PP)/ethylene vinyl acetate (EVA) blends and satisfy limiting cases. In a very recent publication (Lacroix et al. [4]), we have used this modified model, called the LPL model, to predict the morphological evolution of a polypropylene (PP)/ethylene vinyl acetate (EVA)-ethylene methyl acrylate (EMA) blend under simple shear flow. In this model, the time evolution of the anisotropy tensor  $q$ , the time evolution of the interfacial area per unit volume  $Q$  and the extra stress tensor are related by :

$$\frac{\partial q_{ij}}{\partial t} = -q_{ik}\kappa_{kj} - q_{jk}\kappa_{ki} + \frac{2}{3}\delta_{ij}\kappa_{lm}q_{lm} - \frac{Q}{3}\dot{\gamma}_{ij} + \left(\frac{q_{lm}\kappa_{lm}}{Q}\right)q_{ij} - d_1\frac{\alpha}{\eta_M}Qq_{ij} - d_1d_3\frac{\alpha}{\eta_M}\left(\frac{q_{lm}q_{lm}}{Q}\right)q_{ij} \quad (6.1)$$

$$\frac{\partial Q}{\partial t} = -\kappa_{ij}q_{ij} - d_1d_2\frac{\alpha}{\eta_M}Q^2 - d_1d_3\frac{\alpha}{\eta_M}q_{ij}q_{ij} \quad (6.2)$$

$$\sigma_{ij} = \eta_M \left( \frac{1+3/2H}{1-H} \right) \dot{\gamma}_{ij} - \alpha q_{ij} \quad (6.3)$$

with  $H$  given by :

$$H = \phi \frac{2(\eta_I - \eta_M)}{2\eta_I + 3\eta_M} \quad (6.4)$$

here  $\alpha$  is the interfacial tension,  $\eta_M$  and  $\eta_I$  the viscosities of the matrix and of the inclusions respectively,  $\phi$  the volume fraction of the dispersed phase,  $\dot{\gamma}_{ij} = \kappa_{ij} + \kappa_{ji}$  are the components of the rate of deformation tensor and  $\kappa_{ij}$  are the components of the velocity gradient tensor, and  $d_1, d_2, d_3$  ( $\lambda, \mu, \nu$  respectively in Lee and Park) are phenomenological parameters denoted to as degrees of total relaxation, size relaxation, and breakup and shape relaxation (Lee and Park [2]). We use here the summation convention, i.e. summation over repeated indices. With the original mixing rule, the Lee and Park [2] model is expressed as follows:

$$\sigma_{ij} = \left( 1 + \frac{6(\eta_I - \eta_M)}{10(\eta_I + \eta_M)} \phi \right) \eta_M \dot{\gamma}_{ij} - \alpha q_{ij} \quad (6.5)$$

The Lee and Park model will be called later in the article the LP model. We have also proposed a modification of the Grmela and Ait-Kadi model [3] to retrieve from thermodynamic considerations the governing equations developed by Lee and Park [2]. In that case the major difference comes from the contribution of the interface which included non linear terms. With the mixing rule given in Eq. (6.3), we called the modified Grmela/Ait-Kadi model the LGC model. Finally, we have also used a simple linear mixing rule, based on the volume fraction of each component, combined to Eqs. (6.1) and (6.2) and

called this model the LLP model. These different models will be compared with transient shear experiments in a next section.

The development of the interface governing equations assumes affine deformation (Doi and Ohta [1], Lee and Park [2]). We introduce in this article governing equations including non affine deformations. We use the same notation as in our previous work [4] as well as in Grmela and Ait-Kadi [3]. Let us consider first the non dissipative part of the interface evolution equations ( $\Psi \neq 0$ ). We define a conformation tensor  $C$  that characterizes an element of surface.  $C$  is related to  $q$  and  $Q$  by :

$$Qq_{ij} = C_{ij} - \frac{1}{3}Q^2\delta_{ij} \quad (6.6)$$

The convection of this conformation tensor is governed by the lower convected derivative. Non affine deformation can be taken into account by introducing a slip parameter  $\xi$  in such a way that the convection of the tensor  $C$  becomes :

$$\frac{\partial C_{ij}}{\partial t} + C_{kj}\kappa_{ki} + C_{ki}\kappa_{kj} - \frac{\xi}{2} [C_{kj}(\kappa_{ki} + \kappa_{ik}) + C_{ik}(\kappa_{kj} + \kappa_{jk})] = 0 \quad (6.7)$$

We assume here, as in Doi and Ohta [1] and in Grmela and Ait-Kadi [3], that  $C$  is uniform, i.e. independent of the position vector. By introducing Eq. (6.6) into Eq. (6.7) the non dissipative part of the interface evolution equations can be expressed as follows :

$$\begin{aligned} \frac{\partial q_{ij}}{\partial t} = & -q_{ki}\kappa_{kj}(1-\frac{\xi}{2}) + \frac{\xi}{2}q_{ki}\kappa_{jk} - q_{kj}\kappa_{ki}(1-\frac{\xi}{2}) + \frac{\xi}{2}q_{kj}\kappa_{ik} + \frac{2}{3}(1-\xi)\delta_{ij}\kappa_{lm}q_{lm} \\ & - \frac{Q}{3}(1-\xi)\dot{\gamma}_{ij} + (1-\xi)\left(\frac{q_{lm}\kappa_{lm}}{Q}\right)q_{ij} \end{aligned} \quad (6.8)$$

$$\frac{\partial Q}{\partial t} = -\kappa_{ij} q_{ij} (1 - \xi) \quad (6.9)$$

The relaxation mechanism proposed by Lee and Park [2] remains unchanged (the corresponding terms are expressed in Eqs. (6.1) and (6.2)) and can be combined with Eqs. (6.8) and (6.9) to lead to the complete evolution equations of  $q$  and  $Q$ . The stress is then given by :

$$\sigma_{ij} = 2(1 - \xi) C_{ik} \frac{\partial \Phi}{\partial C_{kj}} \quad (6.10)$$

We recall that one of the main advantages of the thermodynamic formulation is that a formula for the stress tensor arises as an integral part of the derivation of the governing equations. Setting  $\xi = 0$  in Eq. (6.8) allows to retrieve the affine deformation. In that case, the equations are governed by the lower convected derivative whereas for  $\xi = 2$ , the tensor evolution obeys an upper convected derivative. In the case when  $\xi = 1$ , the flow is purely rotational and, as seen from Eq. (6.10), no contribution to the stress tensor comes from the interface. A similar observation has been made by Larson [14] when considering the Gordon-Schowalter derivative in another context. This set of equations can also be used in both shear and elongational flows.

Few studies concern the rheological properties in extensional flows of immiscible blends in relation to their morphology. Gramespacher and Meissner [15], Levitt et al. [16] have related the interfacial properties of different blends to their elongational properties but in very well defined extensional flow fields. Since the pioneering works of Taylor [17], elongational flows are recognized to be very efficient for deforming and rupturing initially spherical droplets. Nevertheless, most of the studies have been restricted to Newtonian



fluids and investigated the mechanisms of deformation and rupture of a single droplet (Stone et al. [18], Milliken and Leal [19]). Real processing conditions imply in general the use of viscoelastic materials, relatively concentrated systems with the microstructure of a large number of droplets, and large deformations. The viscoelastic nature of the components has a major influence on the morphology developments as shown by the works of Delaby et al. [20] and Mighri et al. [21] for elongational flows. Even if the Lee and Park [2] governing equations (Eqs. (6.1) and (6.2)) are an empirical extension of the Doi-Ohta [1] theory derived for a mixture of Newtonian fluids, these are the only relations available for describing the morphological evolution dynamics under elongational flows. Here, the processing conditions have been chosen to determine the elongational properties of two different blends and assess the model predictions of the morphological evolution of the blends.

## **6.4) Experimental**

### **6.4.1) Materials**

Two different systems have been investigated: blends of polystyrene and polyethylene PS/PE and polypropylene and ethylene vinyl acetate-ethylene methyl acrylate PP/EVA-EMA. Since EVA and EMA are miscible, binary blends of PP and (EVA-EMA) are then obtained. The commercial polymers were a PP (PP3020GN3), an EVA (EVATANE 2805) and an EMA (LOTTRYL 28MA07) supplied by ELF-ATOCHEM whereas a PS (STYRON D685) and a PE (LLDPE TUFLIN) were obtained from DOW CHEMICAL and UNION CARBIDE respectively. Transient shear experiments have been carried out on a controlled strain rheometer ( Bohlin VOR) under nitrogen atmosphere at a set temperature of 200°C for both PP/EVA-EMA and PS/PE blends. In that case, the blends have been prepared with an internal batch mixer. The blending conditions, the characteristics of the rheological measurements and of the image analysis used for this study are described elsewhere (Lacroix et al., [4,13]). In all cases, the morphology was determined using scanning electron microscopy (SEM) and corrections were applied to account for the fact that the observation plane does not necessarily cut the particles at their equator.

To determine the elongational flow properties, the blends as well as the “pure” components have been prepared with a twin screw extruder Leistritz 30-34 in a corotative mode. A small amount of antioxydant (Irganox B225 from Ciba-Geigy) was added with the blends and with the EVA-EMA. The extruded materials were then pelletized and fed to a single screw extruder (Killion) for pressure drops measurements. The characteristics of the different dies used in this study is described in the following section.

#### 6.4.2) Technique

Determining the elongational viscosity remains a very difficult task. Different techniques can be used as approximate methods for measuring the elongational flow properties, such as jet opposed nozzles, fibre spinning, converging flow. The more rigorous method developed by Meissner [22] using rotary clamps yields true uniaxial elongational measurements, but it is not easily accessible and trivial to use. A technique which is frequently used is based on the entrance pressure drops for the flows through a contraction. Moreover, this technique is particularly adapted to usual processing conditions. In this case the extensional viscosity is determined from the flow rates and pressure drops measurements once knowing the die geometry and eventually the shear viscosity. Several analysis have been proposed to correlate these quantities. Cogswell [23] was the first in this context to study entrance pressure effects. Binding [24] and more recently Mackay and Astarita [25] revisited and extended the works of Cogswell [23, 26, 27]. Cogswell considered that the entrance pressure drop was due to two contributions, one due to shear and another one due to elongation effects whereas in Binding’s analysis, minimization of the power consumption was used. In this study we will use Cogswell [23], Binding [24] and Mackay and Astarita [25] analysis. It should be noted that alternative approaches have been proposed such as those of Gibson [28] or of Tremblay [29] based on the sink flow analysis.

Most studies make use of capillary rheometers for determining the entrance pressure drops. But this is relatively far from the processing conditions, for which the polymer is

conveyed and pumped by an extruder and flows through a die. Therefore a setup has been designed to measure capillary as well as extensional properties from a single screw extruder (see Figure 6.1). This setup allows us to obtain various flow rates by using a by-pass valve without modifying the high rotation screw speed (80 rpm). A static mixer was installed at the reservoir inlet to homogenize as well as possible the blend. Converging dies or capillary dies can be mounted on the extruder exit reservoir after the section where the pressure and temperature are measured. The valve also allows us to extract samples before the converging section for morphological analysis. With this design, the morphology of the blends before die extrusion can be controlled by keeping the thermomechanical history unchanged. The morphology of the extruded samples was frozen by plunging the extrudate in cold water right at the die exit. The cooling rate is high enough to guarantee that no significant relaxation and morphological changes take place after extrusion.

To measure a meaningful elongational viscosity, a constant and controlled elongational strain rate should be applied. This can be achieved by choosing correctly the shape of the converging section. Binding and Jones [30], Kim et al. [31] have used planar hyperbolic shaped dies to measure the extensional flow properties of polymer melts or polymer solutions. James et al. [32, 33] showed that a constant elongational strain rate could be obtained if the shape of a cylindrical converging die was given by  $R_{(z)}^2 = \text{Const}$ , where  $R$  the channel radius depends on  $z$ . For an axisymmetric geometry along the  $z$  axis, the extensional strain rate is defined by :

$$\dot{\epsilon}(z) = \frac{d\langle V_z \rangle}{dz} \quad (6.11)$$

where  $\langle V_z \rangle$  is the average velocity at a given  $z$ . From the expression of the volumetric flow rate  $Q_f$ , it can be deduced that :

$$\dot{\epsilon}(z) = \frac{Q_f}{\pi} \frac{d}{dz} \left( \frac{1}{R_{(z)}^2} \right) \quad (6.12)$$

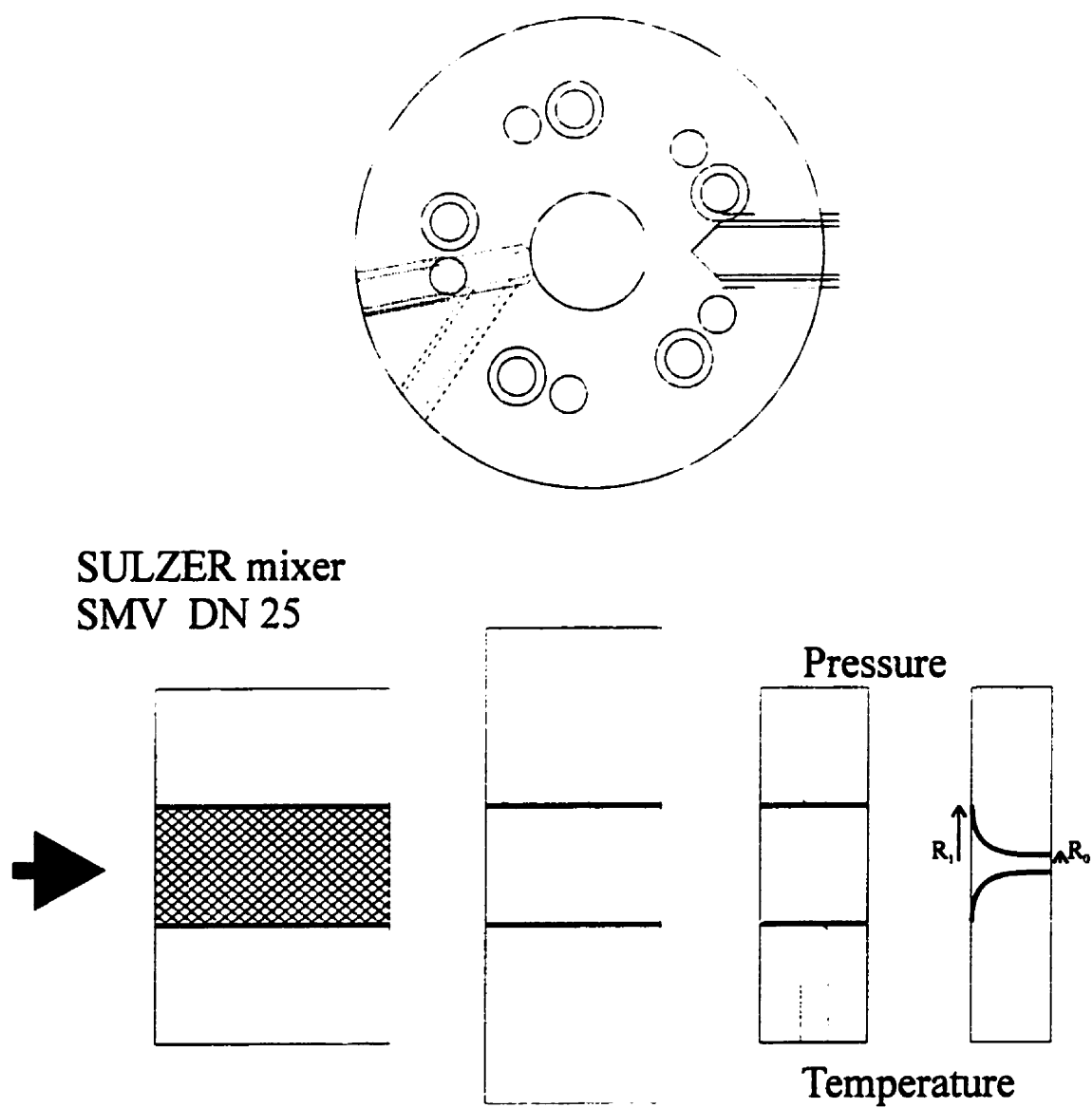


Figure 6.1 : extrusion setup

Imposing a constant elongational strain rate results in the following shape :

$$R_{(z)} = \left( \frac{\dot{\epsilon} \pi z}{Q_f} + \frac{1}{R_1^2} \right)^{-\frac{1}{2}} \quad (6.13)$$

where  $R_1$  is the initial radius of the nozzle die. Two dies of different geometries have been micromachined. Both dies have the same entry radius (12.7 mm). The first one (D1) is 10 mm long with an exit radius of 1.995 mm whereas the second one (D2) is 20 mm long with an exit radius of 2.805 mm. A similar setup has been used by Crevecoeur and Groeninckx [34] to study the fibril formation of thermoplastic/TLCP blends. In our case, we are able to extract the samples just before and after the die so that the resulting morphologies can be analyzed in relation to the elongational effects generated by the die alone. The extensional properties of two different blends, a 70/30 PP/EVA-EMA blend and a 30/70 PP/EVA-EMA blend are compared to the properties of the unblended components. These blends are of particular interest because their zero shear viscosity ratios are either 0.1 or 10 depending on the matrix. Therefore, the effects of the viscosity ratio can be assessed in a dominant elongational flow. As it will be shown in the next section, shear viscosity data, and more precisely power-law parameters of the four different molten polymer or molten blends are needed to determine an equivalent extensional viscosity. Capillary rheometry has been carried out with the single screw extruder. The setup presented in Figure 6.1 is flexible and allows the use of different capillaries instead of a converging section. Here, three different  $L/D$  ratios have been used (8, 16 and 24). The diameters of the dies were 1.6 mm. The whole system described in Figure 6.1 was set at a temperature of 200°C. Before presenting the results in shear and extension, we will explicit the three different approaches (Cogswell, Binding, Mackay and Astarita) in the case of a constrained convergence.

#### 6.4.3) Cogswell analysis.

In Cogswell's [23] analysis, the entry pressure drop is divided into shear and

elongational terms :

$$\Delta P_{ent} = \Delta P_{shear} + \Delta P_{elongation} \quad (6.14)$$

He assumed that the power-law model represents the shear properties of the material. For a capillary of radius  $R_z$  with  $z$  the coordinate along the symmetry axis, the pressure drop due to shear in an element of length  $dz$  assuming fully developed flow and negligible inertial effects, is :

$$dP_s = \frac{2\sigma_w}{R_{(z)}} dz \quad (6.15)$$

where  $\sigma_w$  the shear stress at the wall, is expressed for a power law fluid by :

$$\sigma_w = K \left( \frac{3n+1}{4n} \right)^n \dot{\gamma}_a^n \quad (6.16)$$

with

$$\dot{\gamma}_a = \frac{4Q_f}{\pi R_{(z)}^3} \quad (6.17)$$

In the expression (6.16),  $K$  represents the consistence and  $n$  the index of plasticity,  $\dot{\gamma}_a$  is the apparent shear rate and  $Q_f$  the volumetric flow rate. By inserting the nozzle profile  $R_{(z)}$  given by (Eq. 6.13) and integrating along the die length,  $\Delta P_s$  is expressed as :

$$\Delta P_s = \frac{4}{3} \frac{K Q_f}{(n+1)\pi} \left( \frac{(3n+1)Q_f}{n\pi} \right)^n \left[ \left( \frac{1}{R_0} \right)^{3(n+1)} - \left( \frac{1}{R_1} \right)^{3(n+1)} \right] \quad (6.18)$$

where  $R_0$  and  $R_1$  are respectively the outlet and inlet radii. The elongational contribution to the entrance pressure drop can be derived from energy considerations. If the flow is purely extensional, the pressure difference through a contraction is defined by :

$$\Delta P_e = \int_{z=0}^{l_d} (\sigma_z - \sigma_r) \dot{\epsilon} \frac{\pi R(z)^2}{Q_f} dz \quad (6.19)$$

where  $l_d$  represents the length of the die,  $Q_f$  the volumetric flow rate and  $\sigma_z - \sigma_r$  is the primary normal stress difference. The elongational viscosity is defined by :

$$\eta_e = \frac{\sigma_z - \sigma_r}{\dot{\epsilon}} \quad (6.20)$$

Assuming that the elongational viscosity is constant through the nozzle (notice that for viscoelastic fluids, a constant elongational strain rate is a necessary but not a sufficient condition to have a constant  $\eta_e$ ) and by substituting Eqs. (6.13) and (6.20) into Eq.(6.19) we obtain after the integration :

$$\Delta P_e = \eta_e \dot{\epsilon} \ln \left( \frac{Q_f / \pi R_1^2 + \dot{\epsilon} l_d}{Q_f / \pi R_1^2} \right) \quad (6.21)$$

Because the elongational strain rate is determined from the geometry of the die and the volumetric flow rate, it can be substituted in Eq. (6.21) to yield finally :

$$\Delta P_e = 2\eta_e \frac{Q_f}{\pi l_d} \left( \frac{1}{R_1^2} - \frac{1}{R_0^2} \right) \ln \left( \frac{R_1}{R_0} \right) \quad (6.22)$$

From the entrance pressure drop in a given die, the elongational viscosity can be estimated once we know the shear viscosity.

#### 6.4.4) Binding's analysis

Binding [24] extended the work of Cogswell [23] by using an energy balance and

variational calculus. He assumed, moreover, a power-law form for the extensional viscosity which is then determined from minimization of the power consumption  $W$ . Assumption was made also that the converging angle is small enough so that  $(dR_{(z)}/dz)^2$  or  $d^2R_{(z)}/dz^2$  can be neglected. Recirculating vortex or forced convergence profile are therefore involved in this analysis. The omission of  $(dR_{(z)}/dz)^k$  with  $k>1$  is equivalent to make the lubrication approximation. The power consumption  $W$  that is needed to calculate  $\eta_e$  is related to the entrance pressure drop by  $\Delta P_{ent} Q_f = W$ . In Binding's analysis, the power consumption  $W$  is divided into three contributions due to shear, elongation and kinetic energy variation. We will express more specifically these terms for an hyperbolic shaped die.

The usual assumption in entry flows is that the velocity  $V_z$  of the power law fluid is fully developed. In the converging section,  $V_z$  is given by :

$$V_z = \frac{3n+1}{n+1} \frac{Q_f}{\pi R_{(z)}^2} \left( 1 - \left( \frac{r}{R_{(z)}} \right)^{1+\frac{1}{n}} \right) \quad (6.23)$$

with  $n$  the power law index and  $R_{(z)}$  is the distance to the vortex from the center line or the constrained convergence. Following Binding's analysis [24] the rate of work per unit volume may be expressed by :

$$\dot{W} = \dot{W}_{shear} + \dot{W}_{elongation} + \dot{W}_{kinetic\ energy} \quad (6.24)$$

In contrast to Cogswell, Binding assumes power-law behavior for shear and elongational properties as well. Therefore, in Eq. (6.24) the contributions due to shear and elongation are respectively defined by :

$$\begin{aligned} \dot{W}_s &= K |\dot{\gamma}|^{n+1} \\ \dot{W}_e &= L |\dot{\epsilon}|^{t+1} \end{aligned} \quad (6.25)$$



In cylindrical coordinates,  $\dot{\gamma} = \partial V_z / \partial r$  and  $\dot{\epsilon} = \partial V_z / \partial z$ . Binding expressed the extensional rate of strain by taking the derivative of Eq.(6.23). This constitutes one of the differences with the “full technique” proposed by Mackay and Astarita [25] (see the next paragraph). By substituting the profile of the converging section (Eq. (6.13)) and integrating over the volume of the die we obtain :

$$W = \frac{4KQ_f^2}{3(n+1)\dot{\epsilon}\pi} \left( \frac{(3n+1)Q_f}{n\pi} \right)^n \left[ \left( \frac{1}{R_0} \right)^{3(n+1)} - \left( \frac{1}{R_1} \right)^{3(n+1)} \right] + I_m Q_f L \left( \frac{3n+1}{n+1} \right)^{t+1} \left( \frac{\dot{\epsilon}}{2} \right)^t \ln \left( \frac{1}{\beta^2} \right) + \frac{3}{2} \rho Q_f^3 \frac{(3n+1)^2}{(2n+1)(5n+3)} \frac{1-\beta^4}{\pi^2 R_0^4} \quad (6.26)$$

where  $R_0$  is the outlet radius of the die and  $\beta$  is the inverse of the contraction ratio ( $\beta = R_0/R_1$ ). In Eq.(6.26),  $I_m$  is defined by :

$$I_m = \int_0^1 \left| 2 - \frac{3n+1}{n} \phi^{1+1/n} \right|^{t+1} \phi d\phi \quad (6.27)$$

From the knowledge of the shear viscosity and by using a regression on a log-log plot,  $L$  and  $t$  can be obtained and used to calculate the extensional viscosity (Binding [35]). It was also verified that the fluids followed the imposed profile. In the case of a free convergence, it was assumed by Binding [24] that the fluid will create its own convergence profile so as to minimize the power consumption. When convergence is already imposed,  $dR_z/dz$  is a known function of  $z$  and this leads to a power consumption  $W$  defined by Eq. (6.26). As pointed out by Binding and Jones [30], limiting conditions are implied by the use of Eq. (6.26). Actually, the rate of convergence imposed by the hyperbolic shaped die should not be greater than the one the fluid would adopt to minimize its energy. If this occurs Eq. (6.26) is no longer valid and the minimum power consumption will correspond to the following profile:

$$\left( \frac{-dR_z}{dz} \right)^{t+1} = \frac{K(n+1)^{t+1}}{(3n+1)n^n L I_m} \left( \frac{(3n+1)Q_f}{n\pi R_z^3} \right)^{n-t} \quad (6.28)$$

where  $L_m$  is defined by Eq. (6.27). The condition required to confine the fluid in the imposed geometry is defined by :

$$\left( \frac{-dR_z}{dz} \right) \geq \left( \frac{-dR_z}{dz} \right)_{profile} \quad (6.29)$$

This condition is fulfilled if :

$$Q_f \leq \left( \frac{2l_d R_0^2}{1-\beta^2} \right)^{\frac{1-n}{1-n}} \left( \frac{K(n+1)^{n+1}}{(3n+1)n^n L l_{nt}} \right)^{\frac{1}{1-n}} \left( \frac{n\pi}{3n+1} \right) \left[ \left( \frac{1}{l_d R_0^2} \right)^{3/2} \right]^{\frac{n+1}{1-n}} \quad (6.30)$$

It was checked that for all the measurements this equation is satisfied.

#### 6.4.5) Mackay and Astarita's analysis

Following Binding's approach, Mackay and Astarita [25] derived recently an expression to estimate the extensional viscosity from the minimization of the stress power by using the Generalized Engineering Bernoulli Equation. They call this method a "full technique". As already mentioned in the preceding paragraph, one of the difference between the Binding and Mackay/Astarita analysis stems from the calculation of the extensional rate of strain. Mackay and Astarita have pointed out that the use of Eq. (6.22) implies that the velocity is zero at the edge of the vortex or of the converging profile. Evaluating  $\partial V_z / \partial z$  by taking the derivative of Eq. (6.22) leads to a negative non zero value for the velocity gradient at the boundary. This is therefore in contradiction with the presupposed velocity profile. Instead of taking the derivative of Eq. (6.22), they used an average rate of elongation, as the one assumed in Eq. (6.12), which can be expressed by :

$$\dot{\epsilon} = \frac{d\langle V_z \rangle}{dz} = \frac{2V_z}{R_{(z)}} \left( \frac{-dR_{(z)}}{dz} \right) \quad (6.31)$$

The calculation of the stress power dissipated  $W$  is carried according to the following equation :

$$W = \int \left( L \left| \frac{\partial V_z}{\partial z} \right|^{t-1} \left( \frac{\partial V_z}{\partial z} \right)^2 + K \left| \frac{\partial V_z}{\partial r} \right|^{n-1} \left( \frac{\partial V_z}{\partial r} \right)^2 \right) dV \quad (6.32)$$

Integrating over the volume of the whole system and taking into account the nozzle profile yields the following expression :

$$W = \frac{4KQ_f^2}{3(n+1)\dot{\epsilon}\pi} \left( \frac{(3n+1)Q_f}{n\pi} \right)^n \left[ \left( \frac{1}{R_0} \right)^{3(n+1)} - \left( \frac{1}{R_1} \right)^{3(n+1)} \right] + 2LQ_f J_m \left( \frac{3n+1}{n+1} \right)^{t+1} \ln \left( \frac{1}{\beta^2} \right) \dot{\epsilon} \quad (6.33)$$

with

$$J_m = \frac{t(t+1)n(n+1)}{(t(n+1)+2n)((t+1)(n+1)+2n)} B(t, 2n/1+n) \quad (6.34)$$

where  $B$  is the beta function defined by :

$$B(a,b) = \Gamma(a)\Gamma(b)/\Gamma(a+b) \quad (6.35)$$

with  $\Gamma$  the gamma function. The power-law parameters  $L$  and  $t$  can be determined from an appropriate log-log plot once the shear viscosity is known.

## 6.5) Results and discussion

### 6.5.1) Morphology and simple shear flow properties

For the two systems investigated (PS/PE and PP/EVA-EMA), stress growth shear experiments have been compared to the different model predictions. These start-up experiments are very useful to test the ability of the different models for predicting the morphological evolution of the blend under shear flow. A part of the experimental results

has already been published elsewhere ( Lacroix et al. [4,36] ). Figure 6.2a,b,c reports the start-up experiments at constant shear rates of  $0.0507 \text{ s}^{-1}$ ,  $0.101 \text{ s}^{-1}$  and  $0.32 \text{ s}^{-1}$  for the 80/20 PS/PE blend. As for the PP/EVA-EMA blend (Lacroix et al. [4]) an overshoot is first observed before the transient viscosity reaches a constant value or before the sample is ejected from the geometry. No such overshoots could also be observed for the unblended components at the different shear rates investigated. For this PS/PE system, we have a situation analogous to that of the PP/EVA-EMA blend. The dispersed phase is less viscous than the matrix which means that the inclusions of PE can be deformed and eventually break. The flow was then stopped and the samples were allowed to relax. During this process, the deformed particles should recover their equilibrium shape under the effects of the interfacial tension.

Figure 6.2 reports the different model predictions for the PS/PE system. The parameters used to fit the data with the different models for the PS/PE blend are reported in Table 6.1. Their determination is explained in details in Lacroix et al.[4]. The different abbreviations used to denote the models are explained in the first part of this article. As shown in Figures 6.2a and b, the LP, LLP, LPL and LGC models are able to describe the transient data for a 80/20 PS/PE blend. Even the simple linear mixing rule allows to get satisfactory results. The best description of the rheological data is obtained, however, with the LP model. This in contrast with the PP/EVA-EMA system studied in [4] for which it was not possible to fit the data with the LP and LLP models. For the highest shear rate investigated (Figure 6.2c), only the LGC model can describe these transient data.

Even if these models are descriptive regarding the evolution with time of the transient viscosity, they can be used as predictive ones when considering the morphology. Nevertheless, depending on the chosen mixing rule, different parameters have to be used to fit the data. This choice will modify the predictions of the changes in droplets size occurring during simple shear flow. Here we assess the ability of the models to predict qualitatively or quantitatively the morphological changes following stress growth and stress relaxation

experiments. Indeed, the knowledge of the interfacial area  $Q$  allows us to determine an average diameter if the dispersed phase is present as spherical particles. Results are reported in Table 6.1 for the PS/PE blend and are compared to the experimental determined values using scanning electron microscopy. The corresponding results for the PP/EVA-EMA blend are given in [4].

Table 6.1: Parameters used for predicting the transient rheological behavior of the 80/20 PS/PE blend with the different models; comparison between predicted radii values and SEM determined values.

$d_1=0.6$ $d_3=0.8$ $\alpha = -C_1=5\text{mN/m}$					Calculated radii ( $R_{v, \text{initial}}=2.4\mu\text{m}$ )				
shear rate ( $\text{s}^{-1}$ )	$d_2$ LP	$d_2$ LLP	$d_2$ LPL/LGC	$C_2$ (N)	LP ( $\mu\text{m}$ )	LLP ( $\mu\text{m}$ )	LPL ( $\mu\text{m}$ )	LGC ( $\mu\text{m}$ )	$R_{v, \text{morphology}}$ ( $\mu\text{m}$ )
0.0507	0.28	0.16	0.12	$10^{-11}$	4.3	2.6	2	2	2.8
0.101	0.45	0.24	0.18	$10^{-11}$	4.1	2	1.6	1.6	1.6
0.32	---	---	0.8	$10^{-11}$	---	---	4.6	4.6	1.2

For the PS/PE system, as well as for the PP/EVA-EMA, the predicted radius is very sensitive to the choice of the mixing rule. Table 6.1 shows that the LLP, LPL and LGC models give relatively satisfactory results for the lowest shear rates. Clearly the LP model overestimates the experimentally determined value. But the best description of the rheological data is obtained with the LP model. For the highest shear rate investigated, it was not possible to obtain reasonable fits with the LP and LLP models. In that case, the droplets diameters predicted by the LPL and LGC models are considerably larger than the value determined from scanning electron microscopy (the calculated radius is equal to  $4.6\mu\text{m}$  instead of a value of  $1.2\mu\text{m}$  determined from SEM analysis). For this PS/PE blend, none of these models appear to be adequate for predicting at high shear rates the morphological evolution of the blend even if good descriptions of the viscosity data can be obtained.

a)

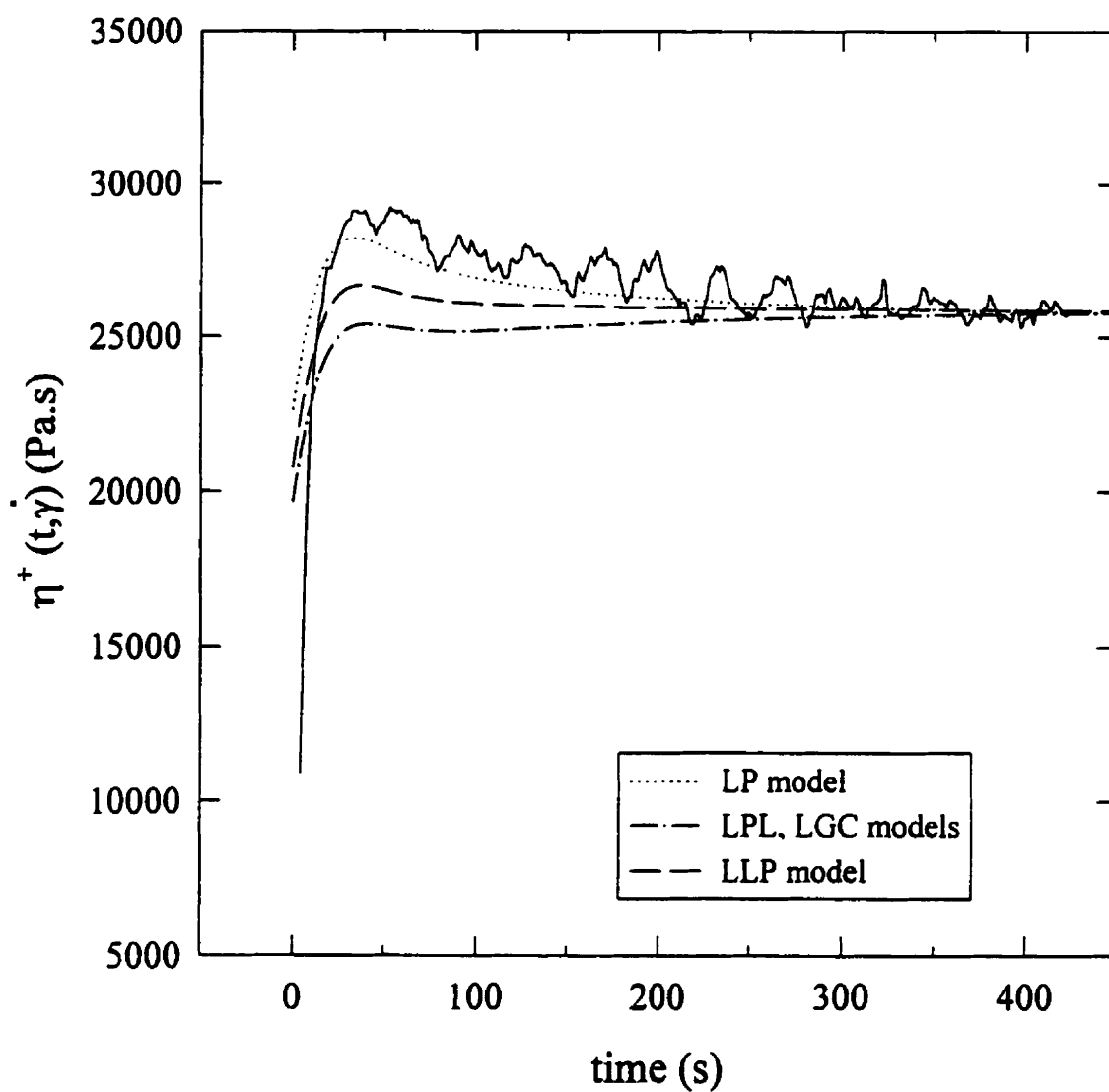


Figure 6.2 : Comparison between stress growth viscosity data and models predictions for a 80/20 PS/PE blend at  $T = 200^\circ\text{C}$  : (a)  $\dot{\gamma} = 0.0507 \text{ s}^{-1}$ , (b)  $\dot{\gamma} = 0.101 \text{ s}^{-1}$ , (c)  $\dot{\gamma} = 0.32 \text{ s}^{-1}$

b)

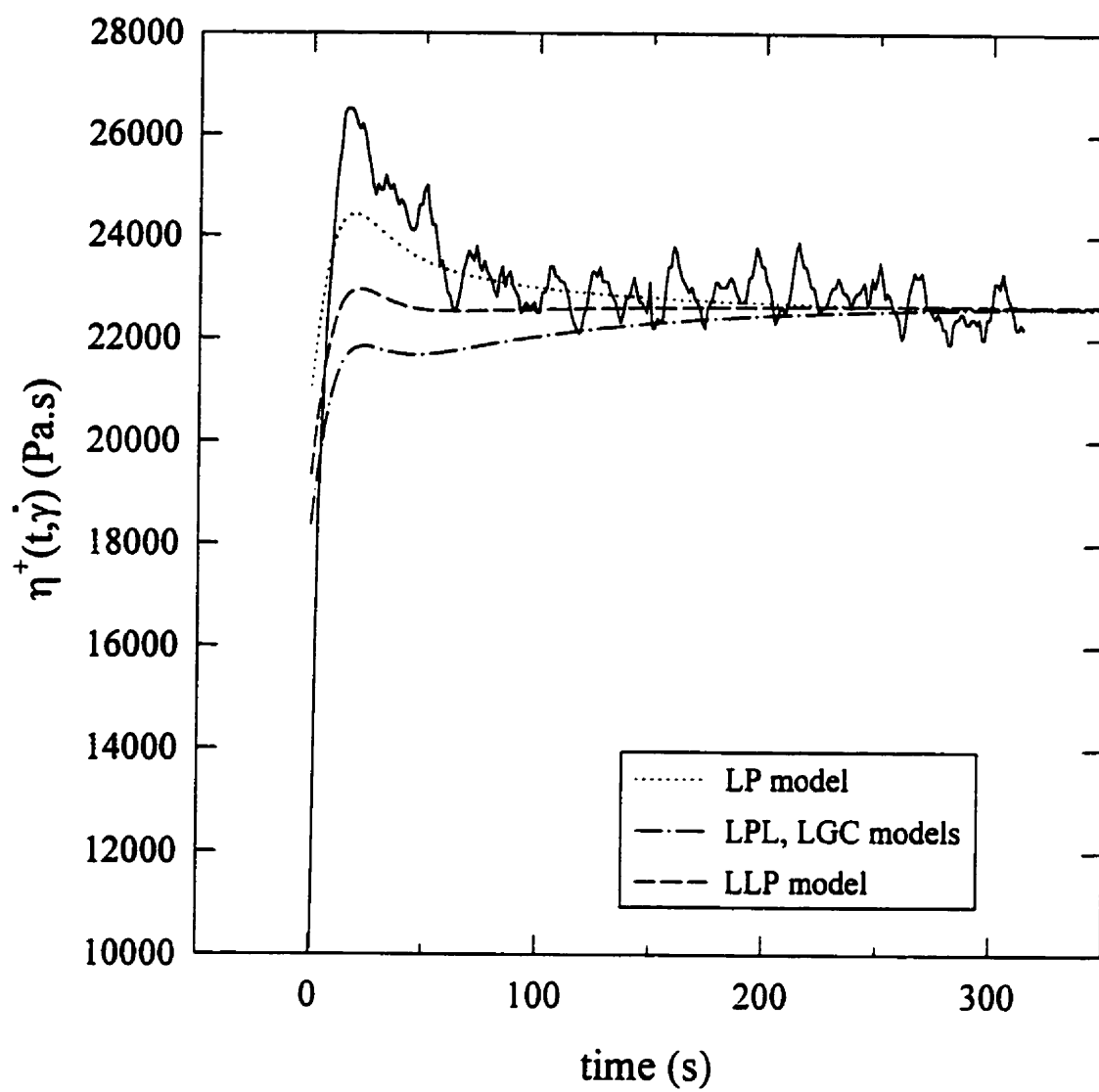


Figure 6.2 (suite)

c)

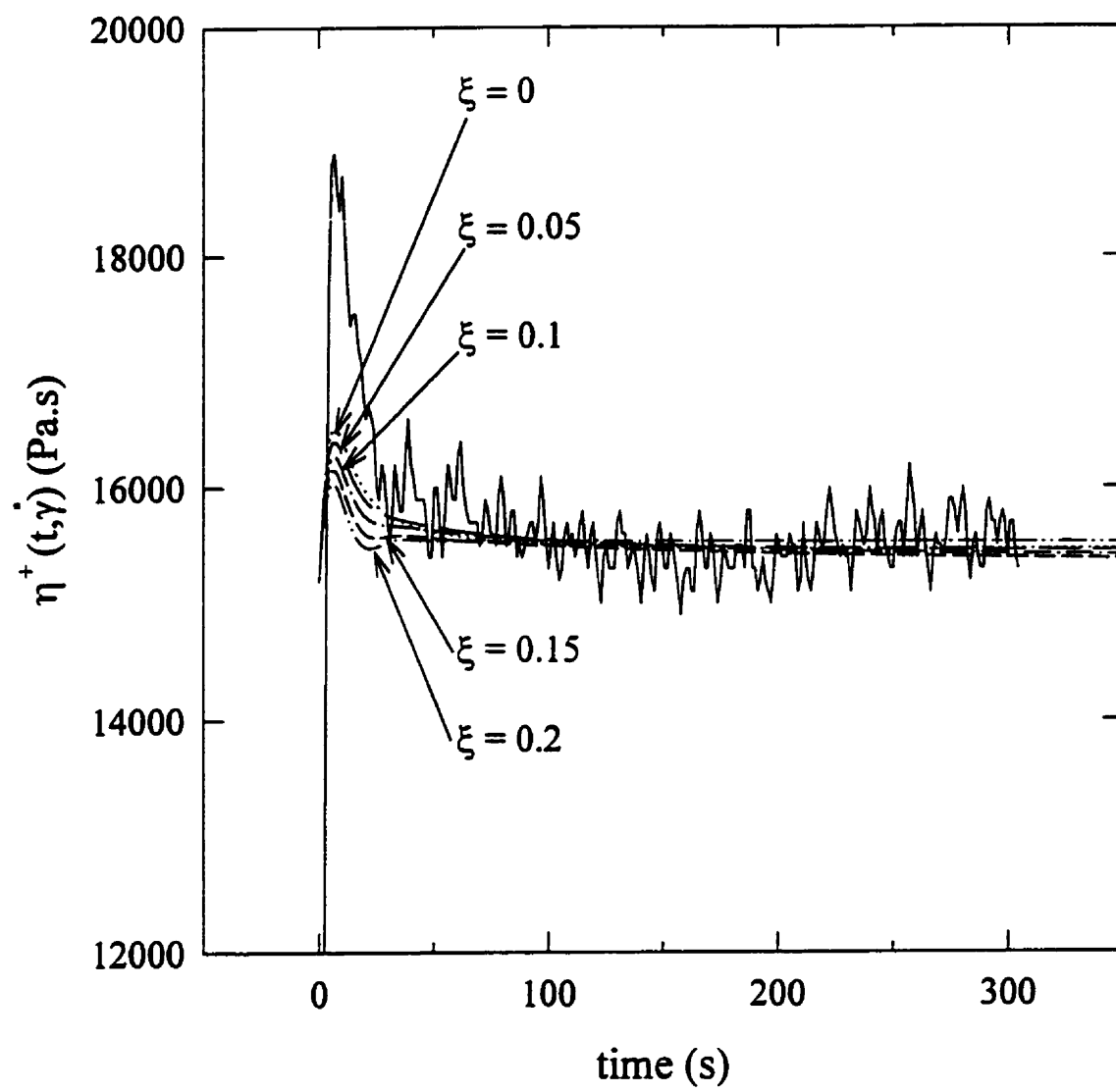


Figure 6.2 (suite)



For all these models affine deformation has been assumed. For the highest shear rate ( $0.32 \text{ s}^{-1}$ ), the LGC model predictions have been tested with the interface evolution equations that include the non affine deformation. The results reported in Figure 6.2c for the PS/PE blend show that when increasing value of the slip parameter  $\xi$ , the peak of the overshoot is decreasing. For values of  $\xi$  higher than 0.2, oscillations start to appear. To describe the rheological data, the parameters  $d_1$  and  $d_2$  have been kept constant but  $d_2$  had to be adjusted when changing the value of  $\xi$ . Table 6.2 shows that when  $\xi$  is increased,  $d_2$  has to be decreased to describe the transient viscosity. The predicted radii range from  $4.6 \mu\text{m}$  for  $\xi = 0$  to  $2 \mu\text{m}$  for  $\xi = 0.2$ . In this later case, the predicted result is closer to the value determined from microscopic analysis. The results presented in Table 6.2 and in Figure 6.2c show that  $\xi$  has a major influence on the calculated radii but it is of minor influence regarding the description of the rheological data.

Table 6.2 : Parameters used for predicting the transient rheological behavior of the 80/20 PS/PE blend and the 70/30 PP/EVA-EMA blend with the LGC non affine model.

PS/PE, shear rate = $0.32 \text{ s}^{-1}$ ,			PP/EVA-EMA $d_1 = 0.5$ , $d_2 = 0.715$ , $\alpha = -C_1 = 1.2 \text{ mN/m}$ , $C_2 = 10^{-11}$				
$\xi$	$d_2$	$R_v$ calculated ( $\mu\text{m}$ )	shear rate ( $\text{s}^{-1}$ )	$\xi$	$d_2$	$R_v$ calculated ( $\mu\text{m}$ )	$R_v$ morphology ( $\mu\text{m}$ )
0	0.8	4.6	0.0126	0.125	0.135	6.6	6
0.05	0.55	3.9	0.126	0.05	0.45	3	3
0.1	0.4	3.5					
0.15	0.3	3.2					
0.2	0.2	2					

The PP/EVA-EMA blend has been investigated at four different shear rates and the results for two different shear rates are presented in Figure 6.3. The LPL and LGC models are able to describe qualitatively and in certain cases quantitatively the breakup and coalescence phenomena. The larger disagreement was obtained for the lowest shear rate (see

Table 5.1 in [4]). When using the LGC model with non affine deformation, the results can be improved. As shown in Table 6.2, an appropriate choice of  $\xi$  and  $d_i$  allows to fit the morphological data. But as shown in Figure 6.3, the rheological data are not better described by releasing the affine deformation assumption. For both blends, PS/PE and PP/EVA-EMA, introducing non affine deformation can improve the results of the model regarding the morphology. The non affine motion requires, however, a supplementary parameter that has to be fitted, and the final morphology is required to determine this parameter. Indeed, we did not succeed to relate the parameter  $\xi$  to quantities such as the viscosities of the phases and the volume fraction which should constitute factors influencing the deformation state of the interface.

Table 6.1 shows that the mixing rule has a major influence on the calculated radius value. We already pointed out that the discrepancies observed can arise from the lack of coupling effects between the orientation tensor and the bulk properties. The bulk and the interfacial properties are treated as separate entities. Even if the contribution of the interface is minor compared to the bulk properties, the effects of the interface deformation is not negligible. We believe that considering the simple additivity of two contributions is valid for the linear viscoelastic domain, for which the deformations of the dispersed droplets remain small. But at moderately large deformations, the morphology (size, shape and orientation) of the dispersed phase will probably affect the rheology of the blend. The experiments show that large deformations have a great influence on the particles size (see Tables 6.1 and 6.2 and Table 5.1 in [4]). One has also to keep in mind that viscoelastic effects and mismatch of the viscosities of the two polymers will influence the behavior of the interface. The introduction of non affine deformation yields better results from a morphological point of view. A supplementary parameter  $\xi$  is, however, added and we do not know if the choice of this parameters is physically sound.

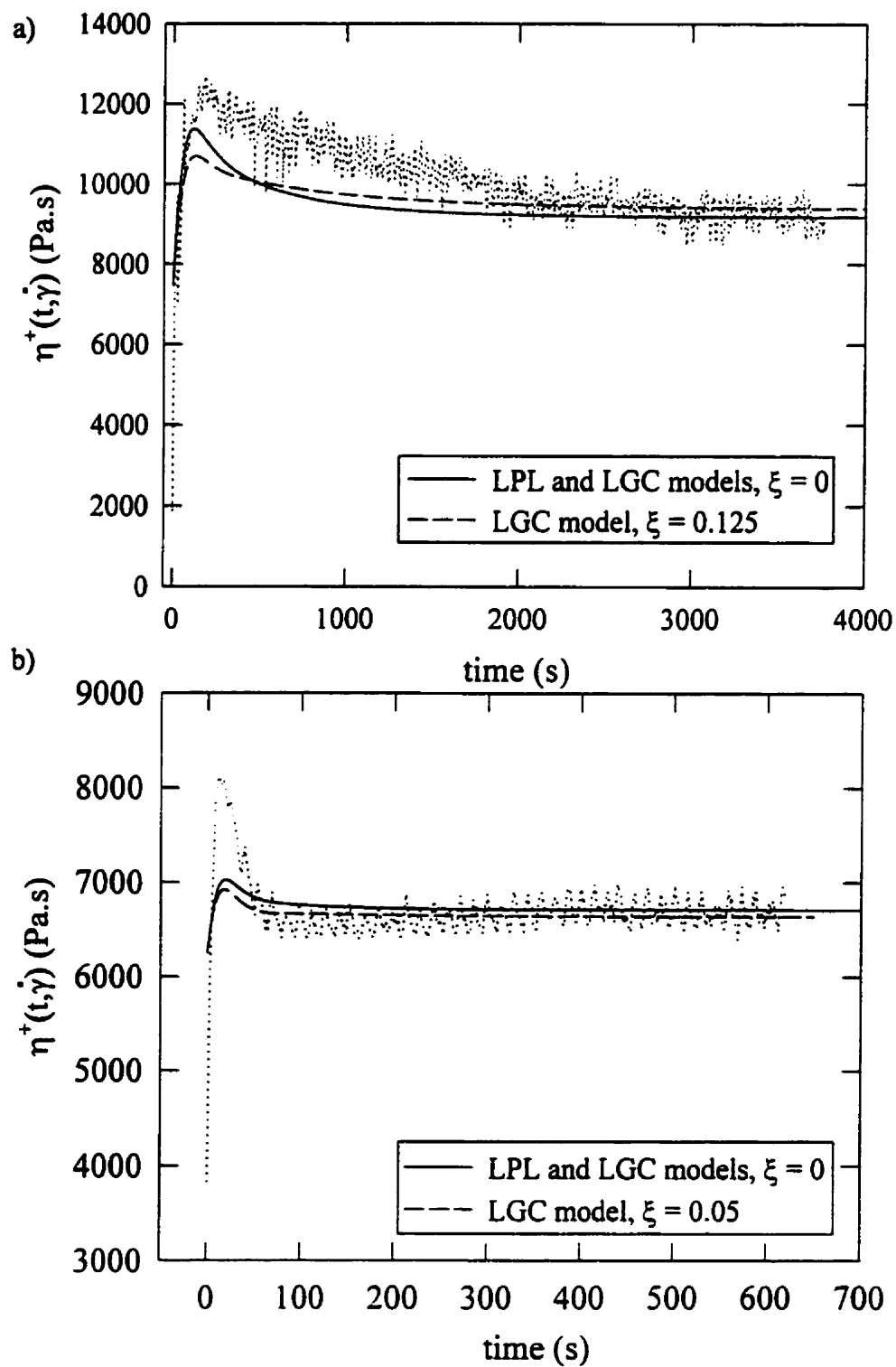


Figure 6.3 : Comparison between stress growth viscosity data and models predictions for a 70/30 PP/EVA-EMA blend at  $T = 200^\circ\text{C}$  : (a)  $\dot{\gamma} = 0.0126 \text{ s}^{-1}$ , (b)  $\dot{\gamma} = 0.126 \text{ s}^{-1}$

More and different rheological data are needed to confirm the assumption of affine deformation. Nevertheless, even with the assumption of affine deformation, the conformation tensor formalism remains very useful. At a macroscopic level of description, conformation tensors can illustrate the different states of the morphology during the flow.

$C$  characterizes an element of surface governed by a lower convected derivative,  $C^I$  is convected according to an upper derivative and represents the droplets. It is then possible to visualize the orientation of the droplets by plotting the conformation ellipses (Ghosh et al. [36]). The conformation tensor is mapped onto a two dimensional plane at different times. The principal axes of the ellipses are determined by the eigenvectors of  $C^I$  whereas the eigenvalues of  $C^I$  represent the major and minor axis respectively. Figure 6.4 illustrates the effects of an imposed shear rate of  $0.126 \text{ s}^{-1}$  on the evolution with the time of the conformation tensors for the 70/30 PP/EVA-EMA blend relatively to the evolution of the normalized interfacial area. Figure 6.4a shows the evolution of the predicted normalized interfacial area in stress growth and relaxation experiment. An increase of  $Q$  indicates that breakup has occurred whereas a decrease of  $Q$  is associated with coalescence or with the recovery of the deformed droplets. Figure 6.4b illustrates the different conformation states of the tensor  $C^I$  corresponding to the morphological changes shown in Figure 6.4a. At  $t = 0$  the isotropic state is represented by a circle. Upon the imposition of the shear rate, the droplets orient themselves along a preferred direction which is given by the major axis of the ellipse. The minor axis gives a qualitative idea of the spread in this preferred direction. Upon cessation of flow, the deformed droplets tend to recover their equilibrium shape under the effects of the interfacial tension to attain the isotropic state back. This representation remains, however, only indicative.

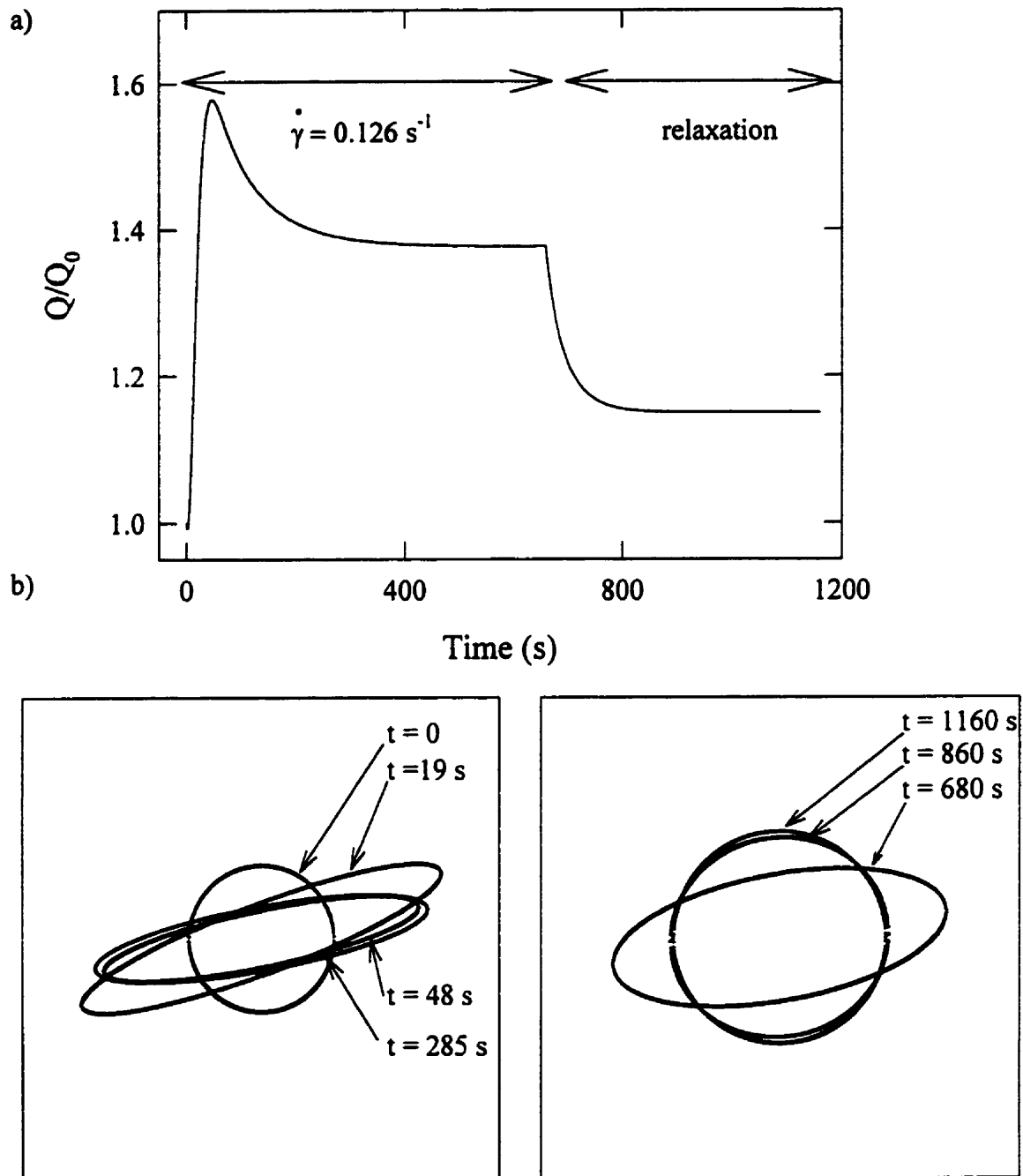


Figure 6.4 : (a) Evolution with time of the normalized interfacial area predicted for the LGC model for the 70/30 PP/EVA-EMA blend in stress growth and relaxation experiment at  $T = 200^{\circ}\text{C}$  with an imposed shear rate of  $\dot{\gamma} = 0.126 \text{ s}^{-1}$ ; (b) Evolution of the conformation tensor  $C'$  during stress growth and relaxation.

### 6.5.2) Morphology and elongational flow

The first step for the estimation of the elongational viscosity according to the Eqs.(6.18, 6.26 and 6.30) is to determine the power-law parameters of the shear viscosity. Results for the components and the blends (PP, EVA-EMA, 70/30 PP/EVA-EMA and 30/70 PP/EVA-EMA) are reported in Table 6.3.

Table 6.3 : Power-law parameters in shear of the different systems.

	PP	EVA/EMA	70/30 PP/EVA-EMA	30/70 PP/EVA-EMA
K (Pa.s <sup>n</sup> )	6455	2884	5755	4730
n	0.47	0.44	0.46	0.43

The range of shear rates covered by the capillary measurements was from 50-100 s<sup>-1</sup> to about 500 s<sup>-1</sup> depending on the polymer and the die. The power-law parameters have been fitted following Bagley corrections and Rabinovitsch analysis. For higher shear rates, outlet instabilities were very pronounced. Since the purpose of this work was not to study instabilities, the data were collected only when no extrudate distortion was visible and for stable extrusion pressures. The onset of the instabilities regions were relatively different for the blends compared to their matrix. With the converging dies, no instabilities were observed whatever the polymer and the flow rate. As shown in Figure 6.5, it was, however, not possible to verify adequately the Cox-Merz rule for the unblended components. The steady shear data are lower than the complex data and of slightly different slope, especially for the PP. This could be explained by viscous dissipation. For all molten polymers or blends investigated in this study, the melt temperature measured at the wall was much higher than the set point of 200°C. The temperature fluctuated between 210°C and 225°C depending on the flow rate.

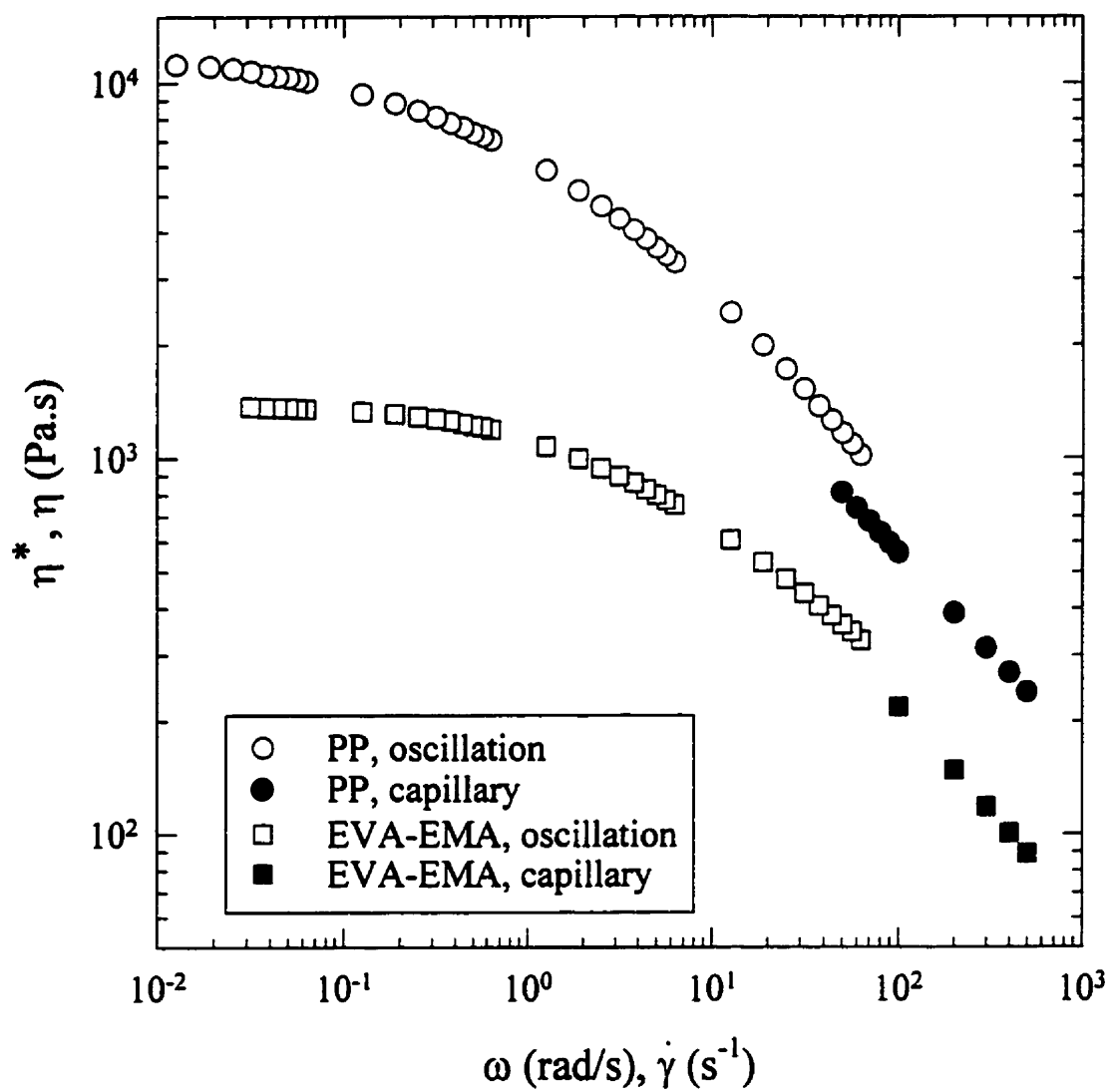


Figure 6.5 : Complex and steady shear viscosities of the PP and the EVA-EMA at  $T = 200^\circ\text{C}$ .

In adiabatic conditions, the variation of the bulk temperature due to viscous dissipation can be calculated according to the following equation (Carreau et al. [37]):

$$\Delta T = \frac{\Delta P}{\rho C_p} \quad (6.36)$$

For the polypropylene,  $\Delta T$  is estimated to be around 5°C at the maximum flow rate. This variation of the bulk temperature is significant enough to affect the rheological measurements which assume isothermal flow and therefore the Bagley corrections.

Figure 6.6 reports the elongational viscosity as calculated by the Cogswell, Binding and Mackay-Astarita methods. Notice that the contribution of the shear components is not negligible and represents around 40% of the total entrance pressure drop. For all the systems investigated, the extensional viscosity determined from the Cogswell analysis is higher than the one calculated with the Binding method. These results are similar to those obtained by Padmanabhan et al. [38]. The results based on the Mackay and Astarita method lie in between. For all the systems studied, the behavior at high extensional strain rate is of a power-law form. The parameters  $L$  and  $t$  of Binding and Mackay/Astarita analysis are reported in Table 6.4. The extensional behavior of the blend is in between those of the matrix and the minor phase for the two composition investigated. The behavior of both blends is dominated by that of the matrix as shown especially in the lower elongational strain rate region. Discrepancies can, however, be observed between the two set of data obtained from the dies D1 and D2. The calculated elongational viscosities do not overlap at a given extensional strain rate except for the 70/30 PP/EVA-EMA blend. We believe that in this later case this is purely fortuitous. The data presented in Figure 6.6 have been duplicated several times and even if temperature variations could be observed, the accuracy is good. But first, if we compare the data at a given extensional strain rate, these values are obtained for different flow conditions because of the die geometry differences. The flow field could be affected by different convergences and possible entry effects could perturb the measured pressure. Second, the pressure measurements cover a wide range of extensional rates of



strain for which the equivalent effective rate of deformation would be given by  $\sqrt{3}\dot{\epsilon}$ . To determine the elongational viscosity from Binding and Mackay/Astarita analysis, the power-law parameters are required. As the range of shear data covers the interval 50-100 s<sup>-1</sup> up to around 500 s<sup>-1</sup>, it is not to be excluded that extrapolating the range of validity of the power-law to relatively small shear rates, equivalent to the lowest extensional strain rates, leads to an overestimation of the parameters K and n. It would affect not only the shear viscosity, especially in the transition zone between the Newtonian and shear thinning behavior, but also the extensional viscosity. Therefore, this would limit the range of validity of the data to the high rate of strain region.

Table 6.4 : Power-law parameters in elongation from the Binding and Mackay/Astarita analysis.

	Binding method		Mackay/Astarita method	
	L (Pa.s <sup>n</sup> )	t	L (Pa.s <sup>n</sup> )	t
PP (D1)	36885	0.5	43370	0.5
PP (D2)	62670	0.35	72185	0.35
EVA/EMA (D1)	12780	0.69	15780	0.69
EVA/EMA (D2)	6725	0.97	8735	0.97
70/30 PP/EVA-EMA (D1)	25980	0.56	30960	0.56
70/30 PP/EVA-EMA (D2)	25575	0.56	30474	0.56
30/70 PP/EVA-EMA (D1)	14315	0.68	17815	0.68
30/70 PP/EVA-EMA (D2)	8025	0.92	10410	0.92

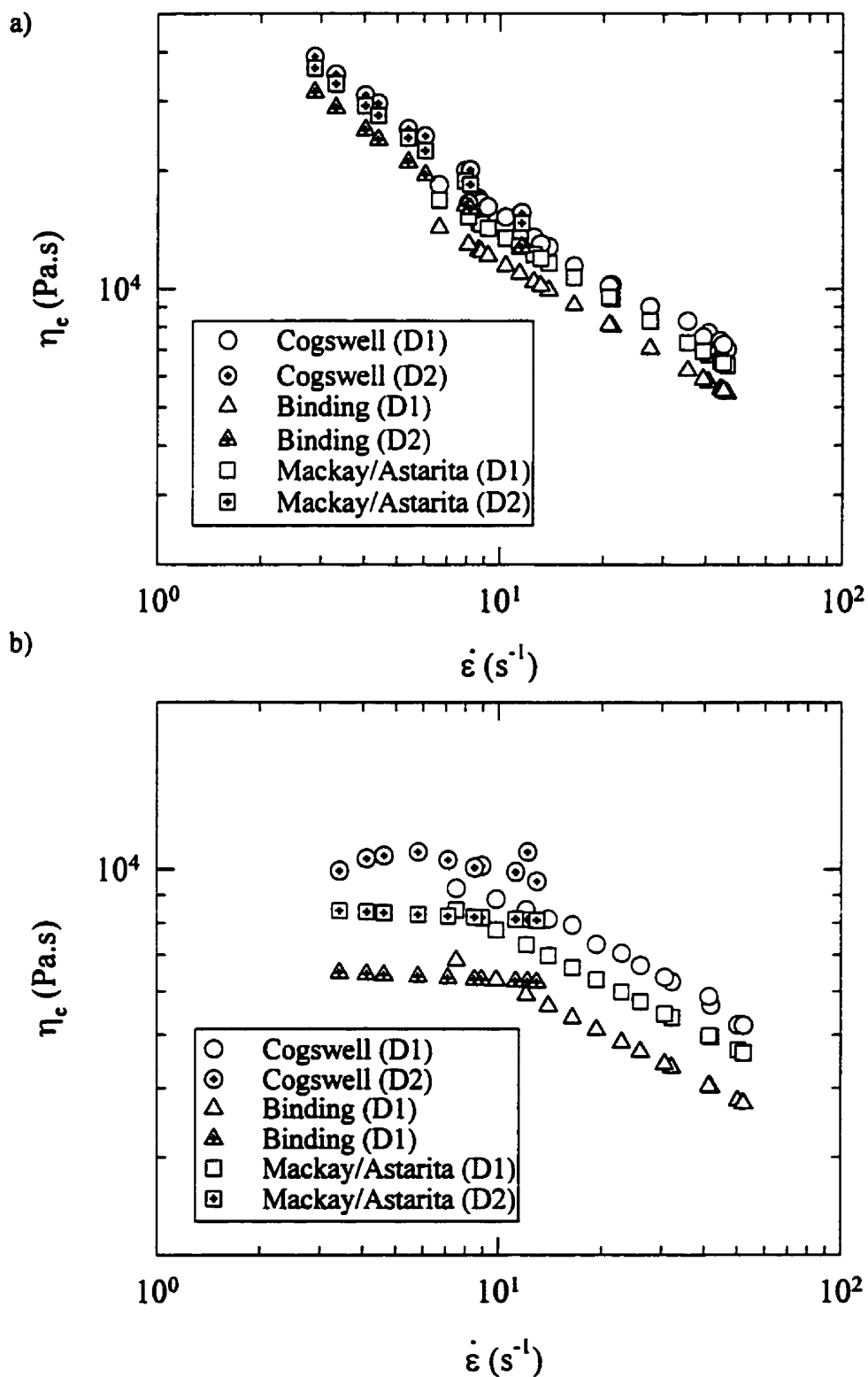


Figure 6.6 : Elongational viscosity of : (a) PP, (b) EVA-EMA, (c) 70/30 PP/EVA-EMA, (d) 30/70 PP/EVA-EMA.

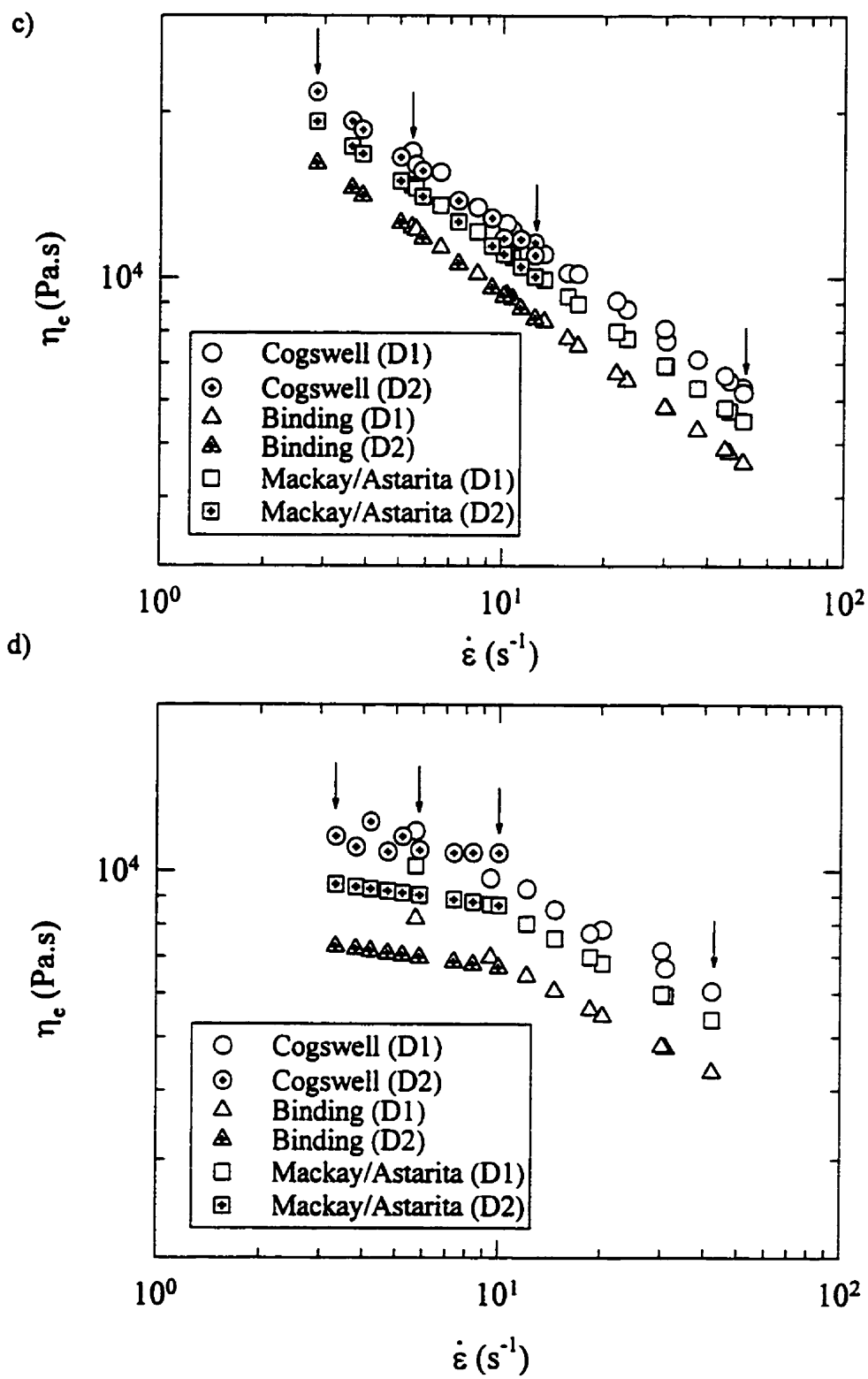


Figure 6.6 (suite)

These data represent apparent extensional properties of the materials. They are nevertheless useful to compare the relative extensional behavior of the blends and of the two matrices. Figure 6.7 reports the Trouton ratios for the four systems investigated as a function of the second invariant of the rate of deformation tensor,  $\bar{\dot{\gamma}}$ , equal to  $\sqrt{3}\dot{\epsilon}$  for uniaxial elongational flow and to  $\dot{\gamma}$  for simple shear flow. As a result of the discrepancies observed between data obtained using the two different dies in Figure 6.6, the lack of overlapping is more visible when plotting the Trouton ratio. It shows nevertheless the pronounced elongational behavior of the different species and the relations between the blends and their matrix. In all cases, the results far exceed the limiting case of Newtonian fluids for which the ratio is equal to 3. The EVA/EMA is strain-hardening and very large values of the Trouton ratio is obtained at the largest elongational rates. The behavior of both blends are also strain-hardening, but the effect is less pronounced with the 70/30 PP/EVA-EMA blend, probably under the influence of the PP phase which is more strain-thinning than strain-hardening. As already mentioned, the setup presented in Figure 6.1 allows us to extract the samples for morphological analysis before the converging section. For both blends, the dispersed phase (EVA-EMA or PP) is present as spherical particles. But for the 30/70 PP/EVA-EMA blend, despite of the static mixer installed at the reservoir entry, the morphology of the extracted samples shows droplets and also not very well defined domain (see Figure 6.8). The volume average diameter of the droplets for both blends is about the same, i.e. independent of the zero shear viscosity ratio (see Table 6.5). The arrows in Figure 6.6 indicate for which conditions the different samples have been extracted at the exit of the die for morphological analysis. The minus and plus signs appearing in Table 6.5 correspond for each die to the lowest and highest flow rates for which morphological analysis has been carried out. As expected through extrusion in the converging die, a transition is observed towards a fibrillar structure (Figure 6.9). The fibril diameters are almost the same for both blends and considering the error included in the fibril diameter determination, one could say that the diameter is not affected by the extensional rate.

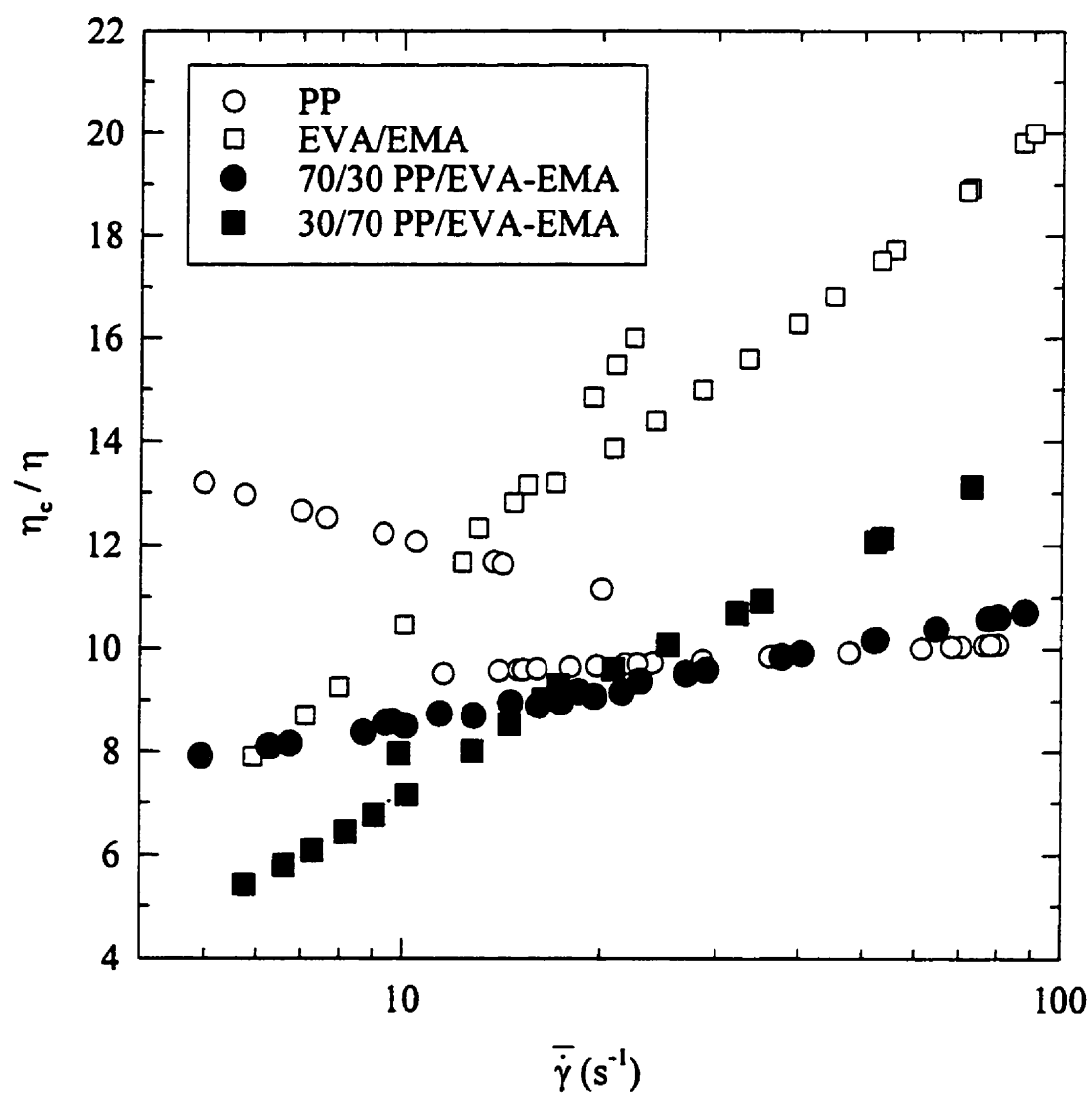
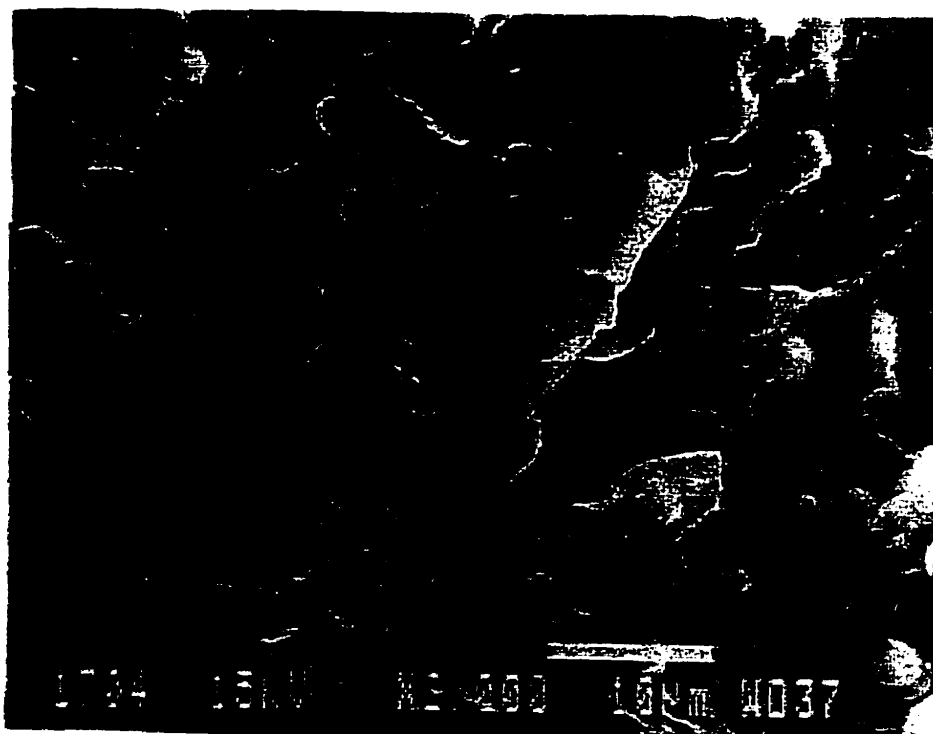


Figure 6.7 : Trouton ratio for the PP, EVA-EMA and the 70/30 PP/EVA-EMA, 30/70 PP/EVA-EMA.blends

a)



b)

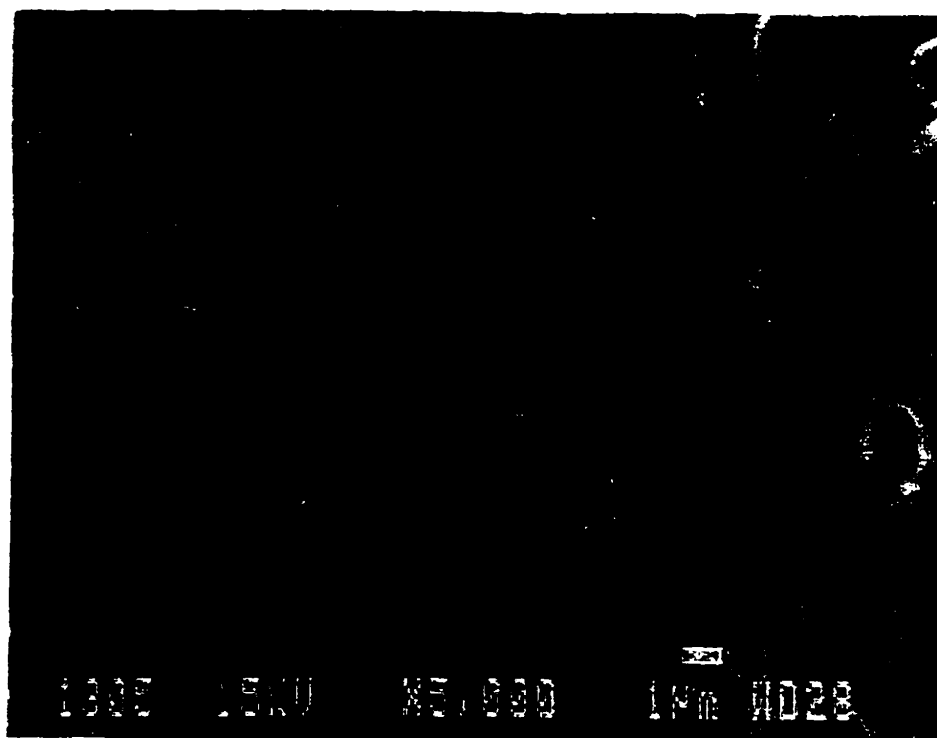
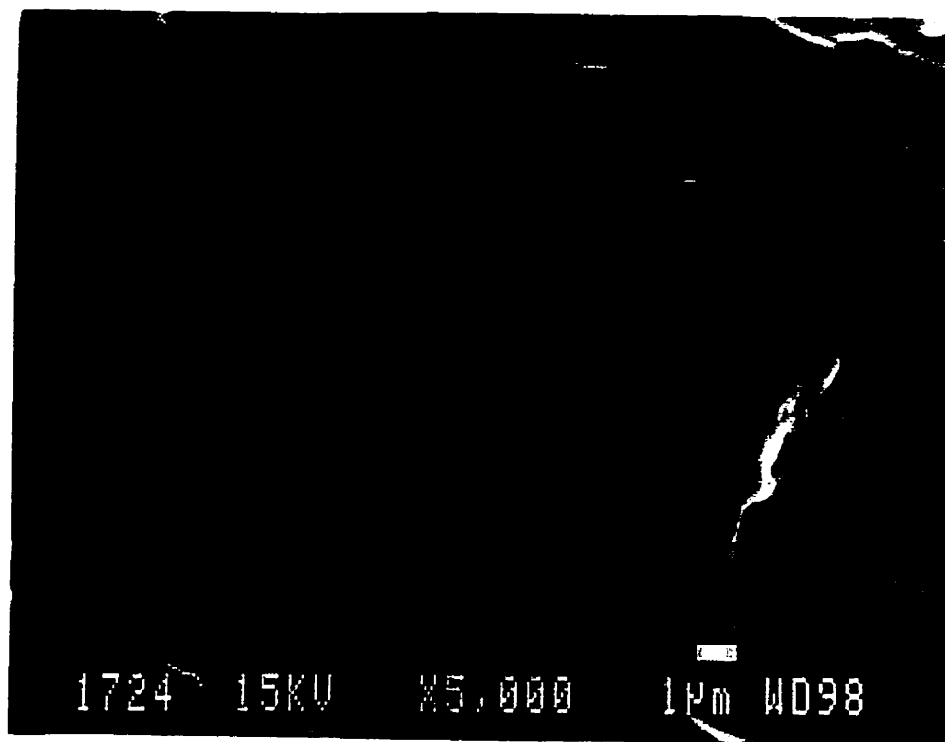


Figure 6.8 : Micrographs of the blends before the converging section : (a) 70/30 PP/EVA-EMA, (b) 30/70 PP/EVA-EMA.

a)



b)

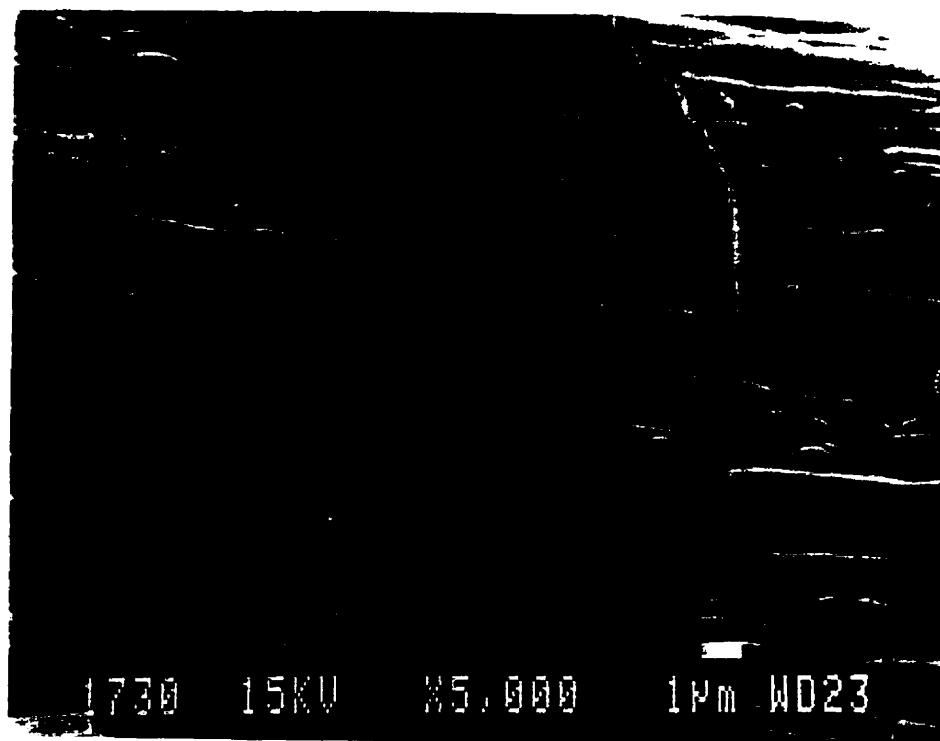


Figure 6.9 : Micrographs of the blends after the converging section with the die D2 at the lowest flow rate : (a) 70/30 PP/EVA-EMA, (b) 30/70 PP/EVA-EMA.

Table 6.5 : Morphology obtained after extrusion through both hyperbolic shaped dies.

	Fibrils diameter ( $\mu\text{m}$ )			
	D1		D2	
	(-)	(+)	(-)	(+)
70/30 PP/EVA-EMA, $R_{v \text{ initial}} = 1.45 \mu\text{m}$	0.8	0.6	0.8	0.7
30/70 PP/EVA-EMA, $R_{v \text{ initial}} = 1.45 \mu\text{m}$ + domains	1	1.1	0.9	0.9
	+ ellipsoids		+ ellipsoids	

For the 30/70 PP/EVA-EMA blend ellipsoids are also present. We believe, however, that these ellipsoids are the result of the not well defined domain deformation. Several particular features can be extracted from this result. For both dies, D1 and D2, the Hencky strain is constant and equal to 3.6 and 3.7 respectively. The resulting morphology is probably dependent on the Hencky strain and not on the extensional strain rate. Even if the initial particles diameter is relatively small, such dominant elongational flows are able to generate fibrillar structure. But the flow is not the only variable to take into account. The pronounced elongational behavior which can be seen from the Trouton ratio values (Figure 6.7) seems to have a great influence on the resulting morphology. It appears therefore that the zero shear viscosity ratio represents only one of the parameters governing the formation of a given morphology. The elasticity, which can be estimated through the analysis of the normal forces should constitute moreover a dominant factor in the establishment of the final morphology (Elmendorp and Malcke [39]). The PP phase in the 30/70 PP/EVA-EMA blend is indeed around ten times more viscous and the formation of a fibrillar structure is still observed in a very short time (the residence time in the die lies about the interval 0.1-1s depending on the flow rate).



Equations (6.1) and (6.2) can be assessed to predict the morphological evolution of the blend in a purely elongational flow. The interface governing equations developed by Doi and Ohta [1] and extended by Lee and Park [2] allow to describe the transition from a spherical morphology to a fibrillar structure. Nevertheless, the predictions remain only qualitative because the predicted interfacial area is greatly overestimated. The calculated radii of fibers are of the order of nm whereas we determine experimentally radii of the order of  $0.4\ \mu\text{m}$ . Moreover, the time needed to reach a fibrillar structure is much longer than the residence time in the die (from about 0.1 to 1 s depending on the flow rate). For non affine deformation, the results were similar. When using Eqs. (6.1) and (6.2) we have considered the flow purely extensional and used for a given extensional strain rate the viscosity as determined by applying one of the method explained in the paragraph below. The values of the elongational viscosity are in the same order of magnitude for Cogswell, Binding and Mackay/Astarita analysis and the different methods used to evaluate the extensional viscosity have been proved to be accurate and comparable with other techniques. Therefore, we think that the discrepancies could arise from the fact that the flow is not purely extensional. We recall that around 40% of the entry pressure drop was found to be due to the shear components of the flow. Moreover, Eqs. (6.1) and (6.2) may not be general enough to describe adequately the morphological evolution under elongational flows. Some work is still needed to characterize adequately these major transitions and test the relaxation mechanism proposed by Lee and Park [2]. Vinckier et al. [11] have indeed reported very recently that this mechanism was not adapted for the breakup of highly extended droplets (fibrils) by end-pinching or Rayleigh instabilities and only correctly predicted the relaxation of slightly deformed droplets. We found, however, a relative agreement between the Lee and Park equations and the predictions of the retraction process induced by Rayleigh instabilities, also used as the breaking thread method. This is obviously relatively far from our experiment for which, even if long thread are formed, residual stresses are still present and coalescence can occur during the relaxation process. We hope that the above observations may be indicative for further developments in this area.

## 6.6) Concluding remarks

The Lee and Park model [2] as well as modified versions (Lacroix et al. [4]) are shown to predict qualitatively the morphological changes in immiscible blends occurring in both shear and elongational flows. In stress growth experiments, an overshoot in the shear stress is observed, which is a characteristic of the deformation of the interface. The linear viscoelastic and stress growth data are used to evaluate the model parameters and predict the size of the dispersed phase following stress relaxation. It has been shown that the predictions of the different models are very sensitive to the choice of the mixing rule used to account for a mismatch of the both phase viscosities. We believe that coupling effects between the bulk properties and the interfacial tensor should be taken into account. This remains nevertheless an open subject. Adding an additional parameter for non affine deformations could lead to better results in certain cases but the predictions remain bounded to the chosen mixing rule. For elongational flows, the Lee and Park governing interface equations are able to predict qualitatively the transition from an initial spherical morphology to a fibrillar structure. The morphologies have been obtained with a nozzle shaped die, for which the flow is mostly extensional. The extensional viscosity used in the Lee and Park equations have been calculated from entrance pressure drop measurements. Cogswell [22], Binding [23] and Mackay/Astarita [24] analysis have been used for this purpose and all the three methods lead to values ranging in the same order of magnitude. The elongational behavior of both 70/30 PP/EVA-EMA and 30/70 PP/EVA-EMA blends is less strain-thinning than the PP and very large Trouton ratio values are obtained for the 30/70 PP/EVA-EMA blend. The elongational properties of the EVA-EMA phase influence greatly those of the blends and appear to be a dominant factor in the resulting morphology. Fibrillar morphology are indeed observed for viscosity ratios of 0.1 and 10.

## Acknowledgments

The authors are thankful for the financial support received from ELF-ATOCHEM. Discussions with Prof. M. Moan are gratefully acknowledged. We are also thankful to

Messrs. L. Parent and C. Painchaud for their help during compounding.

## 6.7) References

- [1] M. Doi and T. Ohta, " Dynamics and Rheology of Complex Interfaces. I ", J. Chem. Phys. **95** (1991) 1242-1248.
- [2] H.M. Lee and O.O. Park, " Rheology and dynamics of Immiscible Polymer Blends ", J. Rheol. **38** (1994) 1405-1425.
- [3] M. Grmela and A. Ait-Kadi, "Comments on the Doi-Ohta theory of blends", J.Non-Newtonian Fluid Mech. **55** (1994) 191-195.
- [4] C. Lacroix, M. Grmela and P.J. Carreau, "Relationships between rheology and morphology for immiscible molten blends of polypropylene and ethylene copolymers under shear flow", J. Rheol. **42** (1998) 41-62.
- [5] Y. Takahashi, N. Kurashima, I. Noda, and M. Doi, "Experimental tests of the scaling relation for textured materials in mixtures of two immiscible fluids", J. Rheol. **38** (1994) 699-712.
- [6] Y. Takahashi, S. Kitade, N. Kurashima, and I. Noda, "Viscoelastic properties of immiscible polymer blends under steady and transient shear flows", Polym. J. **26** (1994) 1206-1212.
- [7] Y. Takahashi and I. Noda, " Domain structures and viscoelastic properties of immiscible polymer blends under shear flow" in Flow-Induced Structure in Polymers, edited by A. Nakatani and M. D. Dadmun (Am. Chem. Soc., Washington D.C., 1995) p 140-152.
- [8] G.K. Guenther and D.G. Baird, "An Evaluation of the Doi-Ohta Theory for an Immiscible Polymer Blend", J. Rheol. **40** (1996) 1-20.
- [9] I. Vinckier, P. Moldenaers, and J. Mewis, "Relationship between Rheology and Morphology of Model Blends in Steady Shear Flow", J. Rheol. **40** (1996) 613-631.
- [10] I. Vinckier, P. Moldenaers, and J. Mewis, "Transient rheological response and morphology evolution of immiscible polymer blends", J. Rheol. **41** (1997) 705-718.
- [11] I. Vinckier, J. Mewis and P. Moldenaers, "Stress relaxation as a microstructural probe for immiscible polymer blends", Rheol. Acta. **36** (1997) 513-523.

- [12] S. Kitade, A. Ichikawa, N. Imura, Y. Takahashi, and I. Noda, "Rheological properties and domain structures of immiscible polymer blends under steady and oscillatory shear flows", *J. Rheol.* **41** (1997) 1039-1060.
- [13] C. Lacroix, M. Aressy, and P.J. Carreau, "Linear viscoelastic behavior of molten polymer blends: a comparative study of the Palierne and the Lee and Park models", *Rheol. Acta* **36** (1997) 416-428.
- [14] R.G. Larson, "Constitutive equations for polymer melts and solutions", Ed. Butterworths (1988)
- [15] H. Gramespacher and J. Meissner, "Melt elongation and recovery of polymer blends, morphology, and influence of interfacial tension", *J. Rheol* **41** (1997) 27-44.
- [16] L. Levitt, C. W. Macosko, T. Schweizer and J. Meissner, "Extensional rheometry of polymer multilayers: A sensitive probe of interfaces", *J. Rheol* **41** (1997) 671-685.
- [17] G. I. Taylor, "The deformation of emulsions in definable fields of flow", *Proc. Roy. Soc. London Ser A* **146** (1934) 501-523.
- [18] H.A. Stone, B.J. Bentley, L.G. Leal, "An experimental study of transient effects in the breakup of viscous drop", *J. Fluid. Mech.* **173** (1986) 131-158.
- [19] W.J. Milliken and L.G. Leal, "Deformation and breakup of viscoelastic drops in planar extensional flows", *J. Non-Newtonian Fluid Mech.* **40** (1991) 355-379.
- [20] I. Delaby, B. Ernst, Y. Germain and R. Muller, "droplet deformation in polymer blends during uniaxial elongational flow: Influence of viscosity ratio for large capillary numbers", *J. Rheol.* **38** (1994) 1705-1720.
- [21] F. Mighri, A. Ajji and P.J. Carreau, "Influence of elastic properies on drop deformation in elongational flow", *J. Rheol* **41** (1997) 1183-1201.
- [22] J. Meissner "Development of a universal extensional rheometer for the uniaxial extension of polymer melts", *Trans. Soc. Rheol* **16** (1972) 405-420
- [23] F. N. Cogswell, "Converging flow of polymer melts in extrusion dies", *Polym. Eng. Sci.* **12** (1972) 64-73.

- [24] D.M. Binding, "An approximate analysis for contraction and converging flows", J. Non-Newtonian Fluid Mech. **27** (1988) 173-189.
- [25] M.E. Mackay and G. Astarita, "Analysis of entry flow to determine elongation flow properties revisited", J. Non-Newtonian Fluid Mech. **70** (1997) 219-235.
- [26] F. N. Cogswell, "Measuring the extensional rheology of polymer melts", Trans. Soc. Rheol. **16** (1972) 383-403.
- [27] F. N. Cogswell, "Converging flow and stretching flow : A compilation", J. Non-Newtonian Fluid Mech. **4** (1978) 23-38.
- [28] A.G. Gibson, "Converging dies" in Rheological Measurements, edited by A.A Collyer and D.W. Clegg (1988) 49-92
- [29] B. Tremblay, "estimation of the elongational viscosity of polyethylene blends at high deformation rates", J. Non-Newtonian Fluid Mech. **33** (1989) 137-164.
- [30] D.M. Binding and D.M. Jones, "On the interpretation of data from converging flow rheometers", Rheol. Acta **28** (1989) 215-222.
- [31] H.C. Kim, A. Pendse and J. R. Collier, "Polymer melt lubricated elongational flow", J. Rheol. **38** (1994) 831-845.
- [32] D. F. James, G. M. Chandler and S. J. Armour, "A converging channel rheometer for the measurement of extensional viscosity", J. Non-Newtonian Fluid Mech. **35** (1990) 421-443.
- [33] D. F. James, "Flow in a converging channel at moderate Reynolds numbers", AIChE J. **37** (1991) 59-64.
- [34] G. Crevecoeur and G. Groeninckx, "Fibril formation in *in situ* composites of a thermotropic liquid crystalline polymer in a thermoplastic matrix", J. Appl. Polym. Sci. **49** (1991) 839-849.
- [35] D. M. Binding, "Contraction flows and new theories for estimating extensional viscosity", edited by A.A Collyer, Chapman and Hall (1993) 1-32.
- [36] T. Ghosch, M. Grmela and P.J. Carreau, "Rheology of short fibers filled thermoplastics" Polym. Composites, **16** (1995) 144-153

- [37] P.J. Carreau, D. De Kee, R.P. Chhabra in "Rheology of polymeric systems : principles and applications", Hansers Publishers (1997)
- [38] M. Padmanabhan and C. W. Macosko, "Extensional viscosity from entrance pressure drop measurements", *Rheol. Acta* **36** (1997) 144-151.
- [39] J. J. Elmendorp and R. J. Maalcke, "A study on polymer blending microrheology: Part I", *Polym. Eng. Sci.* **25** (1985) 1041-1047.

## CHAPITRE 7 - CONCLUSIONS ET PERSPECTIVES

Ce travail est largement basé sur l'analyse et l'utilisation du modèle de Lee et Park (1994). Cette équation d'état, initialement développée pour prendre en considération les changements de morphologie se produisant dans un mélange immiscible lors d'un écoulement, n'avait été étudiée que dans un cadre de viscoélasticité linéaire et ce, pour un seul système. Depuis quelques années, plusieurs équipes de recherche se sont consacrées à l'étude des relations entre la rhéologie de mélanges modèles et leur morphologie tel que prédit par la théorie de Doi et Ohta (1991). Dans le cadre de cette thèse, une démarche systématique a été adoptée pour évaluer l'incidence de différents écoulements sur la rhéologie et la morphologie de mélanges de polymères commerciaux à l'état fondu. Différentes approches (modèle de Lee et Park, modèles de conformation) ont été utilisées pour cerner les paramètres qui influencent et participent à l'établissement d'une morphologie.

Dans le premier article, les prédictions du modèle de Lee et Park (1994) sont confrontées à celles du modèle de Palierne (1990). Cette étude permet ainsi de confirmer que le modèle de Palierne est apte à prédire le comportement viscoélastique linéaire des mélanges sans l'ajustement de paramètres. Cette comparaison, effectuée sur trois mélanges différents, montre que la description des données dans le domaine des basses fréquences est relativement similaire pour les deux modèles étudiés. Ceci justifie donc les équations d'évolution d'interface proposées par Lee et Park et, même si un paramètre doit être ajusté dans ce cas, il confère une certaine flexibilité au modèle. En revanche, pour des phases présentant des propriétés rhéologiques bien différentes, des déficiences entre les résultats expérimentaux et les prédictions du modèle ont pu être observées dans le domaine des hautes fréquences. Ces déficiences sont attribuées à la loi de mélange incluse dans le modèle de Lee et Park (1994). Une relation empirique est de ce fait introduite pour mieux décrire les résultats expérimentaux et satisfaire certains cas limites. Enfin une méthode approximative de détermination du paramètre ajustable dans le modèle de Lee et Park est proposée à partir



de la comparaison entre différents temps caractéristiques associés à l'interface.

Dans le second article, les propriétés viscoélastiques non linéaires des mélanges sont étudiées. Le modèle de Lee et Park (1994), ainsi que le modèle suggéré dans la première partie de ce travail sont évalués dans le cadre d'un écoulement en cisaillement simple parfaitement contrôlé. Une version modifiée du modèle de Grmela et Ait-Kadi (1994), définie de sorte que les modes de relaxation proposés par Lee et Park puissent être retrouvés à partir de considérations thermodynamiques, est aussi testée. Ces différentes relations utilisées pour décrire les données rhéologiques en régime transitoire permettent de prédire l'évolution de la morphologie au cours du cisaillement. Les modèles de Lee et Park et de Grmela et Ait-Kadi modifiés prédisent qualitativement ou quantitativement les phénomènes de coalescence ou de rupture s'opérant sur un mélange PP/EVA-EMA dans un écoulement en cisaillement simple. Une telle exploitation des modèles constitue une nouvelle approche des relations entre la rhéologie d'un mélange et sa morphologie induite dans l'écoulement. La comparaison de ces diverses prédictions avec les données obtenues à partir d'analyses d'images sur des micrographies, montre que la règle de mélange incluse dans chacun des modèles joue un rôle déterminant sur les résultats finaux. Cet accord entre les prédictions théoriques et les mesures expérimentales est malgré tout limité au cas où les inclusions sont déformables.

Dans le troisième article, un autre système (PS/PE) permet de mettre en évidence les limitations de ces modèles. En effet, les changements de morphologie ne peuvent être prédits qualitativement que pour certains taux de cisaillement. Les prédictions des diverses relations demeurent intimement reliées au choix de la loi de mélange. La généralisation des équations d'évolutions d'interface (pour tenir compte d'une différence de viscosité entre les deux phases) n'apporte que de relatives améliorations. Néanmoins, pour des écoulements à dominante élongationnelle, les équations d'évolutions de l'interface permettent de décrire qualitativement la transition d'une morphologie nodulaire à une morphologie fibrillaire. De plus, ces équations traduisent quantitativement la formation de gouttellettes via le mécanisme

d'instabilités capillaires de Rayleigh pour des fibrilles. Pour le mélange PP/EVA-EMA, le caractère élongationnel de l'écoulement agit de manière prépondérante dans l'établissement de la morphologie. Comme le comportement élongationnel du mélange est fortement influencé par celui de la matrice, connaître les données de viscosité élongationnelle des composantes non mélangées peut donc s'avérer très utile dans l'élaboration d'une stratégie de mélange.

Même si des lacunes persistent quant à l'utilisation du modèle de Lee et Park ou des extensions qui ont été proposées dans le cadre de ce travail, la vision macroscopique de l'interface, telle que décrit par un tenseur d'orientation et une aire interfaciale, consitue une voie de recherche prometteuse. En effet, cette approche permet de s'intéresser à l'évolution de la morphologie en cours d'écoulement, ce qui n'avait pu être réalisé auparavant. Etablir une relation qui permettrait de décrire ces changements de morphologie quelque soit le type d'écoulement ou l'intensité de la déformation serait d'une grande utilité pour l'analyse numérique. En effet, ces équations peuvent être résolues ponctuellement et aucune limitation n'est imposée quant à l'écoulement. Pour ce faire, il faudrait prendre en compte les couplages qui peuvent exister entre la morphologie et les propriétés rhéologiques du mélange des deux composantes. Dans une première étude, l'anisotropie pourrait être introduite dans les termes dissipatifs des équations d'évolution de façon à rendre compte des effets d'orientation et de déformation des particules pour des fortes déformations. Déterminer des relations entre les paramètres ajustables des modèles et les propriétés physiques des polymères représenterait alors un pas supplémentaire dans la compréhension des équations d'évolution de l'interface, qui ne sont sans doute pas complètes, et donc dans la rhéologie des systèmes multiphasés.

## CHAPITRE 8 - Références

- BARTHÈS-BIESEL, D. et ACRIVOS, A. (1973). Deformation and burst of a liquid droplet freely suspended in a linear shear field. J. Fluid. Mech., **61**, 1-21.
- BINDING, D.M. (1988). An Approximate Analysis for Contraction and Converging Flows J. Non-Newtonian Fluid Mech., **27**, 173-189.
- BINDING, D.M. et JONES, D.M. (1989). On the interpretation of data from converging flow rheometers. Rheol. Acta, **28**, 215-222.
- BINDING, D. M. (1993). Contraction flows and new theories for estimating extensional viscosity édité par A.A Collyer, Chapman and Hall 1-32.
- BOUSMINA, M. et MULLER, R. (1993). Linear Viscoelasticity in the Melt of Impact PMMA. Influence of Concentration and Aggregation of Dispersed Rubber Particles. J. Rheol., **37**, 663-679.
- BOUSMINA, M., BATAILLE, P., SAPIEHA, S. et SCHREIBER, H.P. (1995). Comparing the Effect of Corona Treatment and Block Copolymer Addition on Rheological Properties of Polystyrene/Polyethylene Blends. J. Rheol., **39**, 499-517.
- BOUSMINA, M. et MULLER, R. (1996). Rheology/morphology/flow conditions relationship for polymethylmetacrylate/rubber blend. Rheol. Acta, **35**, 369-381.
- BRAHIMI, B., AIT-KADI, A., AJJI, A., JERÔME, R. et Fayt, R. (1991). Rheological Properties of Copolymer modified Polyethylene/Polystyrene blends. J. Rheol., **35**, 1069-1091.
- CARREAU, P.J., BOUSMINA, M. et AJJI, A. (1994). Rheological Properties of Blends : Facts and Challenges. Progress in Pacific Polymer Science-3, édité par K.P. Ghiggin, (Springer, New-York), pp. 25-40.
- CARREAU, P.J., DE KEE, D. et CHHABRA, R.P. (1997). Rheology of polymeric systems principles and applications. Hansers Publishers.
- CHOI, S.J. et SCHOWALTER, W.R. (1975). Rheological Properties of Nondilute Suspensions of Deformable Particles. Phys. Fluids, **18**, 420-427.

COGSWELL, F.N. (1972). Converging flow of polymer melts in extrusion dies. Polym. Eng. Sci., **12**, 64-73.

COGSWELL, F.N., (1972). Measuring the extensional rheology of polymer melts. Trans. Soc. Rheol., **16**, 383-403.

COGSWELL, F.N. (1978). Converging flow and stretching flow : A compilation. J. Non-Newtonian Fluid Mech., **4**, 23-38.

CREVECOEUR, G. et GROENINCKX, G. (1991). Fibril formation in *in situ* composites of a thermotropic liquid crystalline polymer in a thermoplastic matrix. J. Appl. Polym. Sci., **49**, 839-849.

DELABY, I., ERNST, B., GERMAIN, Y. et MULLER, R. (1994). Droplet deformation in polymer blends during uniaxial elongational flow. Influence of viscosity ratio for large capillary number. J. Rheol., **38**, 1705-1720.

DICKIE, R.A. (1973). Heterogeneous Polymer-Polymer Composites I Theory of Viscoelastic properties and Equivalent Mechanical Model. J. Appl. Polym. Sci., **17**, 45-63.

DOI, M. (1993). Rheology of Textured Materials édité par L. Garrido, Complex Fluids, Lecture Notes in Physics, (Springer, New York), p 221.

DOI, M. et OHTA, T. (1991). Dynamics and Rheology of Complex Interfaces. I. J. Chem. Phys., **95**, 1242-1248.

ELMENDORP, J.J. et MAALCKE, R.J. (1985). A study on polymer Blending Microrheology, Part 1. Polym. Eng. Sci., **25**, 16, 1041-1047.

ELMENDORP, J.J. et VAN DER VEGT, A.K. (1986). Study on Polymer Blending Microrheology: Part IV. The Influence of Coalescence on Blend Morphology Origination. Polym. Eng. Sci., **26**, 1332-1338.

FORTELNÝ, I. et ŽIVNÝ, A. (1995). Theory of Competition Between Breakup and Coalescence of Droplets in Flowing Polymer Blends. Polym. Eng. Sci., **35**, 1872-1877.

FRIEDRICH, C., GLEINSER, W., KORAT, W.E., MAIER, D. et WEESE, J. (1995). Comparison of sphere-size distributions obtained from rheology and transmission electron microscopy in PMMA/PS blends. J. Rheol., **36**, 1411-1425.

- FRIEDRICH, C., RIEMANN, R.E., MAIER, D. et Korat, E. (1996). Influence of interfacial rheological properties of a PMMA-PS polymer blend. Proc. XII th Int. Congr. On Rheology, p143, Quebec, Canada
- FRÖHLICH, H. et SACK, R. (1946). Theory of the Rheological Properties of Dispersions.. Proc. Roy. Soc. A, 185, 415-430.
- GERMAIN, Y., ERNST, B., GENELOT, O. et DHAMANI, L. (1994). Rheological and Morphological Analysis of compatibilized PP/PA Blends. J. Rheol., 38, 681-697.
- GIBSON, A.G. (1988). Converging dies dans Rheological Measurements, édité par A.A Collyer and D.W. Clegg 49-92.
- GHOSCH, T., GRMELA, M. et CARREAU, P.J. (1995). Rheology of short fibers filled thermoplastics. Polym. Composites, 16, 144-153.
- GODDARD, J.D. et MILLER, C. (1967). Nonlinear effects in the rheology of dilute suspensions. J. Fluid. Mech., 28, 657-673.
- GRAEBLING, D. et MULLER, R. (1990). Rheological Behavior of Polydimethylsiloxane/ Polyoxyethylene Blend in the Melt. Emulsion Model of two Viscoelastic Liquids. J. Rheol., 34, 193-205.
- GRAEBLING, D., MULLER, R. et PALIERNE, J.F. (1993). Linear Viscoelastic Behavior of Some Incompatible Polymer Blends in the Melt. Interpretation of Data with a Model of Emulsion of Viscoelastic Liquids. Macromolecules, 26, 320-329.
- GRAEBLING, D., BENKIRA, A., GALLOT, Y. et MULLER, R. (1994). Dynamic Viscoelastic Behavior of Polymer blends in the Melt. Experimental Results for PDMS-POE, PS/PMMA and PS/PEMA blends. Eur. Polym. J., 30, 301-308.
- GRAMESPACHER, H. et MEISSNER, J. (1997). Melt elongation and recovery of polymer blends, morphology, and influence of interfacial tension. J. Rheol., 41, 27-44.
- GRMELA, M. (1985). Stress tensor in generalized hydrodynamics. Phys. Lett. A, 111, 41-44.
- GRMELA, M. (1988). Hamiltonian dynamics of incompressible elastic fluids. Phys. Lett. A, 130, 81-86.

GRMELA, M. et AIT-KADI, A. (1994). Comments on the Doi-Ohta theory of blends. JNNFM, 55, 191-195.

GUENTHER, G.K. et BAIRD, D.G. (1996). An Evaluation of the Doi-Ohta Theory for an Immiscible Polymer Blend. J. Rheol., 40, 1-20.

GUSKEY, S.M. et WINTER, H.H. (1991). Transient shear behavior of a thermotropic liquid crystalline polymer in the nematic state. J. Rheol., 35, 1191-1207.

HAN, C.D. (1981). Multiphase Flow in Polymer processing. Academic Press.

HAN, J.H., FENG, C.C., LI, D.J. et HAN, C.D. (1995). Effect of flow geometry on the rheology of dispersed two phase blends of polystyrene and polymethylmethacrylate. Polymer, 36, 2451-2463.

HONERKAMP, J. et WEESE, J. (1993). A Non Linear Regularization Method for the Calculation of Relaxation Spectra. Rheol. Acta., 32, 65-73.

JAMES, D.F., CHANDLER G.M. et ARMOUR, S.J. (1990). A converging channel rheometer for the measurement of extensional viscosity. J. Non-Newtonian Fluid Mech., 35, 421-443.

JAMES, D.F. (1991). Flow in a converging channel at moderate Reynolds numbers. AIChE J., 37, 59-64.

KIM, H.C., PENDSE, A. et COLLIER, J.R. (1994). Polymer melt lubricated elongational flow. J. Rheol., 38, 831-845.

KITADE, S., ICHIKAWA, A., IMURA, N., TAKAHASHI, Y. et Noda, I. (1997). Rheological properties and domain structures of immiscible polymer blends under steady and oscillatory shear flows. J. Rheol., 41, 1039-1060.

LACROIX, C., BOUSMINA, M., CARREAU, P.J., FAVIS, B.D. et MICHEL, A. (1996). "Properties of PETG/EVA Blends : Viscoelastic, Morphological and Interfacial Properties, Part I. Polymer, 37, 2939-2947.

LACROIX, C., ARESSY, M. et CARREAU, P.J. (1997). Linear viscoelastic behavior of molten polymer blends: a comparative study of the Palierne and the Lee and Park models. Rheol. Acta, 36, 416-428.

- LACROIX, C., GRMELA, M. et CARREAU, P.J. (1998). Relationships between rheology and morphology for immiscible molten blends of polypropylene and ethylene copolymers under shear flow. J. Rheol., **42**, 41-62.
- LARSON, R. G. (1988). Constitutive equations for polymer melts and solutions édition Butterworth.
- LAVALLÉE, C. (1990). Stéréologie appliquée aux alliages polymères. CNRC, IMI, Boucherville, Qc, Canada.
- LEE, H.M. et PARK, O.O. (1994). Rheology and dynamics of Immiscible Polymer Blends. J. Rheol., **38**, 1405-1425.
- LEVITT, L., MACOSKO, C.W., SCHWEIZER T. et MEISSNER, J. (1997). Extensional rheometry of polymer multilayers: A sensitive probe of interfaces. J. Rheol., **41**, 671-685.
- MACKAY, M.E. et ASTARITA, G. (1997). Analysis of entry flow to determine elongation flow properties revisited. J. Non-Newtonian Fluid Mech., **70**, 219-235.
- MELLEMA, J. et WILLEMSE, M.W.M. (1983). Effective Viscosity of Dispersions Approached by a Statistical Continuum Method. Physica 122A, 286-312.
- MIGHRI, F., AJJI, A. et CARREAU, P.J. (1997). Influence of elastic properties on drop deformation in elongational flow. J. Rheol., **41**, 1183-1201.
- MILLIKEN, W.J. et LEAL, L.G. (1991). Deformation and breakup of viscoelastic drops in planar extensional flows. J. Non-Newtonian Fluid Mech., **40**, 355-379.
- NOBILE, M. R., ACIERNO, D., INCARNATO, L. et NICOLAIS, D. (1990). The rheological behavior of polyetherimide and of its blends with thermotropic copolyester. J. Rheol., **34**, 1181-1197.
- OLDROYD, J.G. (1953). The Elastic and Viscous Properties of Emulsions and Suspensions. Proc. R. Soc. London, Ser. A **218**, 122-132.
- OLDROYD, J.G. (1955). The Effect of Interfacial stabilizing Films on the Elastic and Viscous Properties of Emulsions. Proc. Roy. Soc., A, **232**, 567-577.
- ONUKI, A. (1987). Viscosity enhancement by Domains in Phase -Separating Fluids near the Critical Point : Proposal of Critical Rheology. Phys. Rev. A, **35**, 12, 5149-5155.

PADMANABHAN, M. et MACOSKO, C.W. (1997). Extensional viscosity from entrance pressure drop measurements. Rheol. Acta, **36**, 144-151.

PALIERNE J. F. (1990). Linear Rheology of Viscoelastic Emulsions with Interfacial Tension. Rheol. Acta, **29**, 204-214; (1991) **30**, 497.

RALLISON, J.M. (1984). The deformation of small viscous drops and bubbles in shear flows. Ann. Rev. Fluid. Mech., **16**, 45-66.

SALTIKOV, S.A. (1967). The Determination of the Size Distribution of particles in an Opaque Material from a Measurement of the Size Distribution of their Section dans Stereology, édité par H. Elias, Proc. Second Int. Cong. for Stereology, NY ( Springer, New York), pp 163-173.

SCHOLZ, P., FROELICH, D. et MULLER, R. (1989). Viscoelastic Properties and Morphology of Two-Phase Polypropylene/Polyamide 6 blends in the Melt. Interpretation of Results with an Emulsion Model. J. Rheol., **33**, 481-499.

SCHOWALTER, W.R., CHAFFEY, C.E. et BRENNER, H. (1968). Rheological Behavior of a dilute Emulsion. J. Colloid. Interface Sci., **26**, 152-160.

SONDERGAARD, K. et LYNGBAE-JORGENSEN, J. (1996). Coalescence in an Interface-Modified Polymer Blend as Studied by Light Scattering Measurements. Polym., **37**, 509-517.

STONE, H.A., BENTLEY, B.J. et LEAL, L.G. (1986). An experimental study of transient effects in the breakup of viscous drop. J. Fluid. Mech., **173**, 131-158.

TAKAHASHI, Y., KURASHIMA, N., Noda, I. et DOI, M. (1994a). Experimental tests of the scaling relation for textured materials in mixtures of two immiscible fluids. J. Rheol., **38**, 699-712.

TAKAHASHI, Y., Kitade, S., KURASHIMA, N. et NODA, I. (1994b). Viscoelastic properties of immiscible polymer blends under steady and transient shear flows. Polym. J., **26**, 1206-1212.

TAKAHASHI, Y. et NODA, I. (1995). Domain structures and viscoelastic properties of immiscible polymer blends under shear flow dans Flow-Induced Structure in Polymers, édité par A. Nakatani and M. D. Dadmun (Am. Chem. Soc., Washington D.C.) pp 140-152.



- TAYLOR, G.I. (1932). The Viscosity of a Fluid Containing small Drop of another. Proc. Roy. Soc. A, 138, 41-48.
- TAYLOR, G.I. (1934). The Formation of Emulsions in Definable Fields of Flow. Proc. Roy. Soc. A, 146, 501-523.
- TOMOTIKA, S. (1935). On the Instability of a Cylindrical Thread of a Viscous Liquid Surrounded by Another Viscous Fluid. Proc. Roy. Soc., A, 150, 322-337.
- TREMBLAY, B. (1989). Estimation of the elongational viscosity of polyethylene blends at high deformation rates. J. Non-Newtonian Fluid Mech., 33, 137-164.
- UTRACKI, L.A. et SHI, Z.H. (1992). Development of polymer blend morphology during compounding in a twin screw extruder, Part I : Droplet dispersion and coalescence : A review. Polym. Eng. Sci., 32, 1824-1833.
- VINCKIER, I., MOLDENAERS, P. et MEWIS, J. (1996). Relationship between Rheology and Morphology of Model Blends in Steady Shear Flow. J. Rheol., 40, 613-631.
- VINCKIER, I., MOLDENAERS, P. et MEWIS, J. (1997). Transient rheological response and morphology evolution of immiscible polymer blends. J. Rheol., 41, 705-718.
- VINCKIER, I., MEWIS, J. et MOLDENAERS, P. (1997). Stress relaxation as a microstructural probe for immiscible polymer blends. Rheol. Acta., 36, 513-523.
- WEESE, J. (1993). A Regularization Method for Non Linear Ill Posed Problems. Comput. Phys. Commun., 77, 429-440.